3-29-2019 10:30 AM

The Lotus japonicus SHORT INTERNODES/STYLISH gene family and its role during root nodule development

Arina Shrestha
The University of Western Ontario

Supervisor
Szczyglowski, Krzysztof
The University of Western Ontario Co-Supervisor
Huner, Norman P.A.
The University of Western Ontario

Graduate Program in Biology
A thesis submitted in partial fulfillment of the requirements for the degree in Doctor of Philosophy

ABSTRACT

The ability to host nitrogen-fixing bacteria, which convert atmospheric di-nitrogen to ammonia, inside root cells is a special adaptation of most leguminous and only some non-leguminous plants. It engenders the development of new, root-derived organs, called nodules. Significant research effort has been dedicated to understanding how these ultimate nitrogen-fixing plant organs are built. Nonetheless, important gaps with respect to pertinent knowledge still remain.

My thesis work has focused on deciphering the role of the *SHORT INTERNODES/STYLISH* (*SHI/STY*) transcription factor gene family during nodule formation in *Lotus japonicus*, a model legume plant. I show here that the *SHI/STY* gene family comprises at least nine members, called *STY1* to *STY9*. The RNAseq, qRT-PCR and promoter-GUS localization experiments revealed that expression of all nine *STY* genes associates with nodule development which in most cases required *NF-YA1*, encoding a nodule-specific subunit of a heterotrimeric transcription factor. The activity of the *STY* promoters was associated with nodule primordia and with the vasculature and vascular parenchyma in fully mature nodules. Mutant analysis and a dominant negative approach were used to assess the functional relevance of the *STY* genes during nodule formation. Based on the outcome of experiments with the STY3-SRDX presumed dominant repressor, *STY* genes are shown to be required for both, symbiotic infection and nodule formation in *L. japonicus*. Using *in silico* analysis and a candidate gene approach, *YUCCA1* and *YUCCA11* genes, likely involved in regulation of auxin biosynthesis rates, were identified as potential targets of the *STY*-dependent regulation. My data suggest that *L. japonicus* STYs participate, in a highly redundant manner, in a cascade of transcriptional reprograming that is initiated with the perception of bacterially-encoded nodulation factors by the host roots and leads to local auxin signalling which is required for the differentiation of a fully functional, nitrogen-fixing nodule. The summative findings of my thesis work contribute toward better understanding of the requisite mechanisms for nitrogen-fixing symbiosis, with refinement on the signal transduction pathway that is generated during root nodule organogenesis.

KEYWORDS

Lotus japonicus, legumes, *SHORT INTERNODES/STYLISH*, symbiosis, nitrogen fixation, nodule organogenesis.

DEDICATION

To my parents and family

ACKNOWLEDGEMENTS

I would like to sincerely thank my supervisor Dr. Krzysztof Szczyglowski for his continuous support, encouragement and guidance during my study period. His mentorship has immensely honed my critical thinking abilities. I feel proud and lucky to have had the opportunity to work with such a great person.

I am grateful to my co-supervisor, Dr. Norman P.A. Hüner for his guidance and suggestions throughout my research. I would like to thank my advisor committee members, Dr. Dennis Maxwell and Dr. Susanne Kohalmi for their support and suggestions during my graduate studies.

I would like to thank Loretta Ross and Terry Huebert for their technical and intellectual support. Thanks also for their patience and heart melting attitude which made these years easier and memorable. I am also grateful to past and present members of Szczyglowski lab, Dr. Alexandre Tromas, Dr. Preetam Janakirama, Dr. Erin Zimmerman, Dr. Sihui Zhong, Dr. Mandana Miri, Sanjay Nema, and Jasmine Therrien for their great advice and for creating a wonderful working environment.

I would also like to thank Agriculture and Agri-Food Canada, London Ontario, for providing me with work facilities during my studies. Thanks to all the friends from Agriculture and Agri-Food Canada for such a memorable and nice company during my graduate work. I am thankful to Alex Molnar for his assistance with the preparation of figures and posters. I am grateful to Dr. Sangeeta Dhaubhadel for providing her suggestions and time when needed.

I would like to express my deepest love and gratitude to my beloved parents for all kinds of support and their unconditional love for me.

I am very much grateful to my husband Suresh Chandra Shrestha. This achievement would not have been possible without his support. Thank you for your understanding and for being a wonderful father to Samyak.

TABLE OF CONTENTS

ABSTRACT ..... **i**

KEYWORDS ..... **ii**

DEDICATION ..... **iii**

ACKNOWLEDGEMENTS ..... **iv**

TABLE OF CONTENTS ..... **v**

LIST OF TABLES ..... **viii**

LIST OF FIGURES ..... **ix**

LIST OF APPENDICES ..... **xii**

LIST OF ABBREVIATIONS ..... **xiii**

CHAPTER 1
INTRODUCTION **1**

1.1 Agriculture, nitrogen and the environment 2

1.2 Plant nitrogen nutrition 5

1.3 Nutrient acquisition through plant-microbe interactions 6

1.4 Biological nitrogen fixation 9

1.5 Arbuscular mycorrhiza symbiosis and CSSP 10

1.6 NFS, an AMS on steroids? 13

1.7 Root nodules 16

1.8 Cytokinins and nodule formation 19

1.9 *NIN*, the nodule inception regulator 21

1.10 Nuclear factor Y (NF-Y) and nodule formation 22

1.11 The objectives of the thesis 23

CHAPTER 2

MATERIALS AND METHODS 26

2.1 Seed germination and plant materials 27

2.2 Assessment of plant phenotypes 27

2.3 Identification of *sty* and *yucca* mutant lines and development of higher order mutants 28

2.4 Electrophoretic Mobility Shift Assay 30

2.5 Development of STY3::SRDX dominant negative constructs 31

2.6 Hairy root transformation and fully transgenic *L. japonicus* lines 32

2.7 Gene expression analysis using quantitative RT-PCR 34

2.8 Gene expression analysis using GUS histochemical assay 35

2.9 GUS staining procedure 36

2.10 RNA sequencing 36

2.11 Microscopy 37

2.12 Statistical analyses 37

2.13 Phylogenetic analyses 38

2.14 BLAST analyses 38

CHAPTER 3

RESULTS 41

3.1 *STY1*, *STY2* and *STY3* are likely direct targets of NF-YA1 42

3.2 The *L. japonicus SHI/STY* gene family comprises at least nine members 45

3.3 Activities of *STY* promoters associate with root and nodule development 50

3.4 The level of *STY* mRNAs is regulated during *L. japonicus* nodule development 54

3.5 *L. japonicus sty* mutants 61

3.6 *sty* mutants show weak symbiotic phenotypes 63

3.7 STY3::SRDX blocks infection thread and nodule formation 71

3.8 STYs are required to regulate *YUCCA1* and *YUCCA11* expression during symbiosis 81

3.9 *YUCCA1* and *YUCCA11* promoters are active in nodule primordia and nodules ... 90

3.10 Expression of *YUCCA1* and *YUCCA11* is regulated by NF-YA1 93

3.11 NF-YA1 and NF-YA4 regulate the *YUCCA11* gene expression in a partially redundant manner 96

CHAPTER 4

DISCUSSION 99

4.1 The *L. japonicus SHI/STY* gene family partakes in nodule formation..... 100

4.2 SHI/STY proteins and plant development 101

4.3 *L. japonicus STY*s act in unison to mediate nodule formation..... 102

4.4. *STY* gene expression is regulated by *NF-YA1* dependent and independent mechanisms 103

4.5 Deleterious mutations at *STY* loci have only limited impact on symbiosis 105

4.6 STY3::SRDX blocks nodule formation 106

4.7 STY3::SRDX negatively impacts *M. loti* infection 107

4.8 Both *NF-YA* and *STYs* are required for *YUCCA* gene expression 108

4.9 Nodule differentiation is mediated by *STY*s 110

PERSPECTIVES AND CONCLUSIONS 112

BIBLIOGRAPHY 116

APPENDICES 137

CURRICULUM VITAE..... 142

LIST OF TABLES

CHAPTER 2

Table 2.1 A list of *L. japonicus sty* and *yucca* LORE1 insertion lines and names of the corresponding mutant alleles 39

Table 2.2 *sty3* mutant alleles identified by TILLING approach 40

CHAPTER 3

Table 3.1 Expression of four *L. japonicus STY* genes is significantly upregulated upon *M. loti* infection..... 55

Table 3.2 Segregation of the *pNF-YA1:STY3::SRDX* transgene in two T1 populations, derived from *STY3::SRDX5* and *STY3::SRDX6* independent T0 transgenic plants. 77

Table 3.3 *YUCCA11* is expressed upon *M. loti* inoculation..... 85

Table 3.4 *In silico* analysis of *YUCCA* gene promoters for the presence of a STY binding (ACTCTAC/A) motif..... 89

LIST OF FIGURES

CHAPTER 1

Figure 1.1 Population of the Earth. 3

Figure 1.2 Legume plants engage in beneficial symbioses with both rhizobia and arbuscular mycorrhiza fungi. 8

Figure 1.3 Schematic representation of the nitrogen cycle. 11

Figure 1.4 The endosymbiosis pathway. 14

Figure 1.5 Infection thread. 18

CHAPTER 3

Figure 3.1 *NF-YA1* mediates *STY1*, *STY2* and *STY3* gene expression during nodule development. 43

Figure 3.2 NF-YA1 binds to the promoters of *STY1*, *STY2*, and *STY3* in vitro. 44

Figure 3.3 The *Lotus japonicus* genome contains at least nine *STY* genes. 46

Figure 3.4 *SHI/STY* protein alignment. 48

Figure 3.5 The predicted SHI/STY proteins share two conserved domains. 49

Figure 3.6 Schematics of constructs used to localize the *STY* gene promoter activities. 51

Figure 3.7 *L. japonicus STY* promoters are active during root and nodule development. 53

Figure 3.8 Expression of *STY* genes is regulated upon *M. loti* infection. 58

Figure 3.9 Summary of *STY* genes that responded to *M. loti* infection and the relative dependency of expression changes on presence of functional *NF-YA1*. 59

Figure 3.10 *Lotus japonicus* mutant *sty* alleles. 62

Figure 3.11 *sty* mutants form epidermal infection threads. 64

Figure 3.12 *sty* mutants form fewer nodule primordia..... 66

Figure 3.13 Mutations at most *STY* loci affect shoot growth..... 67

Figure 3.14 Root growth is affected in *sty* mutants. 69

Figure 3.15 A list of double and higher order *sty* mutants..... 70

Figure 3.16 Plant development is affected in *sty1-2 sty2-1 sty3-9* triple mutant..... 72

Figure 3.17 Outlines of constructs used for expression of a presumed STY3 dominant repressor..... 73

Figure 3.18 *pNF-YA1:STY3::SRDX* inhibits nodule formation. 74

Figure 3.19 Transgenic plants carrying *pNF-YA1:STY3::SRDX* do not form nodules. 75

Figure 3.20 *STY*s are required for nodule formation..... 79

Figure 3.21 *STY*s are required for infection thread formation. 80

Figure 3.22 A conceptual outline for identification of downstream STY targets..... 82

Figure 3.23 *L. japonicus* YUCCA proteins have six conserved domains characteristic of flavin monooxygenases..... 83

Figure 3.24 Relationship tree of predicted *L. japonicus* and *M. truncatula* YUCCA proteins..... 86

Figure 3.25 *YUCCA1* and *YUCCA11* respond to *M. loti* infection and this is dependent on *STY*s..... 88

Figure 3.26 The activity of *YUCCA1* and *YUCCA11* promoters associates with nodule development..... 91

Figure 3.27 *Lotus japonicus* mutant *yucca* alleles. 92

Figure 3.28 *NF-YA1* participates in the regulation of *YUCCA1* and *YUCCA11* expression upon *M. loti* infection..... 94

Figure 3.29 *L. japonicus* has nine predicted *NF-YA* genes. 95

Figure 3.30 *NF-YA1* and *NF-YA4* work partially redundantly to regulate *YUCCA11* gene expression. 97

CHAPTER 4

Figure 4.1 A working model for the NF-YA1/STY dependent regulation of nodule organogenesis in a model legume, *L. japonicus*. 109

LIST OF APPENDICES

Appendix A Primers used for *STY* gene study 137

Appendix B Primers used for *YUCCA* gene study 140

LIST OF ABBREVIATIONS

AM	arbuscular mycorrhiza
AMS	arbuscular mycorrhiza symbiosis
ATP	adenosine triphosphate
BNF	biological nitrogen fixation
bp	base pairs
CSSP	common symbiosis signalling pathway
dai	days after inoculation
das	days after sowing
DB	DNA-binding
dCAPS	derived cleavage amplified polymorphic sequence
DNA	deoxyribonucleic acid
eITs	epidermal infection threads
EMSA	electrophoretic mobility shift assay
ERF	ethylene-responsive element binding factor
FAD	flavin adenine dinucleotide
FMO	flavin monooxygenase
GFP	green fluorescent protein
LORE1	*Lotus japonicus* retrotransposon 1
MC	microcolony
MYA	million years ago
Myc	mycorrhizal
N	nitrogen

NAA	1-naphthaleneacetic acid
NADP	nicotinamide adenine dinucleotide phosphate
NCBI	national center for biotechnology information
NF	nodulation or nod factor
NFS	nitrogen-fixing symbiosis
NLS	nuclear localization signals
NP	nodule primordia
ORF	open reading frame
P	phosphorus
PM	plasma membrane
qRT-PCR	quantitative reverse transcription polymerase chain reaction
RING	really interesting new gene
RNA	ribonucleic acid
SE	standard error
SRDX	superman repression domain x
TILLING	Targeting Induced Local Lesions In Genomes
UBI	ubiquitin
UTR	untranslated region

CHAPTER 1

INTRODUCTION

1.1 Agriculture, nitrogen and the environment

Approximately 60 percent of the world's population depends on agriculture for their survival. Global agricultural production has been growing at an average rate of 2 to 4% annually over the past 50 years, while arable land has increased by only 1% annually. The current world population of more than 7 billion is predicted to increase to above 9 billion by 2050 (Figure 1.1) (United Nations Report, 2015; https://esa.un.org/unpd/wpp/Publications/Files/Key_Findings_WPP_2015.pdf). To meet the requirements of the growing population, world food production will need to be increased by a projected 25 to 70% (Hunter et al., 2017). This will have to be accompanied by a dramatic reduction in agriculture-related pollution in order to restore and maintain the key ecosystem services (Steffen et al., 2015; Hunter et al., 2017). Along with or as an integral part of the policy, governance and other management strategy developments, innovative agriculture research has, and will continue to have, a significant role to play in meeting these existential challenges.

A good example in this context is the significant transformation in the capacity for food production that was made possible, thanks to the discovery of a chemical process that converts atmospheric di-nitrogen (N_2) to ammonia and its subsequent industrialization. Known as the Haber-Bosch process, reflecting the names of two German chemists and Nobel Prize laureates (https://www.thechemicalengineer.com/features/cewctw-fritz-haber-and-carl-bosch-feed-the-world/), it is conceivably one of the most impactful scientific inventions of the twentieth century. This invention launched the age of industrial nitrogen fertilization and became an integral part of the Green Revolution that spurred high yielding crop varieties (Pingali, 2012).

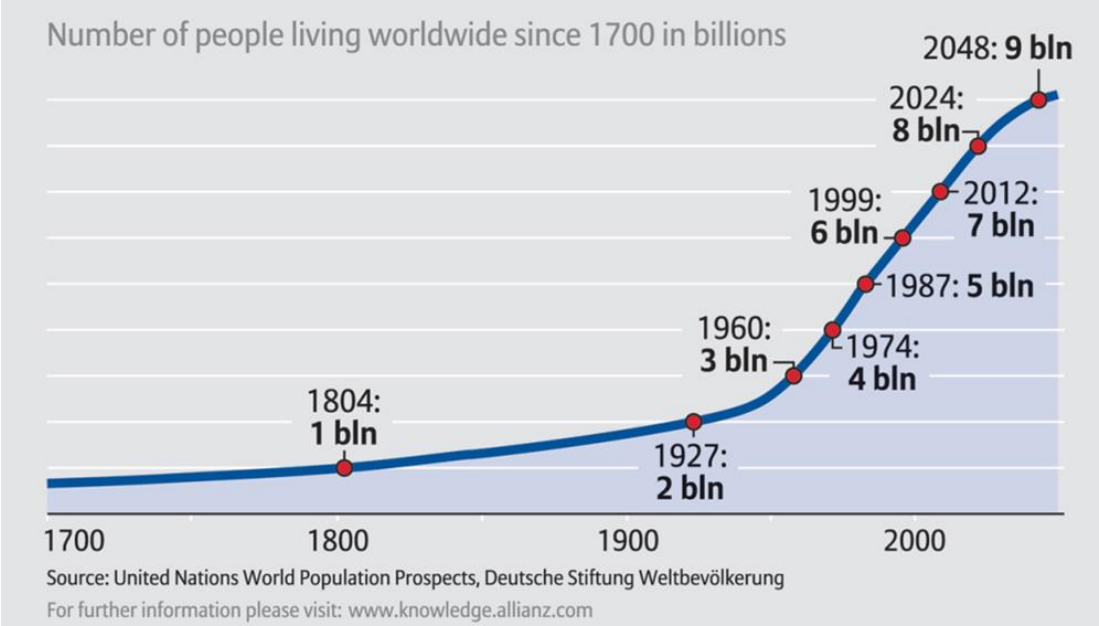

Figure 1.1 Population of the Earth. It had taken all of human history until 1804 for the world population to reach one billion. During 20th century, the global population grew from 1.65 billion to 6 billion. (Figure was modified from https://www.dsw.org/wp-content/uploads/2018/06/weltbevölkerung_final.pdf)

Conventional agriculture, primarily in industrialized countries, has quickly become addicted to Haber-Bosch nitrogen and it was estimated that approximately half of the current human population owe their lives to this very invention (Erisman et al., 2008). However, the costs of producing and using industrial nitrogen fertilizers are no longer considered sustainable. This is because of the need for non-renewable fossil fuel energy in their production and the resulting pollution, as caused by environmental nitrogen enrichment, and its downstream impacts, including greenhouse gas effects, toxic algae blooms, and loss of biodiversity (Vitousek et al., 1997; Rockström et al., 2009).

Pollution of the environment with nutrients is particularly prevalent in several regions of the world, including China, Northern India and also in the USA and Western Europe (Foley et al., 2011). In the United Kingdom, for example, agriculture-derived nitrogen accounts for 66% of nitrous oxide emissions, with very potent greenhouse gas effects (https://uk-air.defra.gov.uk/assets/documents/reports/aqeg/2800829_Agricultural_emissions_vfinal2.pdf), while in Europe 2-3% of the population is exposed to drinking water contaminated with unsafe levels of nitrate (Van Grinsven et al., 2006). Closer to home, in Ontario (Canada), Lake Erie is one of the most productive basins, providing drinking water to millions of people and supporting a multi-billion dollar economy in both Canada and USA. Unfortunately, its efficacy with regard to many key services it provides is threatened by a disturbing trend of recurrent algae blooms and hypoxic conditions. These highly detrimental events are a direct consequence of nutrient, primarily phosphorus and nitrogen, loading (contaminations) caused by agricultural run-offs. Anthropogenic enrichment in P is considered the primary driver behind the size of harmful algae blooms in Lake Erie.

However, there is mounting evidence that combined nitrogen from inorganic fertilizers and manure is the chief culprit influencing the toxicity of the bloom, a more important factor when it comes to public health (https://cen.acs.org/articles/94/web/2016/01/Nitrogen-Triggers-Extra-Toxic-Algal.html).

These few examples highlight the dark side of nitrogen, as used in agriculture. While critically needed to maintain high yields, at least under current production schemes, their use, or rather overuse, has already reached the critical planetary boundary level and become unsustainable (Rockström et al., 2009) .

1.2 Plant nitrogen nutrition

Nitrogen is one of the most widespread elements on the Earth. In its elemental, diatomic (N_2) form, it comprises approximately 78% of the Earth's atmosphere. However, N_2 is unusable to most organisms due to the triple bond connectivity of the two atoms, which makes its conversion to any biologically active molecule highly challenging. Thus, while being abundant, nitrogen represents one of the most growth-limiting macronutrients for the majority of organisms in natural settings, including plants.

Nitrogen is a major component of chlorophyll, the pigment required for photosynthesis, as well as amino acids, the building blocks of proteins. It is also found in biomolecules, like ATP and nucleic acids. Plants can only utilize nitrogen in its reduced forms and nitrate (NO_3^-) is the most preferable source of mineral nitrogen for many plants, although they can also utilize other nitrogen forms, such as ammonium and amino acids (Masclaux-Daubresse et al., 2010). Root-localized nitrogen sensing and uptake machinery facilitate these processes and are dynamically regulated at local and systemic levels, responding to

availability and distribution of external nitrogen while also integrating the information on internal demand (Gent and Forde, 2017; Poitout et al., 2018).

Plants acquire NO_3^- from the soil by absorbing it across the plasma membrane (PM) of root epidermal and cortical cells, which is facilitated by high- and low-affinity transporters. Once inside, NO_3^- is reduced by nitrate reductase (NR) and nitrite reductase (NiR) to ammonium (NH_4^+), which is then assimilated into an organic (amino acid) form *via* the GOGAT cycle. Only a proportion of absorbed nitrate is assimilated within the roots whereas the remaining amount is transported to the shoot via xylem and then assimilated in leaves (Miller and Smith, 1996; Forde and Clarkson, 1999).

Scavenging for nitrogen and also other nutrients is an active process. One of the strategies common to all plants is reflected by the plasticity of growth, where the root system architecture, the three-dimensional geometry of root morphology in the soil (Lynch, 1995), is adjusted depending on nutrient availability and other pertinent external and internal factors. For example, under severe nitrogen limitation, the root growth is stalled to preserve dwindling internal resources (Niu et al., 2013; Giehl et al., 2014; Peret et al., 2014), but appearance of a localized nitrogen patch would quickly stimulate directional lateral root growth toward the nutrient source, allowing for a targeted exploration of the soil (Forde, 2009).

1.3 Nutrient acquisition through plant-microbe interactions

In their quest for limited nutrients, plants are supported not only by their intrinsic abilities to adjust the growth patterns but also by their microbiomes. Both loosely associated microorganisms residing in the rhizosphere and phyllosphere, and also those

habitating the plant endosphere compartments, classified as either extracellular or intracellular endophytes, are likely germane in this context. However, owing to their intimate nature the latter group is more likely to provide a reliable support for nutrition (van der Heijden et al., 2016). This is keenly exemplified by one of the most widely occurring intracellular plant-microbe interactions, pertinent to the majority of extant plant species, which is the symbiosis of plant roots with phosphate-acquiring arbuscular mycorrhiza (AM) fungi (Parniske, 2008; MacLean et al., 2017). Another prominent example is nitrogen-fixing root nodule symbiosis (NFS), although this interaction is restricted to a phylogenetically much smaller group of plants in comparison to AM symbiosis (AMS) (see below) (Figure 1.2).

Among many edaphic factors, elevated levels of soil N and P were shown to influence taxonomic and functional traits of soil microbial communities (Ikeda et al., 2014; Pan et al., 2014; Leff et al., 2015) and their adverse effects on NFS and AMS, respectively, are well-documented (Fred and Graul, 1916; Carroll and Gresshoff, 1983; Delves et al., 1986; Streeter, 1988; Vessey and Waterer, 1992; Mortier et al., 2012; Cabeza et al., 2014; Saito et al., 2014; Konvalinková et al., 2017; Liese et al., 2017). Long-term exposure to chemical fertilization has also been linked to favoring selection of less effective plant mutualists (Johnson, 1993; Kiers et al., 2007; Toby Kiers et al., 2010; Vandenkoornhuyse et al., 2015; Weese et al., 2015). This highlights the existence of important balancing mechanisms and underpins the key dilemma. In agricultural settings, where limiting productivity by any factor is unacceptable, industrial fertilization, while fulfilling most nutritional needs, likely restricts many benefits the plants would have otherwise received through microbial-based services. How to resolve this apparent conundrum, while also addressing the compounding

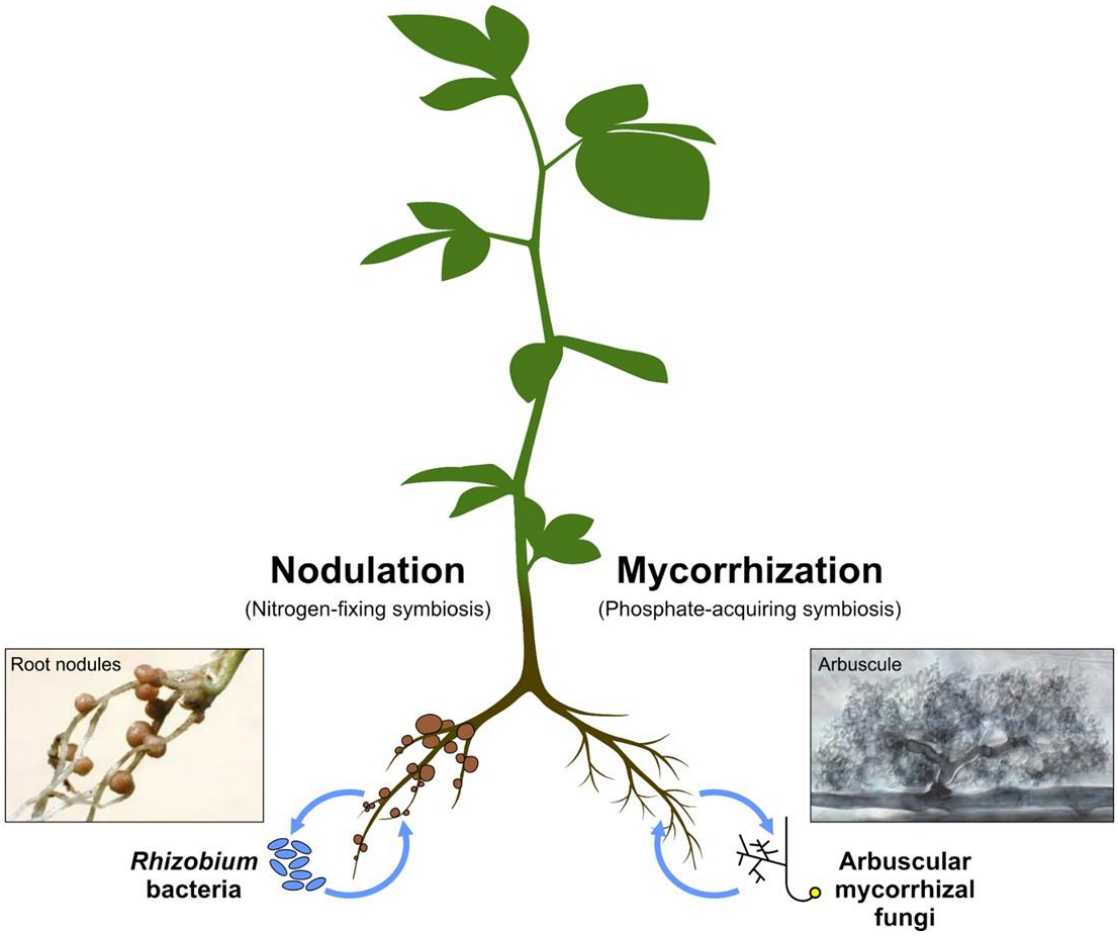

Figure 1.2 Legume plants engage in beneficial symbioses with both rhizobia and arbuscular mycorrhiza fungi. (Picture of the arbuscule was modified from https://mycorrhizas.info/vam.html)

factor of anthropogenic nutrients escaping to the environment and causing its degradation, constitutes one of the main challenges of our generation.

Investments from public and private organizations have been supporting research on so called “self-fertilizing” crops. In terms of nitrogen, exploring the possibility of extending NFS to crops that are currently unable to engage in this type of interaction, or even directly engineering N_2-fixation in cereals by *in planta* expression of a prokaryotic nitrogenase enzyme, are at the forefront of these efforts (Good and Beatty, 2011; Curatti and Rubio, 2014; Mus et al., 2016; Liu et al., 2018). Selecting natural or devising synthetic microbiomes that boost nitrogen acquisition and working toward so called ‘designer roots’ with improved foraging properties are other promising research avenues (Gewin, 2010; Bishopp and Lynch, 2015; Panke-Buisse et al., 2015; Sessitsch and Mitter, 2015). To succeed in these conceivably transformative endeavors will require a thorough understanding of the underlying processes, for which selected aspects of the current knowledge, especially those pertinent to NFS, are briefly summarized in following sections.

1.4 Biological nitrogen fixation

Early during the evolution of the prokaryotic life, long before the Haber-Bosch process was conceived, an enzymatic complex, called nitrogenase, was produced to catalyze the ATP-dependent conversion of N_2 to ammonia (Navarro-Gonzalez et al., 2001). This reaction is known as biological nitrogen fixation (BNF) and although taxonomically restricted to only limited groups within Archea and bacteria, it accounts for at least half of the reduced nitrogen circulating today on the Earth (Falkowski, 1997) (Figure 1.3). Free-

living soil bacteria, such as *Klebsiella* and *Azotobacter*, bacteria that form associative relationships with plants, including *Azospirillum*, *Gluconacetobacter* and cyanobacteria, and also rhizobia and Frankia that can live inside plant cells, exemplify microorganisms that are capable of BNF (Vitousek et al., 2013). On the other hand, not a single eukaryotic organism has gained the ability to carry out this process on it own, although different symbiotic associations with N_2-fixing prokaryotes are known in all crown groups of eukaryotic life, including protists, fungi, animals and plants (Kneip et al., 2007). The nitrogen-fixing root nodule symbiosis of legumes with rhizobia is conceivably the most intricate and is also the best studied interaction.

What evolutionary event or events engendered the ability of legumes and a restricted number of non-legume plants to host N_2-fixing bacteria intracellularly remains the subject of great interest. The current theory, supported by extensive phylogenomic analyses, posits that this trait was attained in an ancestor of the N_2-fixing clade as a result of refurbishing the regulatory elements of pre-existing gene networks (Szczyglowski and Amyot, 2003; Griesmann et al., 2018; van Velzen et al., 2018). One of these gene networks, based on which the capability for NFS evolved, turned out to support AMS (Stracke et al., 2002; Kistner et al., 2005; Markmann and Parniske, 2009; MacLean et al., 2017).

1.5 Arbuscular mycorrhiza symbiosis and CSSP

AMS between plants and the fungi of phylum *Glomeromycota* is ancient, with a predicted origin early during the evolution of terrestrial flora, approximately 460 million years ago (MYA) (Remy et al., 1994; Taylor et al., 1995; Parniske, 2008; Bonfante and Genre, 2010; Corradi and Bonfante, 2012). It has been speculated that plants would have

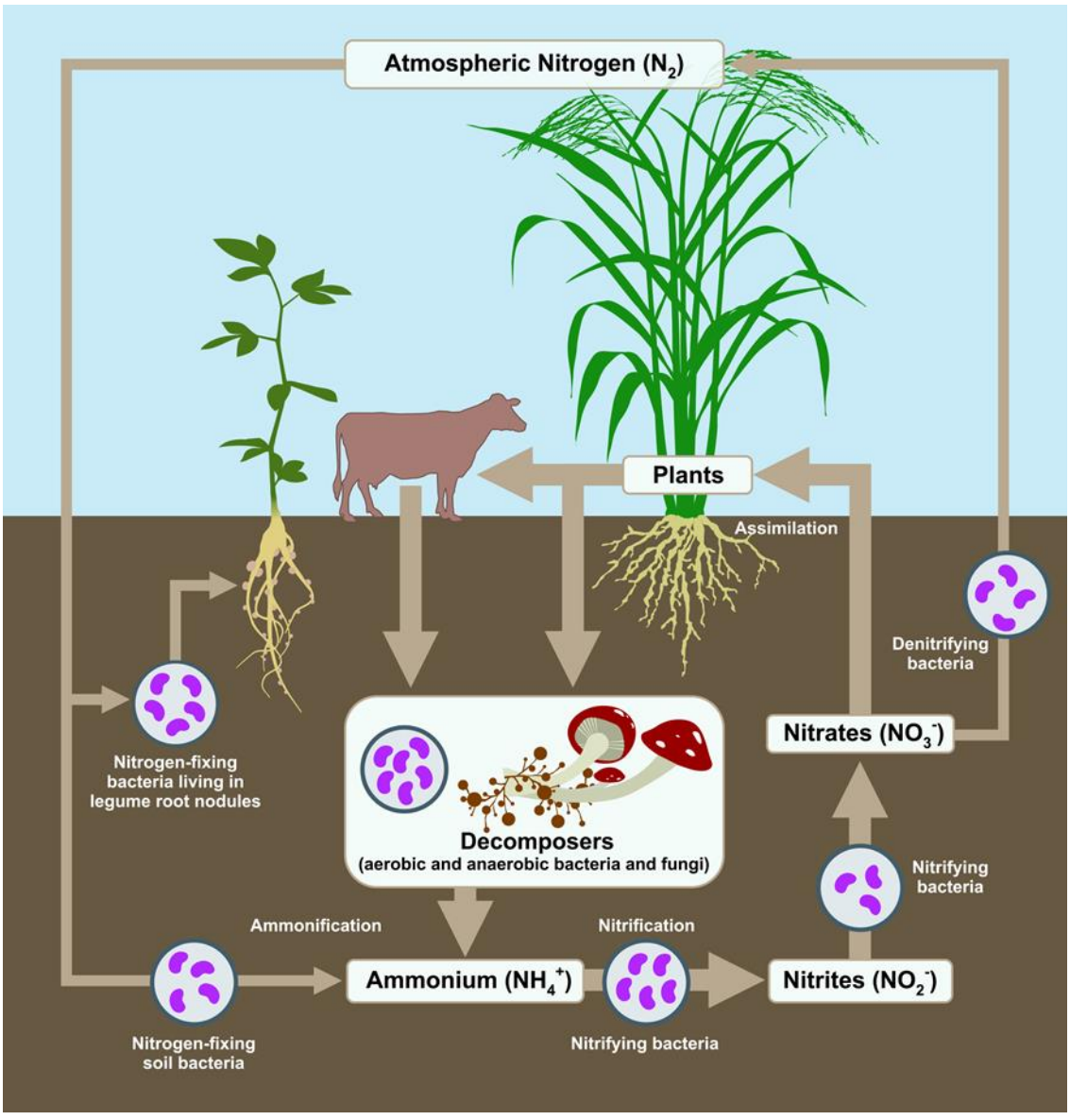

Figure 1.3 Schematic representation of the nitrogen cycle.

(Figure was modified from https://en.wikipedia.org/wiki/Nitrogen_cycle)

been unable to colonize land without being assisted by the fungi. These early land plants had no or very rudimentary root systems and fungal hyphae were likely essential in fulfilling the life-sustaining functions of supplementing water and nutrients, such as P and N to their primitive hosts (Pirozynski and Malloch, 1975).

Extending far beyond the physical constraints of the roots, extra-radical AM hyphae dramatically increase both the distance and the surface area available for soil exploitation (Govindarajulu et al., 2005; Kistner et al., 2005) while highly branched intra-radical hyphae, called arbuscules, serve to trade externally captured nutrients for plant-derived sugars and fatty acids (Yang and Paszkowski, 2011; Luginbuehl et al., 2017; MacLean et al., 2017). Progression of intra-radical hyphae and the establishment of arbuscules without triggering any adverse defense mechanisms, mark an important evolutionary step that was taken by plants in learning of how to tame cooperative fungi through intracellular symbiosis. Evolution has apparently tinkered with this innovation further which, circa 60 MYA, allowed the progenitor of legumes and some non-legume plants to learn how to accommodate N_2-fixing bacteria, which is the basis of the extant NFS. This fascinating picture of the evolutionary progression first surfaced based on the discovery of pea plants carrying monogenic mutations that simultaneously impaired both AMS and NFS (Duc et al., 1989). Subsequent research revealed the presence of the so-called common symbiotic signalling pathway (CSSP) (Oldroyd, 2013), which is shared by and essential for the initiation of the plant accommodation program during both AMS and NFS (Stracke et al., 2002; Kistner et al., 2005; Oldroyd, 2013; MacLean et al., 2017) (Figure 1.4).

The known elements of the CSSP signal transduction include a leucine-rich repeats (LRR) type receptor SYMRK/DMI2 (Endre et al., 2002; Stracke et al., 2002), two ion

channels CASTOR and POLLUX/DMI1 (Ané et al., 2004; Charpentier et al., 2008) and three nucleoporins NUP88, NUP133 and NENA (Kanamori et al., 2006; Saito et al., 2007; Groth et al., 2010), which all contribute to epidermal events that stimulate cellular calcium (Ca^{2+}) influx and rapid oscillations of Ca^{2+} concentration within the perinuclear space, called Ca^{2+} spiking (Ehrhardt et al., 1996; Sieberer et al., 2012; Morieri et al., 2013; Charpentier et al., 2016). Two more downstream components of the CSSP, namely CALCIUM and CALMODULIN-DEPENDENT RECEPTOR KINASE (CCaMK/DMI3) and its phosphorylation target CYCLOPS/IPD3, transduce these Ca^{2+} evolutions into relevant downstream outputs (Levy et al., 2004; Mitra et al., 2004; Messinese et al., 2007; Yano et al., 2008; Hayashi et al., 2010; Madsen et al., 2010; Singh et al., 2014). In *M. truncatula*, DELLA proteins, which are central to gibberellic acid signalling, were shown to promote CCaMK/IPD3 complex formation and be required for both symbioses, hence also belonging to the CSSP (Jin et al., 2016). Downstream from the CSSP, a cascade of transcription factors mediates divergent processes that establish rhizobial and mycorrhizal symbioses (Kalo et al., 2005; Smit et al., 2005; Middleton et al., 2007; Gobbato et al., 2012; Soyano and Hayashi, 2014; Sun et al., 2015; MacLean et al., 2017) (Figure 1.4).

1.6 NFS, an AMS on steroids?

Activation of CSSP during NFS and AMS involves the perception of microsymbiont-derived chemical signals or a mixture of chemically-related signals, termed Nod Factor (NF) and Myc Factor (MycF), respectively (Genre et al., 2013; Russo et al., 2018). NF and MycF are lipo-chitooligosaccharide molecules, where a variety of bacterial strain-specific modifications at the reducing and non-reducing end of the former are considered as

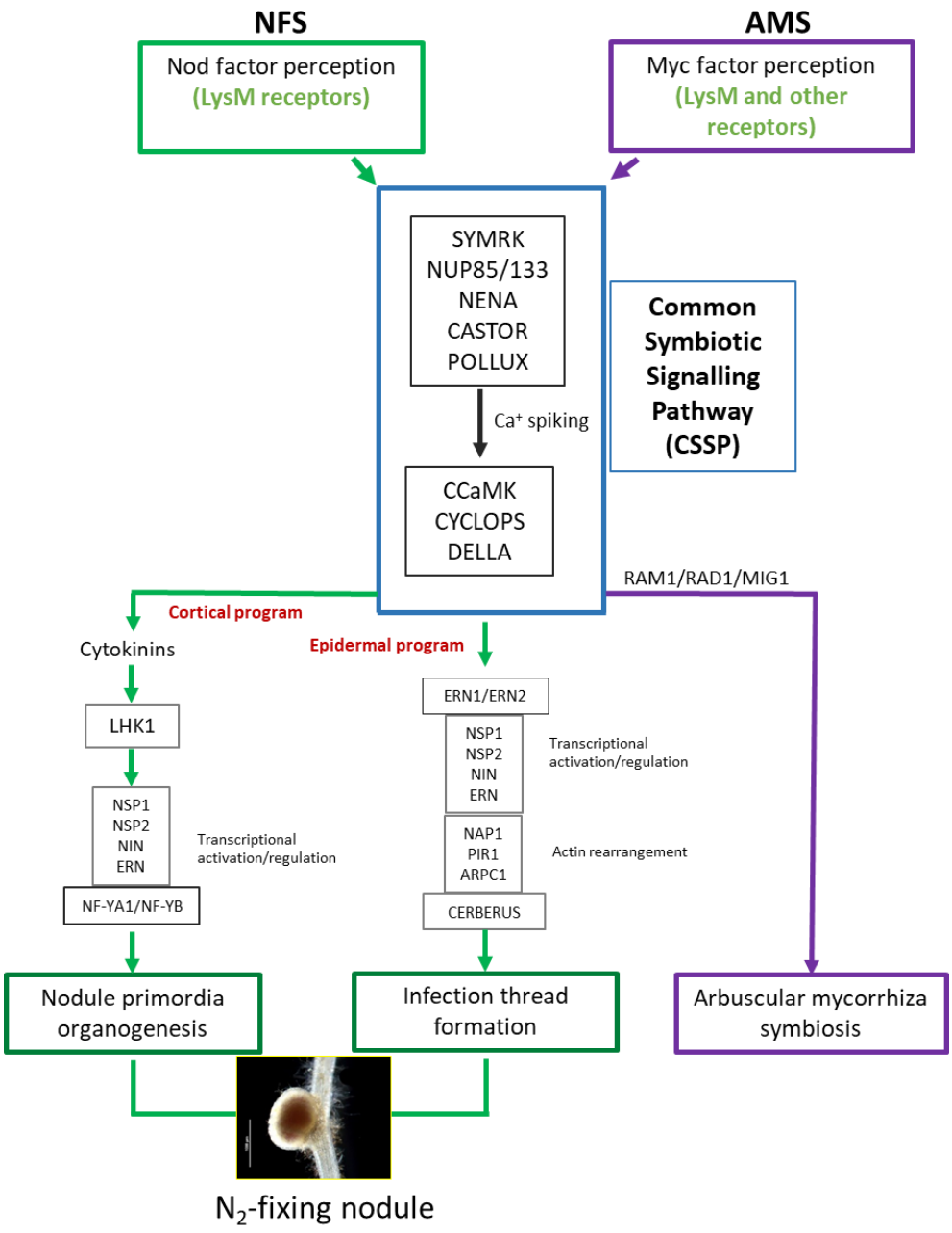

Figure 1.4 The endosymbiosis pathway. An overview of plant proteins that mediate nitrogen-fixing (NFS) and arbuscular mycorrhiza (AMS) symbioses is provided. Note that many additionally regulatory proteins, not included in the schematic, are involved in the establishment of AMS (for comprehensive review on this topic, see MacLean et al., 2017). Furthermore, apart from CSSP, other proteins, such as some of the Nod factor receptors and several transcription factors, including NSP1/2 and NIN, while crucial for NFS, were also shown to play a role during AMS. For more details, please see text.

adaptations from the rather rudimentary chitin backbone of the latter (Maillet et al., 2011). This difference in chemical complexity (i.e. the extent of chemical decorations on the chitin backbone) between NF and MycF was postulated to account, at least in part, for the high level of selectivity in plant-*Rhizobium* interactions as opposed to the rather promiscuous nature of AMS (Maillet et al., 2011; MacLean et al., 2017).

The MycF-specific receptor has yet to be identified while NF receptors have been characterized and were shown to be indispensable for NFS while also being partially involved in, but non-essential for, AMS (Zipfel and Oldroyd, 2017). Interestingly, however, in *Parasponia andersonii,* the only non-legume plant known to form N_2-fixing symbiosis with rhizobia, a single LysM kinase receptor was found to be critical for both symbioses. This observation suggests that like other known CSSP elements, the NF-perception receptors have evolved based on the pre-existing recognition mechanism relevant to AM signalling (Op den Camp et al., 2011).

Activation of the NF or MycF receptors by their respective ligands drives the CSSP-dependent reactivation of cell cycle-related processes in both the root epidermis and subtending cortex. This is apparently important for subsequent intracellular accommodation of both fungal and bacterial partners inside roots (Held et al., 2010; Breakspear et al., 2014; Xiao et al., 2014; Murray, 2017; Russo et al., 2018). However, during NFS only, the re-activated cell cycle results in extensive cell divisions that lead to the formation of distinct accommodation organs, root nodules, which host N_2-fixing and other associated bacteria (Martínez-Hidalgo and Hirsch, 2017). By contrast, sporadic, ectopic cell divisions associated with the progression of fungal hyphae inside roots do not support any macroscopic organ formation and the development of AMS culminates in

microscopic structures only, as represented by arbuscule-containing cells (Russo et al., 2018). Thus, in terms of symbiotic organ formation, NFS could be considered as AMS on steroids.

As outlined below, a functional link between NF perception and the downstream host plant responses involving cytokinins may account for this ostensibly augmented, cellular-level impact that makes a nodule during NFS.

1.7 Root nodules

Only a restricted number of extant plant genera, belonging to one of the four orders, Fabales, Fagales, Rosales and Cucurbitales, within Fabids (formerly eurosid 1) form nodules (Doyle, 2011). This developmental process requires a coordinated, CSSP-dependent response of both root epidermis and subtending root cortex and pericycle (Timmers et al., 1999; Xiao et al., 2014), which commences as a result of the selective recognition and binding of NFs to their cognate, root epidermis-localized receptors. Like in *Parasponia*, these belong to the lysine motif (LysM) receptor-like kinase protein family and are known as NF receptor 1 (NFR1) and NFR5 in *L. japonicus* (Madsen et al., 2003; Radutoiu et al., 2003; Radutoiu et al., 2007; Broghammer et al., 2012) or MtLYK3 and MtNFP in *Medicago truncatula* (Limpens et al., 2003; Arrighi et al., 2006).

The selectivity of the NF recognition by the receptors, which determines the compatibility between the host plant and its N_2-fixing micro-symbiont, has been postulated to have evolved through a neo-functionalization of the plant innate immunity mechanism that uses transmembrane receptors to recognize microbial-associated molecular patterns, such as chitin (Jones and Dangl, 2006; Zhang and Zhou, 2010; Liang et al., 2013; Liang et

al., 2014; Zipfel and Oldroyd, 2017). More recently, a mechanism wherein NF perception induces expression of EPR3, an exopolysaccharide receptor belonging to the LysM receptor kinase family, has been documented. EPR3 apparently acts in a sequential manner with the NFR1/NFR5 complex to reinforce the recognition, thereby allowing the efficient entry of *Mesorhizobium loti*, an N_2-fixing partner of *L. japonicus*, into roots (Kawaharada et al., 2015; Kawaharada et al., 2017b). Additional LysM receptors are also known to participate in fine-tuning the symbiotic process, which altogether points to the involvement of a rather intricate mechanism (Murakami et al., 2018).

At the root epidermis, mutual compatibility between symbiotic partners drives symbiotic infection, which in most plants involves the formation of root hair plasma membrane-derived trans-cellular shafts, called infection threads (IT) (Figure 1.5) (Sprent, 2007). These shafts are actively built by the host plant to guide the orderly progression of rhizobia inside the roots (Fournier et al., 2015; Miri et al., 2016), where a presumed cell non-autonomous root epidermis to cortex signalling has already activated mitotic cell divisions for nodule primordia (NP) formation (Madsen et al., 2010; Held et al., 2014). In most cases, the release of rhizobia from IT inside NP cells marks the beginning of functional symbiosis. Residing within symbiosomes, membrane-bound organelle-like structures present within the cytoplasm of infected nodule cells, differentiated forms of rhizobia, called bacteroids, begin N_2 fixation while assimilating the photosynthetic carbon (Kereszt et al., 2011).

The root nodule provides an ideal environment to protect the rhizobia-encoded nitrogenase complex which catalyzes the reduction of atmospheric N_2 to ammonia

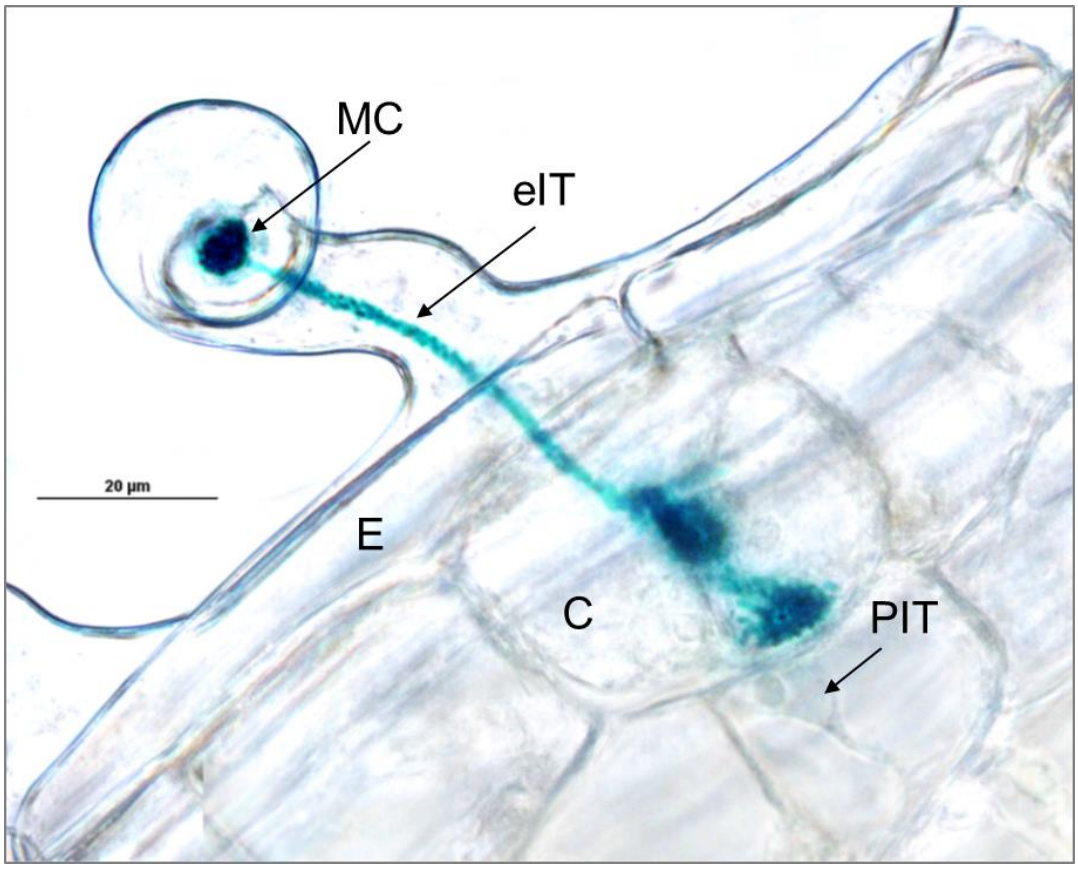

Figure 1.5 Infection thread. Image showing infection thread penetrating root hair and descending into subtending cortex. Presence of *M. loti* inside the infection thread is marked by blue colour, reflecting the activity of the *LacZ* reporter gene. MC, microcolony; eIT, epidermal infection thread; PIT, a preinfection thread that marks one possible route for progression of the infection towards subtending nodule primordium (not shown); E, root epidermis; C, root cortex.

(Coba de la Pena et al., 2017). This is readily assimilated by the host plant, supporting its vigorous growth (Udvardi and Poole, 2013). From this perspective, nodules represent the ultimate N_2-fixing hubs and their engineering in non-nodulation plants is considered as one of the essential steps in extending NFS to some important cereal crops (Rogers and Oldroyd, 2014). Interestingly in this context, acting downstream from NF perception and CSSP, cytokinins, a class of plant hormones regulating a variety of developmental processes in all higher plants, turned out to be key plant endogenous mediators of nodule organogenesis (Cooper and Long, 1994; Murray et al., 2007; Frugier et al., 2008; Sasaki et al., 2014; Gamas et al., 2017; Reid et al., 2017). Why formation of nodules, as mediated by ubiquitous cytokinins, is limited to some plants only, remains an unanswered question.

1.8 Cytokinins and nodule formation

Pertinent to many regulatory processes, (Zürcher and Muller, 2016) cytokinins partake in mechanisms that mediate acquisition of soil nutrients by systemically communicating plant nitrogen status to direct root foraging activities (Kiba et al., 2011; Krouk et al., 2011; Ruffel et al., 2011; Ruffel et al., 2016; Poitout et al., 2018). Their important role during NFS has also been firmly documented. This was initially inferred 24 years ago following the observation that a mutant strain of *Sinorhizobium meliloti*, unable to produce NF but engineered for secretion of trans-zeatin, an isoprenoid cytokinin, was able to induce nodule-like structures on *M. sativa* roots (Cooper and Long, 1994). This early observation is in line with the current understanding that suggests a rapid accumulation of cytokinin in roots as a key step in the nodule primordium inception (Frugier et al., 2008; Held et al., 2014; van Zeijl et al., 2015; Boivin et al., 2016). Importantly, cytokinins have also turned

out to be important in mediating the root susceptibility to rhizobial infection (Murray et al., 2007; Held et al., 2014; Miri et al., 2016; Tsikou et al., 2018).

How bio-active cytokinins are generated in roots upon NF perception and CSSP activation remains a matter of intensive study. Nonetheless, current data indicate that both, *de novo* cytokinin biosynthesis and direct activation of a pre-existing, inert cytokinin pool(s) by LONELY GUY (LOG) proteins (Kurakawa et al., 2007; Tokunaga et al., 2012) contribute to or account for this process (Mortier et al., 2014; van Zeijl et al., 2015; Reid et al., 2017).

Within 3 hours of NF application, trans-zeatin and isopentenyl adenine, the most potent endogenous cytokinins, were detected at a significantly elevated level in *M. truncatula* roots (van Zeijl et al., 2015) and similar observations have been made in *L. japonicus* (Reid et al., 2016). The majority of early (i.e. within the first 3 hours) transcriptional changes to NF perception in *M. truncatula* roots were shown to be dependent on the *MtCRE1* cytokinin receptor gene (van Zeijl et al., 2015), further confirming that cytokinin signalling in roots is one of the key, positive effectors of nodule organogenesis. Indeed, deleterious mutations in *MtCRE1* or its *L. japonicus* orthologue, *LHK1*, result in hugely defective NFS (Gonzalez-Rizzo et al., 2006; Murray et al., 2007; Plet et al., 2011) and the *L. japonicus lhk1-1 lhk1a-1 lhk3-1* triple cytokinin receptor mutant does not form nodules (Held et al., 2014). On the other hand, ectopic cytokinins were shown to trigger cortical cell divisions and formation of nodule-like structures in the absence of rhizobia on roots of several leguminous species (Bauer et al., 1996; Fang and Hirsch, 1998; Mathesius et al., 2000a; Heckmann et al., 2011). Furthermore, axenically grown *L. japonicus* plants carrying *snf2*, a gain-of-function *LHK1* allele, developed empty nodules (Tirichine et al., 2007;

Heckmann et al., 2011; Reid et al., 2017), showing that the cytokinin receptor was not only required but also sufficient for stimulating nodule organogenesis.

1.9 *NIN*, the nodule inception regulator

In *L. japonicus*, expression of the *NODULE INCEPTION REGULATOR* (*NIN*) gene is required for spontaneous nodule formation, as mediated by *snf2*, and *NIN* mRNA level was upregulated in *snf2* roots in the absence of rhizobia (Tirichine et al., 2007). Furthermore, empty nodule-like structures were induced in *L. japonicus* roots by expressing *NIN* under the control of the constitutive, *UBIQUITIN* promoter (Soyano et al., 2013), indicating that by acting downstream from *LHK1*, *NIN* is a key mediator of nodule formation. Consistent with this, *NIN* was shown to be indispensable for nodule formation not only in *L. japonicus* (Schauser et al., 1999) but also in other legume species from Fabales, including pea (*Pisum sativum*) (Borisov et al., 2003) and *Medicago truncatula* (Marsh et al., 2007; Vernie et al., 2015) and in *Casuarina glauca* (order Fagales), an actinorhizal plant (Clavijo et al., 2015; Chabaud et al., 2016).

NIN genes encode RWP-RK domain-containing transcription regulators, belonging to the NIN-like protein (NLP) family (Chardin et al., 2014). Deleterious mutations at *NIN* loci in various nodulating plant species block the development of NFS, including bacterial infection and nodule organogenesis (Schauser et al., 1999; Marsh et al., 2007; Murray et al., 2007; Madsen et al., 2010; Xie et al., 2012; Soyano et al., 2013; Yoro et al., 2014; Vernie et al., 2015). In *M. truncatula*, *NIN* was shown also to play an important role during AM infection, although the *Mtnin-1* mutant was still able to establish AMS (Guillotin et al., 2016), perhaps due to the presence of a partially redundant function(s).

CYCLOPS, the direct phosphorylation target of CCaMK (Yano et al., 2008; Singh et al., 2014) and a component of CSSP (Figure 1.4) was shown to initiate a cascade of transcriptional reprogramming that leads to nodule formation (Limpens and Bisseling, 2014; Soyano and Hayashi, 2014). Its artificial activation in *L. japonicus* was sufficient to stimulate the formation of empty nodule structures in the absence of any external stimulus (Limpens and Bisseling, 2014; Singh et al., 2014). This required *NIN*, which is subjected to CYCLOPS-dependent regulation (Singh et al., 2014). *NIN* has a central, yet complex and not fully understood function(s) during symbiosis. In *L. japonicus* NIN was shown to directly regulate *LjNF-YA1* and *LjNF-YB1* transcription factor genes, which are required for normal nodule development (Soyano et al., 2013) (Figure 1.4).

1.10 Nuclear factor Y (NF-Y) and nodule formation

Nuclear Factor Y (NF-Y) proteins, known also as Heme Activator Proteins (HAP) or CAAT-box binding transcriptional factors (CBF), are heterotrimeric protein complexes composed of the NF-YA, NF-YB and NF-YC subunits (Mantovani, 1999; Dolfini et al., 2012; Laloum et al., 2013). Unlike in animals and fungi, plants have evolved multiple copies of genes encoding each of the three NF-Y subunits and some of these have been shown to play important regulatory functions during nodule formation (Combier et al., 2006; Combier et al., 2008; Zanetti et al., 2010; Laloum et al., 2013; Soyano et al., 2013; Battaglia et al., 2014; Laloum et al., 2014; Laporte et al., 2014).

The *M. truncatula MtNF-YA1* (*MtHAP2-1*) gene, which encodes an A subunit of the NF-Y complex, was the first to be identified as essential for indeterminate (i.e. those which contain a persistent meristem) nodule development (Combier et al., 2006; Combier et al.,

2008). It was shown to be required for regulation of cell proliferation and proper nodule meristem formation. Its role during symbiotic root infection by *S. meliloti*, exerted through a partially redundant function with *MtNF-YA2*, was also highlighted (Laloum et al., 2014; Laporte et al., 2014).

NF-Ys have emerged as important also for determinate, meristem-deprived nodules. For example, in common bean (*Phaseolus vulgaris*), *PvNF-YC1* was shown to be required for nodule formation and also for rhizobial infections, including a mechanism by which the host plant selects for a more efficient symbiotic partner (Zanetti et al., 2010; Battaglia et al., 2014). By contrast, various impediments to the *L. japonicus NF-YA1* did not lead to defective *M. loti* infection but, as in *P. vulgaris* and *M. truncatula*, were detrimental to nodule formation (Soyano et al., 2013; Hossain et al., 2016).

Analysis of independent *L. japonicus* variants, carrying different mutant *nf-ya1* alleles, showed that *LjNF-YA1* became indispensable only downstream from the initial cortical cell divisions but prior to nodule differentiation, including cell expansion and nodule vascular bundle formation (Hossain et al., 2016). Although it remains unclear what specific mechanism(s) is being regulated, a hypothesis was formulated that NF-YA1 may partake in the generation of local auxin maxima. These maxima are known to be produced in *M. loti*-inoculated *L. japonicus* roots downstream from *LHK1* and *NIN* and were deemed essential for nodule formation (Suzaki et al., 2012).

1.11 The objectives of the thesis

Microarray experiments previously done in our laboratory identified 17 genes as potential direct targets of the *NF-YA1*-dependent regulation during *L. japonicus* root nodule

formation (Hossain et al., 2016). Three of the 17 genes, namely *STY1*, *STY2* and *STY3*, were characterized as members of the *L. japonicus SHORT INTERNODE/STYLISH* (*SHI/STY*) transcription factors gene family and the microarray data showed that, as compared to the wild-type counterpart, their expression was significantly downregulated in *nf-ya1* mutants, which was associated with defective nodule organogenesis (Hossain et al., 2016). In *A. thaliana* and *Physcomitrella patens*, STY proteins act as important components of various gene networks, including those pertinent to regulation of cell expansion and auxin biosynthesis. *YUCCA* genes, encoding the indole-3-pyruvic acid (IPyA) decarboxylase, a rate-limiting enzyme in auxin biosynthesis (Cheng et al., 2006; Zhao, 2012) are among the identified, direct targets of the STY-dependent regulation (Sohlberg et al., 2006; Eklund et al., 2010a; Eklund et al., 2010b). As our microarray data suggested that at least some of the *L. japonicus STY* genes are regulated by NF-YA1, a nodule-specific transcription regulator, verifying this and characterizing the role of *STY*s during the transcriptional reprogramming of roots toward nodule formation constituted the primary goal for my thesis work.

The following hypotheses were formulated and tested:

(1) In response to *M. loti* infection, *L. japonicus* NF-YA1 regulates expression of several *SHI/STY* genes.

(2) Members of the *L. japonicus SHI/STY* gene family act redundantly to regulate root nodule formation.

(3) *SHI/STY* genes are essential only after the initial cell divisions for nodule primordia formation.

(4) *YUCCA* genes, encoding auxin biosynthesis enzymes, are downstream targets of the NIN/NF-YA1/STY-dependent regulatory cascade.

The long-term objective of this work is to make significant contributions to our understanding of mechanisms by which nodule formation is achieved. This is expected to resolve at least part of the puzzle, as associated with the ability of legumes and some non-leguminous plants to host nitrogen-fixing bacteria.

CHAPTER 2

MATERIALS AND METHODS

2.1 Seed germination and plant materials

Lotus japonicus ecotype Gifu was used in all experiments (Handberg and Stougaard, 1992). Seeds were scarified using sand paper, followed by two consecutive one-minute washes with 0.1% (w/v) sodium dodecyl sulfate (SDS) in 70% (v/v) ethanol and 0.1% (w/v) SDS in 20% (v/v) bleach. The seeds were then rinsed with sterile Milli-Q water ten times and incubated overnight in sterile water to imbibe. They were transferred to Petri dishes containing six layers of sterilized filter paper (Fisher #09-801A) moistened with sterilized Milli-Q water and allowed to germinate for 7 days at 23° C, under 16/8 hour light/dark regime. Unless otherwise specified, seedlings were transferred to pots containing a 6:1 mixture of vermiculite and sand that was soaked with a 1x B&D nutrient solution (Broughton and Dilworth, 1971), containing 0.5mM KNO_3 and grown under sterile conditions as follows: 16/8 hours day/night at 23/18 °C with humidity of 70%.

For analysis of non-symbiotic plant root and shoot phenotypes, un-inoculated *L. japonicus* wild-type and mutant seedlings were transferred to pots containing a mixture of vermiculite and sand (6:1) that was supplemented with B&D solution containing 1mM KNO_3. Plants were harvested and analyzed at various time-points after sowing.

2.2 Assessment of plant phenotypes

Wild type and mutant *L. japonicus* seedlings were grown under sterile conditions and were inoculated 7 days after sowing using wild-type *Mesorhizobium loti* strain NZP2235 or the same *M. loti* strain carrying the *hemA::LacZ* reporter cassette. The latter guided the visualization and scoring of bacterial infection and early nodule primordia formation via histochemical root staining for β-galactosidase activity (Wopereis et al., 2000). Briefly,

wild-type and mutant roots were collected at various time-points upon inoculation (7 and 21 days) and were vacuum infiltrated for 15 minutes with a fixative solution (1.25% v/v glutaraldehyde solution buffered with 0.2 M sodium cacodylate pH 7.2) and incubated in the same buffer for an additional 1 hour. The fixed roots were rinsed twice with 0.2M sodium cacodylate, pH 7.2, for 15 min and stained for β-galactosidase activity for 16 hours at room temperature using a solution containing sodium cacodylate (0.17M , pH 7.2), $K_3[Fe(CN)_6]$ (5.3mM), $K_3[Fe(CN)_6]$ (5.3mM), and 5-bromo-4-chloro-3-indolyl-D-galactoside substrate (X-Gal, PhytoTechnology Laboratories, USA; 0.085% w/v). The following day, stained roots were rinsed successively with 0.2M sodium cacodylate buffer (pH 7.2; 3 times for 10 min), distilled water (2 times for 5 min), and cleared using the protocol described by (Malamy and Benfey, 1997). This involved the following steps: (1) incubation in solution containing 0.24 M HCl in 20% (v/v) methanol for 15 minutes at 57°C, (2) incubation in a 7% (w/v) NaOH solution in 60% (v/v) ethanol for an additional 15 minutes at room temperature; (3) gradual re-hydration of the roots using an aqueous (v/v) ethanol series of 40%, 20% and 10%, incubating for 5 minutes at each step. Finally, the root specimens were vacuum infiltrated for 15 minutes with a 25% (v/v) glycerol solution containing 5% (v/v) ethanol and mounted on standard, glass microscope slides (Ultident Scientific Inc., Canada) using 50% (v/v) glycerol.

2.3 Identification of *sty* and *yucca* mutant lines and development of higher order mutants

The *sty* and *yucca* mutant lines were identified using the *L. japonicus* LORE1 retrotransposon insertion lines collection at Aarhus University in Denmark

(https://lotus.au.dk/; Mun *et al*., 2016). These are listed in Table 2.1. For all the selected LORE1 insertion lines, the corresponding seeds were received through the Lotus Base (https://lotus.au.dk/). They were germinated and the resulting plants were genotyped using the gene and LORE1 specific primers (Appendix A and Appendix B), following the established procedure (Urbanski et al., 2012).

For the *STY3* locus, nine additional mutant alleles (Table 2.2), called *sty3-1* to *sty3-9,* were identified using the *L. japonicus* TILLING (Targeting Induced Local Lesions In Genomes) resource at the John Innes Centre (RevGenUK; https://www.jic.ac.uk/technologies/genomic-services/revgenuk-tilling-reverse-genetics/; (Perry et al., 2009) . Two alleles, *sty3-1* and *sty3-9*, carried nucleotide changes that resulted in predicted premature translation termination codons and these were analyzed further. The seeds for the two TILLING lines were obtained from RevGenUK. To identify homozygous plants, genotyping was carried out using derived cleavage amplified polymorphic sequence (dCAPS) markers for both alleles, and subsequently confirmed by sequencing of the relevant genomic regions. Both genotyping and sequencing primers used for *sty3-1* and *sty3-9* are listed in Appendix A.

The double mutant lines were developed by performing genetic crosses between selected homozygous single mutants, using manual pollination. The F1 plants were allowed to self fertilize to produce segregating F2 populations and homozygous double mutants were selected using the corresponding genotyping primers (Appendix A). The *sty1-2 sty2-1 sty3-9* triple mutant was developed by crossing homozygous *sty1-2 sty2-1* with *sty2-1 sty3-9*. The triple mutant was selected from the resulting F2 population. The F3 progeny derived

from the confirmed, homozygous double and triple mutant lines were utilized for subsequent phenotypic analyses.

2.4 Electrophoretic Mobility Shift Assay

For the Electrophoretic Mobility Shift Assay (EMSA) a C-terminal portion of the *NF-YA1* mRNA encompassing the DNA binding (DB) domain (i.e. amino acid residues 184 to 332) was amplified using the *NF-YA1*_DB-F and *NF-YA1*_DB-R primers (Hossain et al., 2016). Restriction enzyme recognition sites for HindIII and BglII, along with three random nucleotides, were introduced at 5'-ends of forward and reverse primers, respectively, in order to aid cloning into the pT7-FLAG-2 expression vector (Sigma-Aldrich, Canada). The integrity of the resulting *NF-YA1DB-FLAG* expression plasmid was confirmed by sequencing. To generate the *nf-ya1-2* version of the same construct, a site-directed mutagenesis was carried out using the *NF-YA1DB-FLAG* (above) as the template and the 5'-phosphorylated forward (5'-AAGGGGATGTGGTG***A***TCGGTTCTTGAACA-3') and reverse (5'-GGCCGGCGCATTGCATGTAGATGGC-3') primers. The resulting vector was sequenced to confirm the presence of the *nf-ya1-2* mutation (i.e. A to G substitution, as shown in bold and italics in the forward primer above). The recombinant NF-YA1 and NF-YA1G^{213D} DB domains with C-terminal FLAG tag were produced and purified using ANTI-FLAG M2 Affinity Gel (Sigma-Aldrich, Canada), following the manufacturer's instructions.

EMSA assays were carried out using the LightShift Chemiluminescent EMSA kit (ThermoFisher, USA). For *STY1*, the region spanning nucleotide positions from -1615 to +88 (where +1 reflects A in the predicted ATG translation initiation codon) was amplified

as three overlapping fragments (-1615 to -1079, -1101 to -539 and -558 to +88). These fragments were biotin end-labeled using the Biotin 3' End DNA Labeling Kit (ThermoFisher, USA) and tested for the binding of NF-YA1DBFLAG in vitro. The middle fragment, -1101 to -539, which showed binding, was subsequently divided into three additional sub-fragments, with only the -953 to -729 region demonstrating the specific binding activity. The same -953 to -729 *STY1* promoter fragment was used to test for the binding activity of the mutant, NF-YA1DBG^{213D}-FLAG. A similar procedure was used to select the *STY2* (-357 to -104) and *STY3* (-293 to -82) promoter fragments, which were specifically recognized by NF-YA1DB-FLAG *in vitro*. The corresponding non-labeled promoter fragments were used as cold competitors.

2.5 Development of STY3::SRDX dominant negative constructs

As described in (Hossain et al., 2016), the *UBIQUITIN* promoter (Maekawa et al., 2008) was synthesized by Bio Basic Inc (Canada), with attL1 and attR5 recombination sites at its 5' and 3' ends, respectively. A fragment, containing a cDNA fragment encompassing the entire *STY3* coding region (gene ID Lj2g3v1728900.1, www.kazusa.or.jp/lotus/), translationally fused with the 36-bp sequence for the ERF-associated amphiphilic repression domain (superman repression domain X, called SRDX) (Hiratsu et al., 2003), and the attL5 and attL2 recombination sites at the 5' and 3' ends, respectively, was also prepared by gene synthesis (Bio Basic Inc., Canada). These two synthetic fragments were recombined directly into the pKGWD,0 destination vector (Karimi et al., 2002) (https://gateway.psb.ugent.be/), which has a green fluorescent protein

(GFP) marker in the T-DNA region, using MultiSite Gateway technology (Invitrogen, USA), giving rise to the *UBI$_{Pro}$:STY3::SRDX* vector.

Another DNA fragment encompassing the *L. japonicus NF-YA1* promoter (position -3045 to -1, where -1 denotes the first base upstream from the predicted ATG initiation codon; gene ID Lj5g3v0841080.1; www.kazusa.or.jp/lotus/) transcriptionally linked to the *STY3::SRDX* coding region and followed by the *NF-YA1* 3'UTR, was synthesized with attL1 and attL2 sites (Bio Basic Inc., Canada). This DNA fragment was recombined directly into the pKGWD,0 destination vector (Karimi et al., 2002) (https://gateway.psb.ugent.be/), giving rise to *NF-YA1$_{Pro}$:STY3::SRDX:NFYA1-3'UTR* vector.

2.6 Hairy root transformation and fully transgenic *L. japonicus* lines

After validation by sequencing, the *UBI$_{Pro}$:STY3::SRDX* and *NF-YA1$_{Pro}$:STY3::SRDX:NFYA1-3'UTR* vectors were transformed separately into *Agrobacterium rhizogenes* strain AR1193 and *Agrobacterium tumefaciens* strain LBA4404 via electroporation. Empty pKGWD,0 vector was used in parallel, as a negative control.

Transgenic hairy roots on non-transgenic *Lotus japonicus* shoots were generated following the previously established procedure (Lombari et al., 2005; Murray et al., 2007). Briefly, wild-type *L. japonicus* seeds were sterilized and germinated for 4 days in the dark at room temperature, on Petri dishes containing ½ x Gamborg B5 Basal medium (pH 5.6) with 1% (w/v) phytagel, in order to stimulate hypocotyl growth. *A. rhizogenes* strains carrying either the empty vector or the same vector containing one of the two *STY3::SRDX* constructs were grown for 2 days at 28°C on solid LB plates containing rifampicin

(100µg/ml), histidine (50µg/ml), spectinomycin (100µg/ml), and streptomycin (20µg/ml). On the fourth day after germination, the elongated hypocotyls were inoculated with the appropriate *A. rhizogenens* strain by poking three times with the 28G needle of a sterile 0.5cc hypodermic syringe (Becton Dickinson and Company, USA) that was dipped into the *Agrobacterium* streak. The remaining bacteria on the needle were spread over the punctured hypocotyl region and plates with wounded plants were re-sealed using surgical tape and put back in the dark at room temperature for overnight incubation. The following day, the plates were moved to a tissue culture incubator for 1-2 weeks (23°C; 16h day/8h night). Hairy roots began to appear approximately 7-10 days post inoculation, first as localized tissue swellings (calluses) and subsequently as small root protrusions. At this stage, the original roots were removed at the hypocotyl/root junction. The rootless shoots with emerging hairy roots were transferred to liquid ½ x B5 medium containing 2% (w/v) sucrose and 300 µg/ml of cefotaxime in order to promote hairy root growth and to kill *Agrobacterium*. After two weeks of incubation, the composite plants were transferred to pots containing sterile vermiculite and sand mixture (6:1) moistened with B&D solution and inoculated seven days later with *M. loti*. Symbiotic phenotypes were evaluated 21 dai with *M. loti* by scoring all nodulation events on GFP-fluorescing hairy roots.

Fully transgenic *L. japonicus* plants were generated following the previously described hypocotyl transformation procedure (Lombari et al., 2005). The primary transgenic T0 plants were allowed to self and the resulting T1 populations were genotyped for the presence of the *pNF-YA1:STY3::SRDX* transgene (Appendix A) and evaluated for the associated nodulation phenotypes. The transgene containing non-nodulating T1 plants are currently being grown to produce T2 progeny in order to identify true-breeding,

homozygous T1 plants. The T2 progeny of these plants will be used to generate plant material for next-generation RNA sequencing experiments.

For gene expression analysis (qRT-PCR; section 2.7) of the primary transformants, T0 plants STY3::SRDX5 and STY3::SRDX6 were propagated by cuttings, as follows; briefly, shoot tip segments of approximately 4 cm in length were cut from branches of T0 plants, along with control wild-type plants, and set into vermiculite-sand (6:1) mixture soaked in B&D solution, where they were grown for 14 days under sterile conditions.

2.7 Gene expression analysis using quantitative RT-PCR

L. japonicus ecotype 'Gifu' wild-type and mutant *L. japonicus* seedlings were sown into vermiculite-sand and grown for 7 days, under sterile conditions as described above, while transplanted cuttings of primary T0 transgenic and similarly treated wild-type control plants were grown for 14 days. Control un-inoculated plants were harvested at this time, while the remainder were inoculated with *M. loti* strain NZP2235. Plants were harvested at various time-points after inoculation (4, 7, 12 or 21 days). Immediately upon harvest 5-10 roots (depending on the age of the plants) constituting a single biological replicate, were cut from the adjoining shoots and transferred to a single 2 ml Safe-Lock tube (Eppendorf, Germany) containing a 5mm stainless steel bead (Qiagen, USA), which was flash frozen in liquid nitrogen. Frozen root samples were ground to a fine powder using a Retsch bead mill (Retsch, Germany) and total RNA was extracted using the Plant/Fungi Total RNA Purification Kit (Norgen Biotek, Canada) according to manufacturer's instructions. Following treatment with TURBO DNase (Invitrogen, USA), the concentration and purity of RNA were determined using the QIAxpert (Qiagen, USA) and the integrity was

confirmed by running a 400ng aliquot on an agarose gel. cDNA was prepared from 1µg of total RNA using the SuperScript IV VILO Master Mix (Invitrogen, USA). Negative control reactions, to which no reverse transcriptase was added (-RT), were included for each RNA sample. Quantitative RT-PCR reactions were performed in triplicates (i.e. three biological and three technical replicates) on a CFX-384 Real-Time PCR Detection System (BioRad) using SensiFAST™ SYBR No-ROX Kit (Bioline, Canada). qRT-PCR was carried out using the following conditions: 95°C for 2 min, followed by 45 cycles of 95°C for 5 s and 60°C for 30 s, depending on a given primer set. The expression levels were normalized against three reference genes, UBQ, PP2A, and ATPs (Tirichine et al., 2007). The list of primers used is given in Appendix A and Appendix B.

2.8 Gene expression analysis using GUS histochemical assay

Depending on the genomic sequence availability, fragments encompassing the *STY1* to *STY9* promoter regions, ranging in size from 2.5 to 4.0 kb, were prepared by gene synthesis (Bio Basic Inc., Canada). These were recombined in the pKGWFS7 destination vector containing a GFP/GUS reporter fusion (Karimi et al., 2002); (https://gateway.psb.ugent.be/) using GatewayTM technology (Invitrogen, USA). The TAC/BAC clones, LjT09B24 (TM2451) and LjB04P03 (BM2658), were used to amplify the promoter regions of *YUCCA1* (position -2466 to -1) and *YUCCA11* (position -2249 to -1), respectively, where -1 denotes the first base upstream from the predicted ATG initiation codon. This was done using the conditions: 98°C for 30 s, followed by 30 cycles of 98°C for 5 s and 55°C for 30 s and 72°C for 90 s with final elongation step at 72°C for 5 min, and the primers as listed in Appendix B. The resulting promoter fragments were

directionally cloned into the pENTR/D-TOPO vector (Invitrogen, USA) and subsequently recombined in the pKGWFS7 destination vector (Karimi et al., 2002); (https://gateway.psb.ugent.be/). After validation by sequencing, the constructs were transformed into *A. rhizogenes* strain *AR1193*, which was used for hairy root transformation, as described above. At least ten independent hairy root systems were generated for each construct and these were analyzed for the GUS reporter activity.

2.9 GUS staining procedure

For histochemical staining, roots and nodules collected at various time-points were analyzed. Detection of the GUS reporter activity was conducted using a staining solution containing 0.1M potassium phosphate buffer, 5mM EDTA, 0.5mM potassium ferric- and ferrous-cyanides, 20% (v/v) methanol and 0.5mg/ml 5-bromo-4-chloro-3-indolyl glucuronide cyclohexyl ammonium salt (X-GLUC; Inalco, Italy). All tissues were vacuum-infiltrated for 15 min and stained overnight at either 37°C or room temperature. After overnight incubation, the roots were rinsed successively with 0.2M sodium cacodylate buffer (pH 7.2; 3 times for 10 min), distilled water (2 times for 5 min) and were cleared following the protocol described above in section 2.2.

2.10 RNA sequencing

L. japonicus wild-type Gifu root samples were scarified, germinated, and grown as described in section 2.1. Root samples were harvested 4 dai with *M. loti* and also from the corresponding un-inoculated plants of the same age. Three independent biological replicates per treatment were collected. Total RNA was extracted using the Plant/Fungi

Total RNA Purification Kit (Norgen Biotek, Canada) and its quality was checked on an Agilent Bioanalyzer 2100 RNA Nano chip following the manufacturer's instructions (Agilent Technologies, USA). The RNA library was constructed and sequenced at the Center for Applied Genomics at Sick Kids Hospital in Toronto (Canada) using Illumina Hi-Seq 2500 paired-end reads. The bioinformatics analysis to identify differentially expressed genes was performed through a collaboration with Drs. Terry Mun, Stig U. Andersen and Jens Stougaard at Aarhus University in Denmark.

2.11 Microscopy

All microscopic observations were performed using either Nikon Eclipse Ni upright or the Nikon SMZ25 stereo microscopes (Nikon, Japan). Both microscopes were integrated with a DsRi2 digital camera (Nikon, Japan). The Nikon Eclipse Ni microscope was fitted with 4, 10, 20, 40, and 100X objectives, while the magnification for the NikonSMZ25 scope varied between 3.15x and 78.75x. All images captured were taken in a TIFF format and were subsequently processed using Adobe Photoshop CS6. The nodulation events on GFP-fluorescing hairy roots were counted under a Leica MZFLIII fluorescence stereomicroscope (Leica Microsystems Inc., USA).

2.12 Statistical analyses

Statistical analyses were performed using Microsoft Excel spreadsheet software. Pair-wise comparisons were made using a Student's t-test with either equal or unequal variance based on the result of an F-test. Significant differences between means for three or more data sets were calculated using the one-way analysis of variance (ANOVA) followed by a

post-hoc test. Unless otherwise stated, variance shown represents the 95% confidence intervals of the mean.

2.13 Phylogenetic analyses

The protein sequences were aligned with ClustalW and the tree was generated using MEGA 7 (Molecular Evolutionary Genetics Analysis) software and the neighbor-joining method with bootstrap replicates of 1000.

2.14 BLAST analyses

The Blast Local Alignment Sequence Tool (BLAST) was used for comparison of predicted STY and YUCCA protein sequences using the default parameters, as provided at (http://www.ncbi.nlm.nih.gov/).

Table 2.1 A list of *L. japonicus sty* and *yucca* LORE1 insertion lines and names of the corresponding mutant alleles

Plant ID	Mutant allele	Plant ID	Mutant allele
30052423	*sty1-1*	30092737	*sty7-4*
30032212	*sty1-2*	30097763	*sty7-5*
P1687	*sty2-1*	30088537	*sty8-1*
30010699	*sty3-10*	30089290	*sty8-2*
30083039	*sty4-1*	30109651	*sty8-3*
30007756	*sty4-2*	30034946	*sty9-1*
30115636	*sty5-1*	30109475	*sty9-2*
30120414	*sty5-2*	30058721	*sty9-3*
30089004	*sty5-3*	30120352	*yucca1-1*
30136178	*sty6-1*	L8288	*yucca1-2*
30060832	*sty7-1*	30050160	*yucca11-1*
30074305	*sty7-2*	30086558	*yucca11-2*
30084924	*sty7-3*	30057384	*yucca11-3*

Table 2.2 *sty3* mutant alleles identified by TILLING approach

Plant ID	Mutant allele	Mutation (gDNA)	Mutation (Amino acid)
SL0946-1	*sty3-1a*	C_{1934} - T	Q_{63} - STOP
SL5263-1	*sty3-1b*	C_{1934} - T	Q_{63} - STOP
SL1150-1	*sty3-2*	G_{2070} - A	G_{108} - E
SL4187-1	*sty3-3*	G_{2073} - A	G_{109} - E
SL0070-1	*sty3-4*	G_{2081} - A	A_{112} - T
SL4855-1	*sty3-5a*	C_{2082} - T	$A_{11}2$ - V
SL5707-1	*sty3-5b*	C_{2082} - T	A_{112} - V
SL4170-1	*sty3-6*	G_{2211} - A	R_{155} - H
SL1418-1	*sty3-7*	G_{2214} - A	R_{156} - H
SL0174-1	*sty3-8*	G_{2216} - A	E_{157} - K
SL0541-1	*sty3-9*	C_{2240} - T	Q_{165} - STOP

CHAPTER 3

RESULTS

3.1 *STY1*, *STY2* and *STY3* are likely direct targets of NF-YA1

To confirm the microarray data, quantitative reverse transcription-polymerase chain reaction (qRT-PCR) experiments were carried out, targeting the three *SHI*/*STY* genes. Both, control un-inoculated roots and the equivalent root samples collected at 4 dai with *M. loti* were analyzed in *L. japonicus* wild type and the *nf-ya1-2* mutant (Figure 3.1). In the control roots, steady-state levels of *STY1* and *STY2* mRNAs were at or below the detection limit, while *STY3* mRNA was detectable, albeit at a relatively low level, and this was similar between the two genotypes tested. The levels of the three *STY* mRNAs were significantly upregulated upon *M. loti* infection in wild type but not in *nf-ya1-2* mutant roots, which confirmed the microarray data (Figure 3.1).

These confirmatory observations were followed by testing whether NF-YA1 protein could directly interact with *STY1*, *STY2* and *STY3* promotors *in vitro*. The electrophoretic mobility shift assay (EMSA) was used for this purpose (Figure 3.2).

EMSA, also known as a gel retardation assay, is a commonly used affinity electrophoresis technique for studying protein-DNA or protein-RNA interactions. It can determine whether a given protein or protein mixture binds to a DNA or RNA sequence, *in vitro* (Fried, 1989). In the case of NF-YA1, such an interaction was expected if the corresponding *SHI*/*STY* promoters indeed constitute its direct targets.

Recombinant protein fragments encompassing either the DNA-binding (DB) domain of the wild-type *L. japonicus* NF-YA1 (NF-YA1^{DB}) or its mutant NF-YA1^{DBG213D} version, carrying the glycine (G) to aspartic acid (D) substitution at the amino-acid position 213, were prepared as FLAG-tags and used for testing. The substitution was engineered to

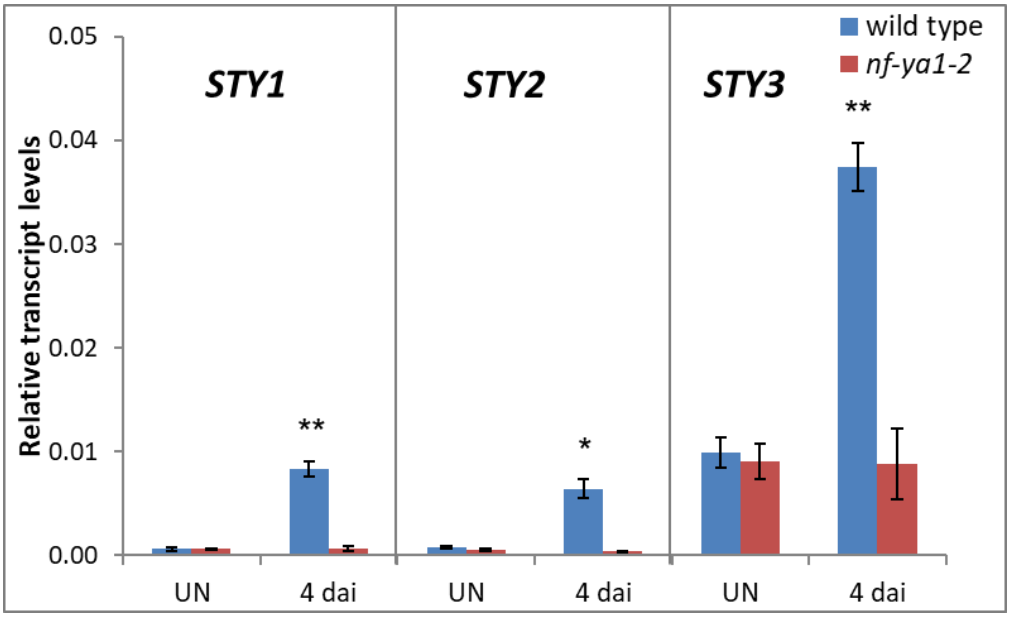

Figure 3.1 *NF-YA1* mediates *STY1*, *STY2* and *STY3* gene expression during nodule development. Quantitative reverse transcription-polymerase chain reaction (qRT-PCR) analysis of the steady-state levels of *STY1*, *STY2*, and *STY3* mRNAs in *Lotus japonicus* wild type and *nf-ya1-2* mutant roots. UN, un-inoculated roots harvested 7 days after sowing; 4 dai, roots harvested 4 days after inoculation (dai) with *M. loti*. Average values for three biological replicates ± standard error are given. Asterisks indicate statistically significant differences. (*P ≤ 0.05; **P ≤ 0.01) in expression between wild type and the mutant, as determined using the Student's t test.

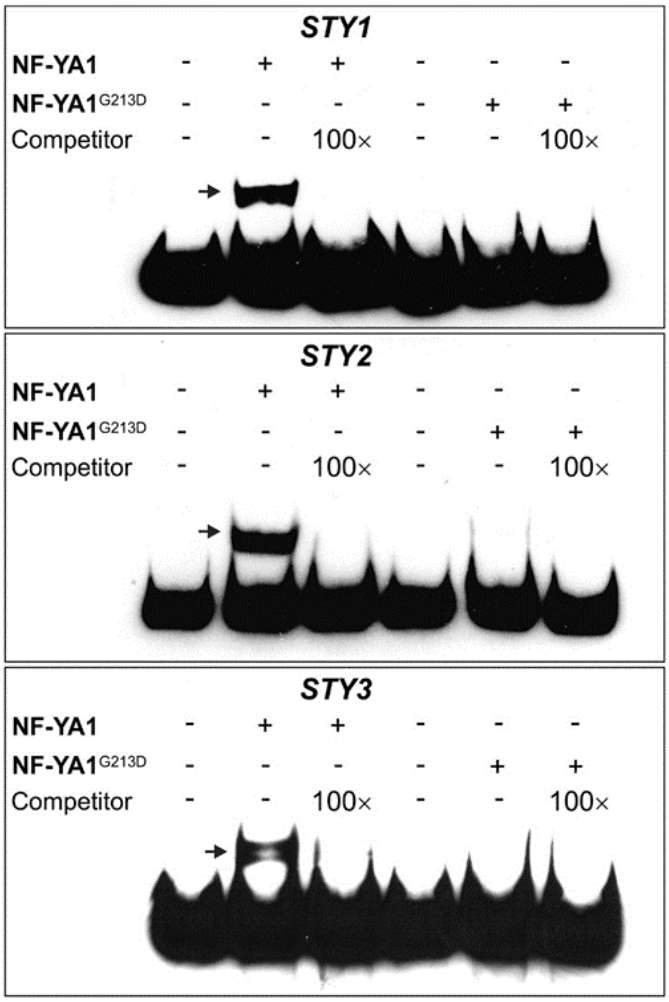

Figure 3.2 NF-YA1 binds to the promoters of *STY1*, *STY2*, and *STY3* in vitro. Electrophoretic mobility shift assays show specific binding of NF-YA1 to *STY* gene promoters *in vitro*. The migration of biotinylated *STY1*, *STY2*, and *STY3* promoter fragments in the absence (-) or the presence (+) of 1 µg of purified FLAG-NF-YA1 wild-type or FLAG-NF-YA1^{G213D} mutant DNA-binding domain is shown. Note that the latter represents the predicted amino acid change in the *nf-ya1-2* allele. The corresponding, non-labeled, wild-type probe in 100-fold molar excess (100×) relative to the biotinylated probes has been added as competitor. Arrows indicate the specific binding of the wild-type FLAG-NF-YA1 protein.

mimic the predicted effect of the *nf-ya1-2* mutation (Hossain et al., 2016). While NF-YA1^{DB} was able to specifically bind to promoters of the three *STY* genes *in vitro*, NF-YA1^{DBG213D} failed to do so (Figure. 3.2).

These *in vitro* data supported the notion that *STY1*, *STY2* and *STY3* constitute direct targets of the NF-YA1-dependent regulation upon *M. loti* infection. They also provided a plausible explanation for the defective symbiotic phenotype of *nf-ya1-2* by indicating that the resulting mutant NF-YA1-2 ^{DBG213D} protein, carrying an amino acid substitution within the DNA binding domain, is likely unable to bind to its *STY* gene targets. Given the defective symbiotic phenotype of *nf-ya1-2* (Hossain et al., 2016), *SHI*/*STY*s were considered as likely essential for root nodule formation, hence prompting their further detailed investigation.

3.2 The *L. japonicus SHI/STY* gene family comprises at least nine members

Using *STY1*, *STY2* and *STY3* DNA and the corresponding protein sequences as queries, non-redundant sequence collections at the NCBI server (https://www.ncbi.nlm.nih.gov/), the Lotus databases (www.kazusa.or.jp/lotus/ and https://lotus.au.dk/) were analyzed. Six additional *STY* genes were predicted, signifying the presence of at least nine members in the predicted *L. japonicus SHI/STY* gene family, which was based on the current, 3.0 version of the *L. japonicus* genome sequence release (http://www.kazusa.or.jp/lotus/index.html) (Figure 3.3).

Subsequently, a variety of on-line tools, including GenScan (www.genes.mit.edu/GENSCAN.html), Splign

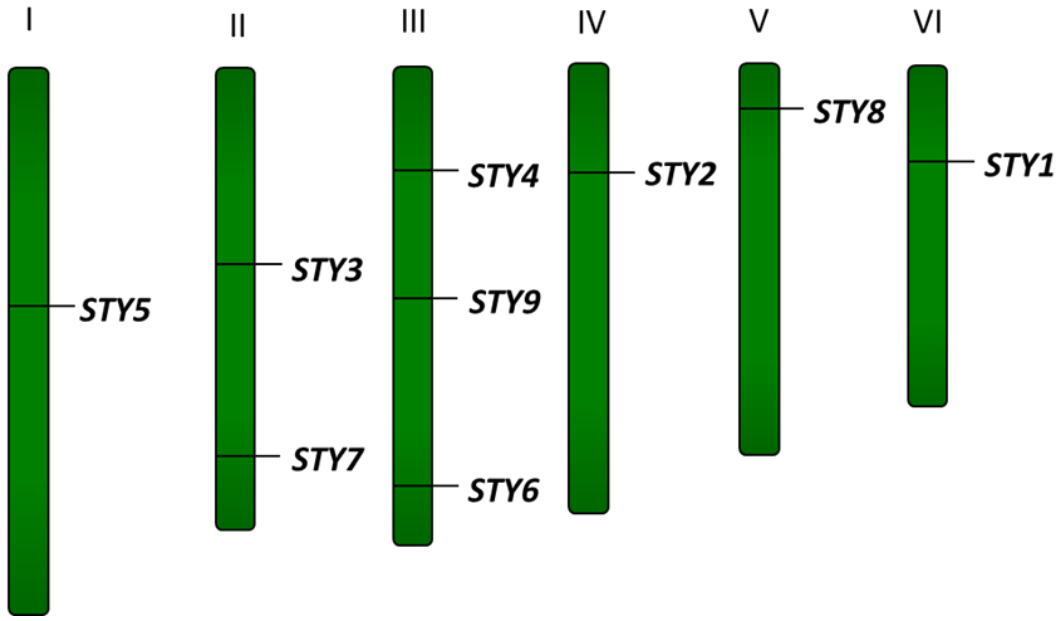

Figure 3.3 The *Lotus japonicus* genome contains at least nine *STY* genes. Approximate location of the *SHI/STY* genes on six *L. japonicus* chromosomes is shown.

(www.ncbi.nlm.nih.gov/sutils/splign/splign.cgi) and Open Reading Frame Finder (www.ncbi.nlm.nih.gov/orffinder/) were utilized to determine the exon/intron structures and predict the corresponding coding and protein sequences. These analyses showed that the *L. japonicus SHI/STY* genes encode predicted proteins ranging in size from 246 to 348 amino acids. In spite of a relatively low overall protein sequence similarity, they contained two conserved amino acid domains, namely the RING-type zinc finger (IPR001841) and the IGGH domains (Figure 3.4). The amino acid identity within the RING finger motif of the *L. japonicus SHI/STY* proteins ranges from 62 to 95% and in the IGGH domain from 40 to 81%.

The RING fingers of the *L. japonicus* SHI/STY proteins encompass circa 31 amino acid stretches that are cysteine (C)-rich and have the consensus sequence of C-X2-C-X7-C-X-HX2-C-X2-C-X7-C-X2-H, or C3HC3H (Figure 3.5). This is similar to the classical zinc-binding C3HC4 RING finger motif (Freemont, 1993; Lovering et al., 1993), which is known to mediate protein-protein interactions in numerous otherwise unrelated proteins in various eukaryotes (Borden, 2000). Immediately downstream of the RING domains, putative nuclear localization signals (NLS) were predicted to be present in *L. japonicus*

Further downstream, the IGGH domain is present (Figure 3.5B). This domain has no primary amino acid sequence similarity to any functionally characterized motifs and could be SHI/STY protein family specific. It is thought to partake in homo and/or heterodimerization between SHI/STY proteins (Eklund et al., 2010a).

The RING finger and IGGH domains are conserved in all known SHI/STY proteins including those from dicotyledonous plants, such as *L. japonicus*, *Arabidopsis thaliana, Nicotiana benthamiana,* and the basal eudicot, *Eschscholzia californica,*

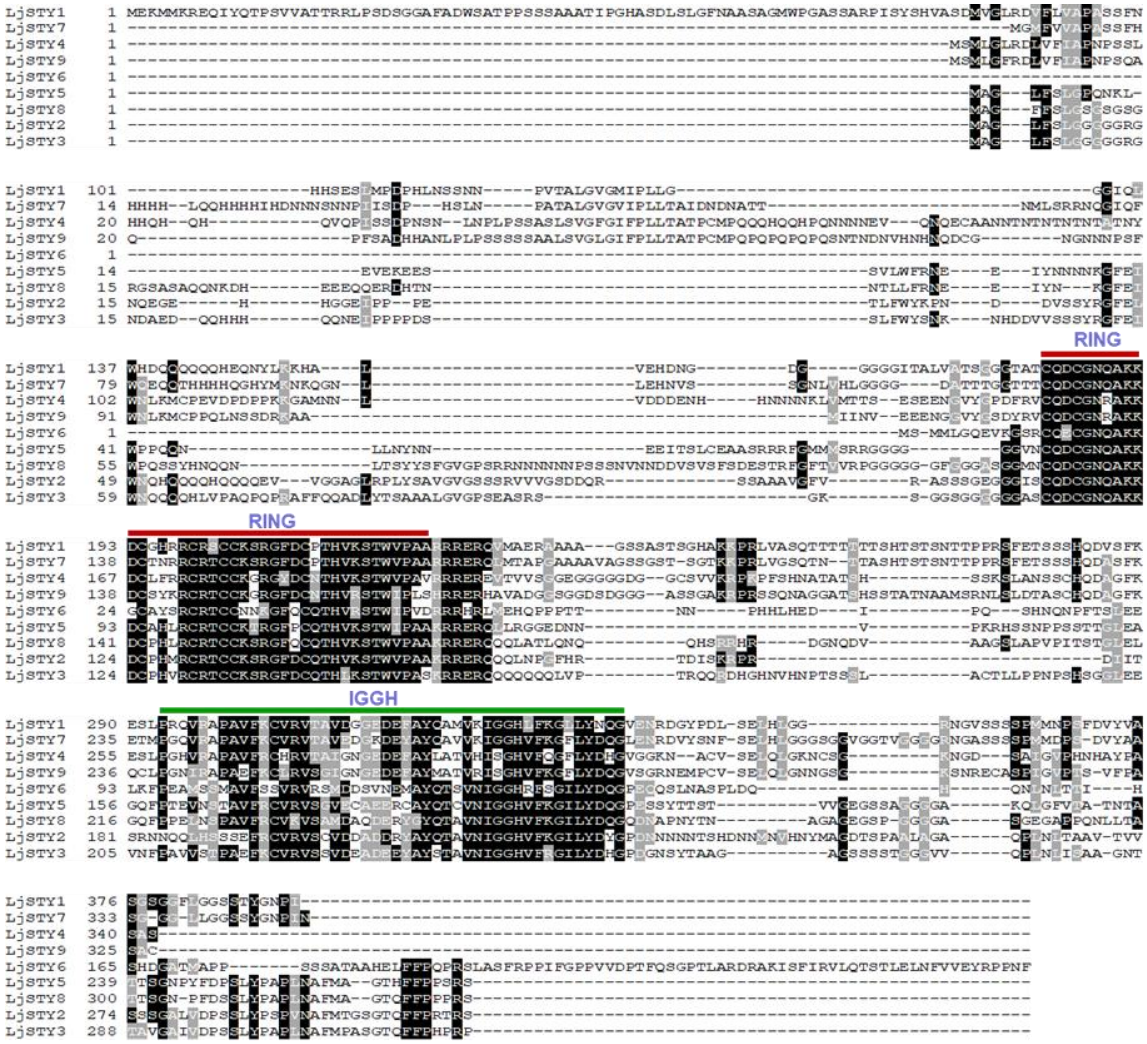

Figure 3.4 *SHI/STY* protein alignment. Nine STY proteins of *Lotus japonicus* were aligned using default settings in the Clustal Omega program. The BoxShade Server version 3.21 was used to generate the final output. A threshold of ≥ 60% conservation was used. Black shading indicates identical residues, whereas gray indicates presence of conservative substitutions. The following accession numbers refer to the protein sequences used: (1) *L. japonicus:* LjSTY1 (Lj6g3v0959410), LjSTY2 (Lj0g3v0059359), LjSTY3 (Lj2g3v1728900), LjSTY4 (Lj3g3v0766120), LjSTY5 (Lj1g3v2140900), LjSTY6 (Lj3g3v3376040), LjSTY7 (Lj2g3v3044220), LjSTY8 (Lj5g3v0155490), and LjSTY9 (Lj0g3v0258549)

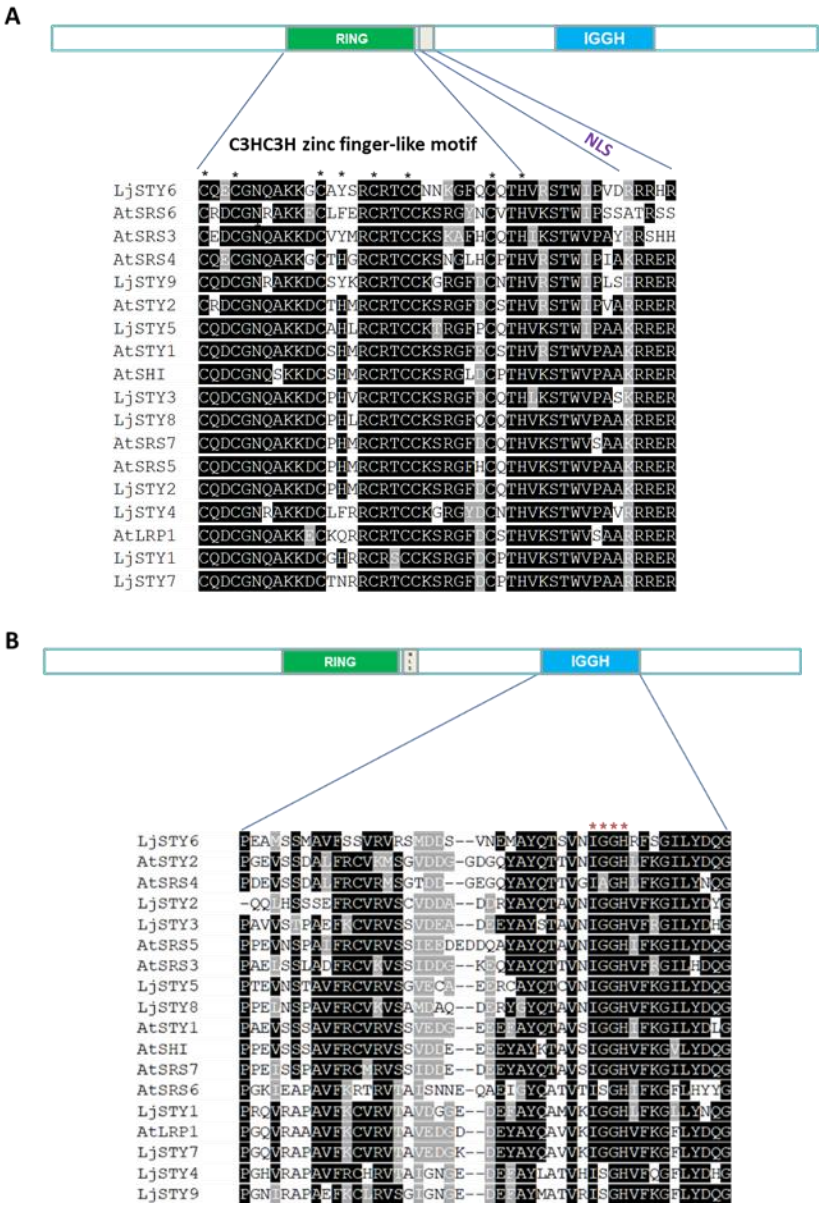

Figure 3.5 The predicted SHI/STY proteins share two conserved domains. Lotus japonicus STY proteins have two conserved domains namely, the putative RING zinc-finger domain (A) and the IGGH domain (B). The domain sequence alignments in A and B were generated using the Clustal Omega program with default settings. The BoxShade Server version 3.21 was used to generate the final output. A threshold of ≥ 60% conservation was used. Black shading indicates identical residues, whereas gray indicates presence of conservative substitutions. The corresponding domains of known *Arabidopsis thaliana* SHI/STY protein were used for comparison.

(Gomariz-Fernandez et al., 2017), and also in *Physcomitrella patens* (Eklund et al., 2010b).

Noteworthy, several *L. japonicus* SHI/STY proteins contain homo-polymeric stretches of glutamine (Q) residues, a feature described in association with the activation domains of various transcription regulators and shared with some of the *Arabidopsis* and the two *Physcomitrella* SHI/STY proteins (Kuusk et al., 2006; Eklund et al., 2010b). Other homo-polymeric regions, including those composed of glycine, histidine and/or asparagine residues were also apparent in some but not all *L. japonicus* SHI/STY proteins (Figure 3.4), but their functional significance is unknown.

3.3 Activities of *STY* promoters associate with root and nodule development

Having identified nine *L. japonicus STY* genes, follow-up experiments were performed to determine whether any other *STY*s, in addition to *STY1*, *STY2* and *STY3*, are relevant to root nodule formation. The association of their expression patterns with nodule development was used as the initial criterion and two parallel experiments, namely histochemical localization of promoter activities and quantification of mRNA levels were employed to assess the attribute.

The promoter-GUS reporter constructs (*LjSTY*$_{PRO}$:GUS), encompassing 2.5 to 4.0 kb regions upstream from the predicted ATG initiation codons, were developed for each of the nine *STY* genes (Figure 3.6) and their activities were tested in *Agrobacterium rhizogenes*-induced transgenic hairy roots formed on wild-type *L. japonicus* shoots.

All nine *STY* promoters were found to be active in hairy roots (Figure 3.7). The GUS reporter activity was found to associate with early lateral root primordia, including the

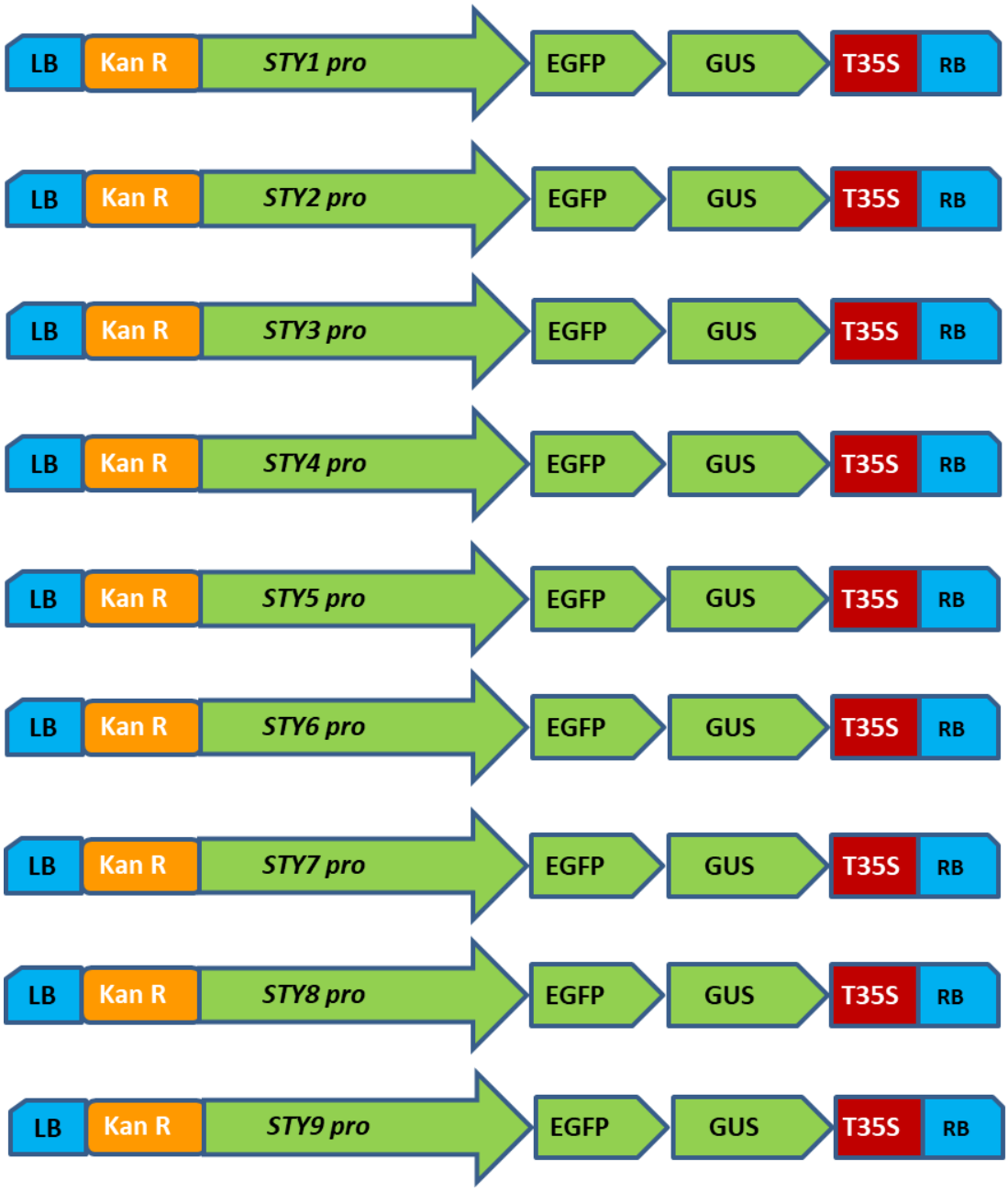

Figure 3.6 Schematics of constructs used to localize the *STY* gene promoter activities. LB: T-DNA left border; *STYpro*: DNA fragments for each of the nine *L. japonicus* STY genes spanning promoter regions of 2.5 kb or more immediately upstream of the predicted translational initiation (ATG) codons; Kan R: the kanamycin resistance gene; EGFP: gene encoding an enhanced green fluorescence protein; GUS: gene encoding the β-glucuronidase; T35S: CaMV 35S terminator sequence; RB: T-DNA right border.

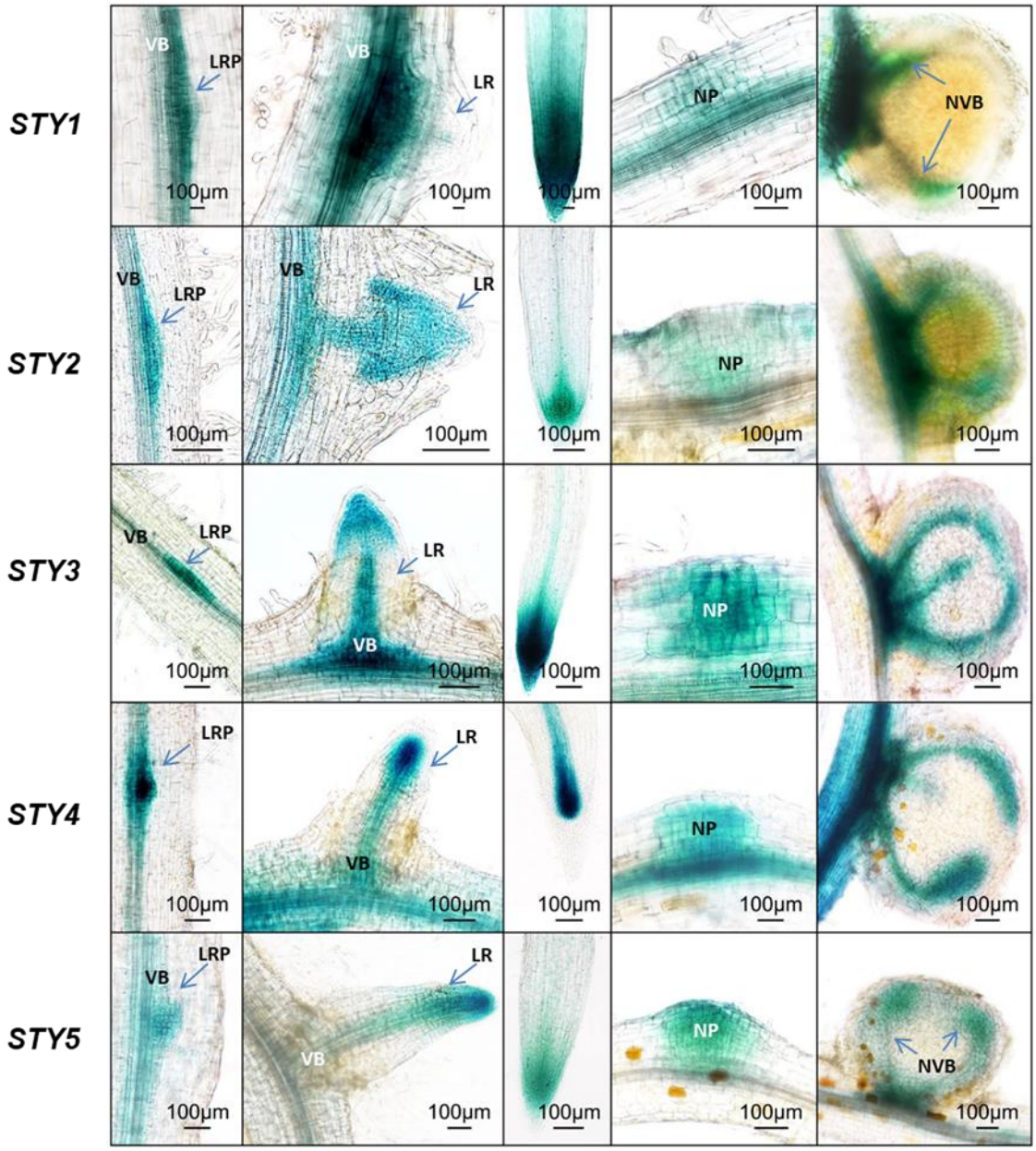

Figure 3.7 (see next page for the figure legend)

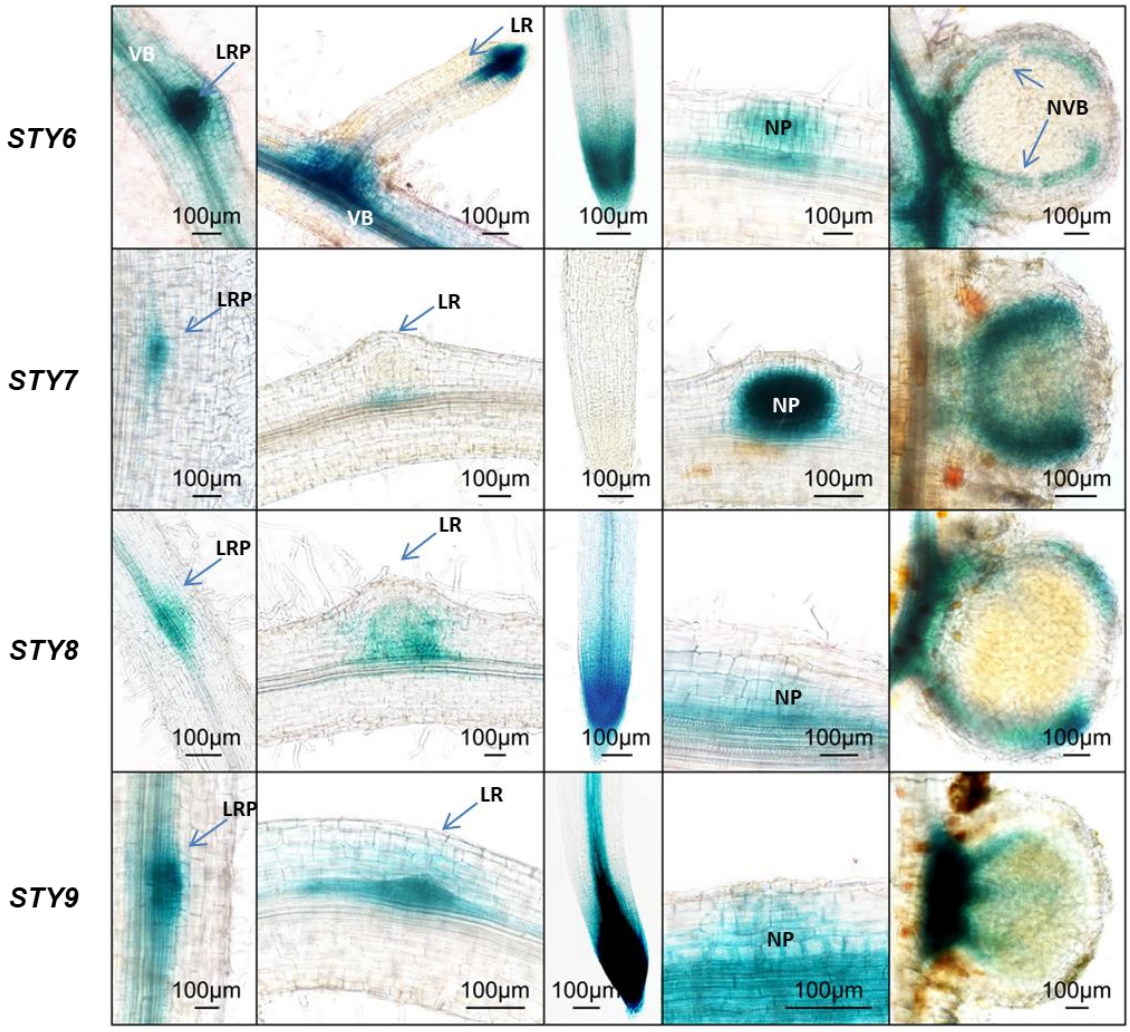

Figure 3.7 *L. japonicus STY* promoters are active during root and nodule development. Representative images of hairy-root segments showing activities of the *STY* promoters, as monitored using the GUS reporter (blue colour). Columns from left to right show the GUS activity as associated with small lateral root primordia (LRP), lateral roots (LR), root apical regions, nodule primordia (NP) and fully mature nodules. The specimens were collected 10-14 dai with *M. loti*. For each promoter:GUS construct, 5-10 individual plants were analysed. (NVB): nodule vascular bundle.

initial pericycle cell divisions. At more advanced stages, encompassing cortical cell divisions and emerging to fully emerged lateral roots, GUS activity was detectable in tissues of the central vasculature and in the root apices, with the latter persisting in the fully emerged lateral and main roots. These activity patterns were shared by most of the *STY* promoters, except *STY7*, for which GUS staining was only very weakly detectable at the base of the emerging lateral root and was not found in the root apices. Furthermore, GUS expression in the central, cylinder region of roots was variable, depending on a particular construct and also on a given developmental stage. It persisted in mature root vasculature for *STY1*, *STY3*, *STY4*, *STY8* and *STY9*, while appearing only transient for *STY2*, *STY5* and *STY6*. Remarkably, all nine *STY* promoters were active in dividing cortical cells of young nodule primordia and also later during development, in the vasculature of mature nodules (Figure 3.7). This was reminiscent of the *NF-YA1* promoter activity in developing *L. japonicus* nodules (Hossain et al., 2016), indicating the presence of overlapped expression domains for these two classes of regulatory genes.

3.4 The level of *STY* mRNAs is regulated during *L. japonicus* nodule development

To further characterize *STY* gene expression during the root nodule symbiosis, an *in-silico* analysis of next-generation RNA sequencing (RNAseq) data (P. Janakirama, and K. Szczyglowski, unpublished data) was carried out. Comparing transcriptomes of the control *L. japonicus* un-inoculated roots with equivalent (i.e. the same age) root samples collected 4 dai with *M. loti* showed that the steady-state levels of *STY1*, *STY2* and *STY3* mRNAs were significantly upregulated in the latter group (Table 3.1), which was consistent with

Gene ID	Gene name	log2FC	Fold change	P-value	FDR-value
Lj6g3v0959410	*STY1*	2.46	5.49	4.774E-15	3.72E-12
Lj0g3v0059359	*STY2*	2.69	6.45	7.994E-15	5.95E-12
Lj2g3v1728900	*STY3*	2.43	5.40	2.22E-16	2.02E-13
Lj3g3v0766120	*STY4*	-0.29	-1.23	0.4424	0.9999
Lj1g3v2140900	*STY5*	0.99	1.98	0.1216	0.9999
Lj3g3v3376040	*STY6*	-0.57	-1.48	0.5983	0.9999
Lj2g3v3044220	*STY7*	1.05	2.06	3.5E-07	6.58E-05
Lj5g3v0155490	*STY8*	1.43	2.69	0.0012	0.0675
Lj0g3v0258549	*STY9*	0.56	1.47	0.2544	0.9999

Table 3.1 Expression of four *L. japonicus STY* genes is significantly upregulated upon *M. loti* infection. Wild-type, un-inoculated roots and roots of the same age collected 4 dai with *M. loti* were analyzed using next-generation RNA sequencing. Of the nine *STY* genes, *STY1*, *STY2*, *STY3*, and *STY7* were found to be significantly (FDR<0.001) upregulated upon *M. loti* inoculation (highlighted in yellow) Log2FC: log2 fold change; Fold change: absolute fold change value; P-value: uncorrected P-value; FDR-value: false discover rate (corrected P value).

the qRT-PCR results (Figure 3. 1). In addition, the level of *STY7,* but not the remaining *STY* mRNAs, was also significantly upregulated in the inoculated roots at this relatively early stage during symbiosis (Table 3.1).

Considering that the histochemical data described above pointed to all nine *STY* promoters being active during nodule formation, additional analyses were warranted. Thus, the steady-state level of the nine *STY* mRNAs was further evaluated across various time-points. Wild-type roots collected at 4 , 7, 12 and 21 dai with *M. loti* and the control, 7-day-old un-inoculated roots, were comparatively analyzed (Figure 3.8). The equivalent total RNA samples derived from roots of *nf-ya1-2* were also included in these experiments in order to determine whether, like *STY1, STY2* and *STY3*, any of the remaining six *STY* genes is also regulated by *NF-YA1* upon *M. loti* infection.

Apart from *STY7,* all other *STY* mRNAs were found to be at relatively low steady-state levels in control, un-inoculated roots and this was genotype independent (Figure 3.8). At 4 dai, five *STY* mRNAs, namely *STY1*, *STY2*, *STY3*, *STY7,* and *STY8,* were significantly upregulated, above control levels, in wild-type roots. This upregulation was lost in *nf-ya1-2*, except for *STY7*, which showed only a partial dependency on *NF-YA1*. *STY7* was still upregulated by *M. loti* infection in *nf-ya1-2,* albeit to a slightly (yet significantly) lower level than in wild-type roots (Figures 3.8 and 3.9).

At 7 dai, levels of these five *STY* mRNAs were further enhanced and two additional *STY* mRNAs, *STY5* and *STY9,* were also significantly upregulated (Figures 3.8 and 3.9). Interestingly, while the latter two showed strict dependency on *NF-YA1*, the group of five initially upregulated *STY* mRNAs (i.e. *STY1*, *STY2*, *STY3*, *STY7* and *STY8*) displayed only a partial dependency at this particular stage after *M. loti* infection. This was evidenced by

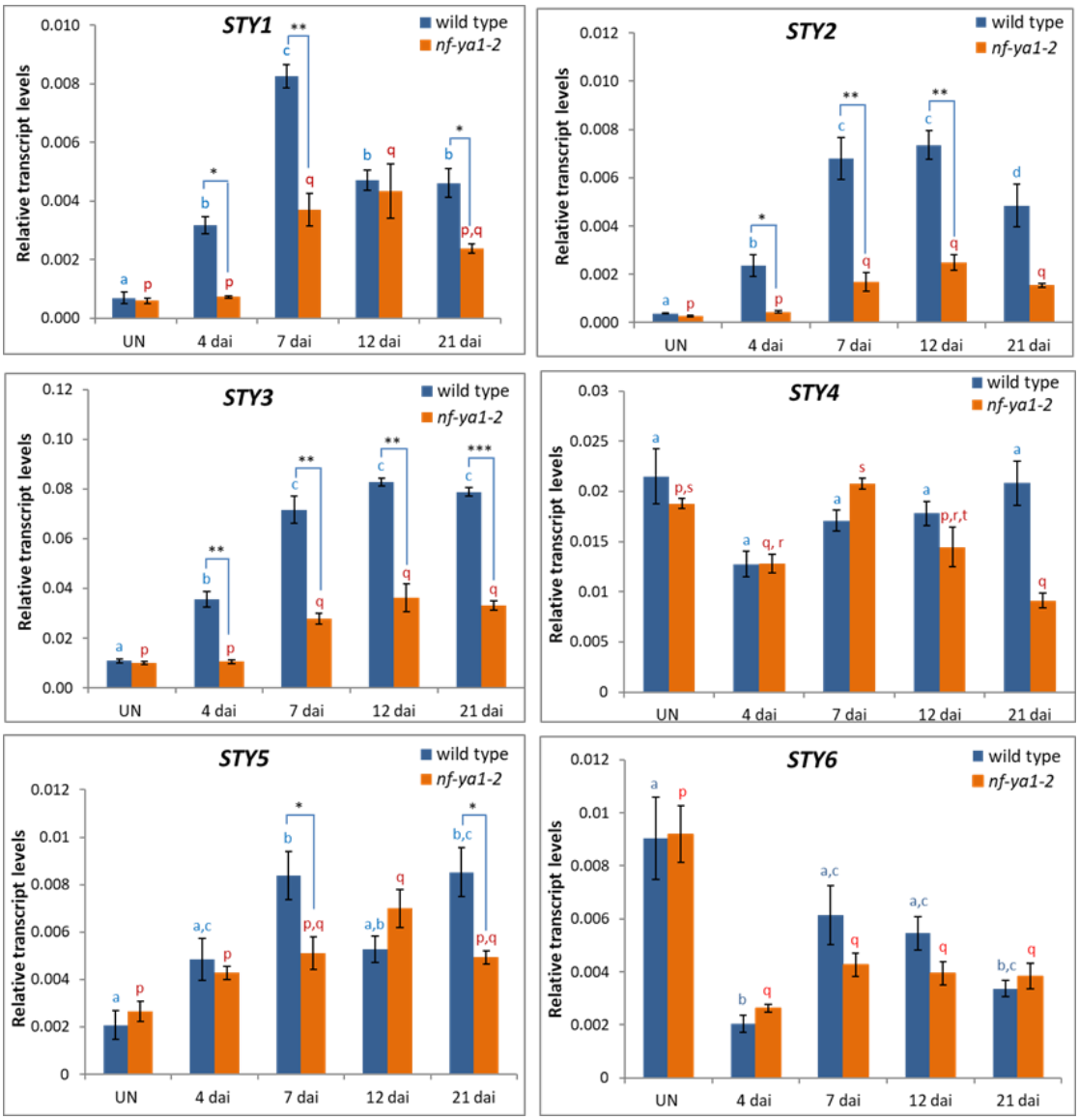

Figure 3.8 (see next page for the figure legend).

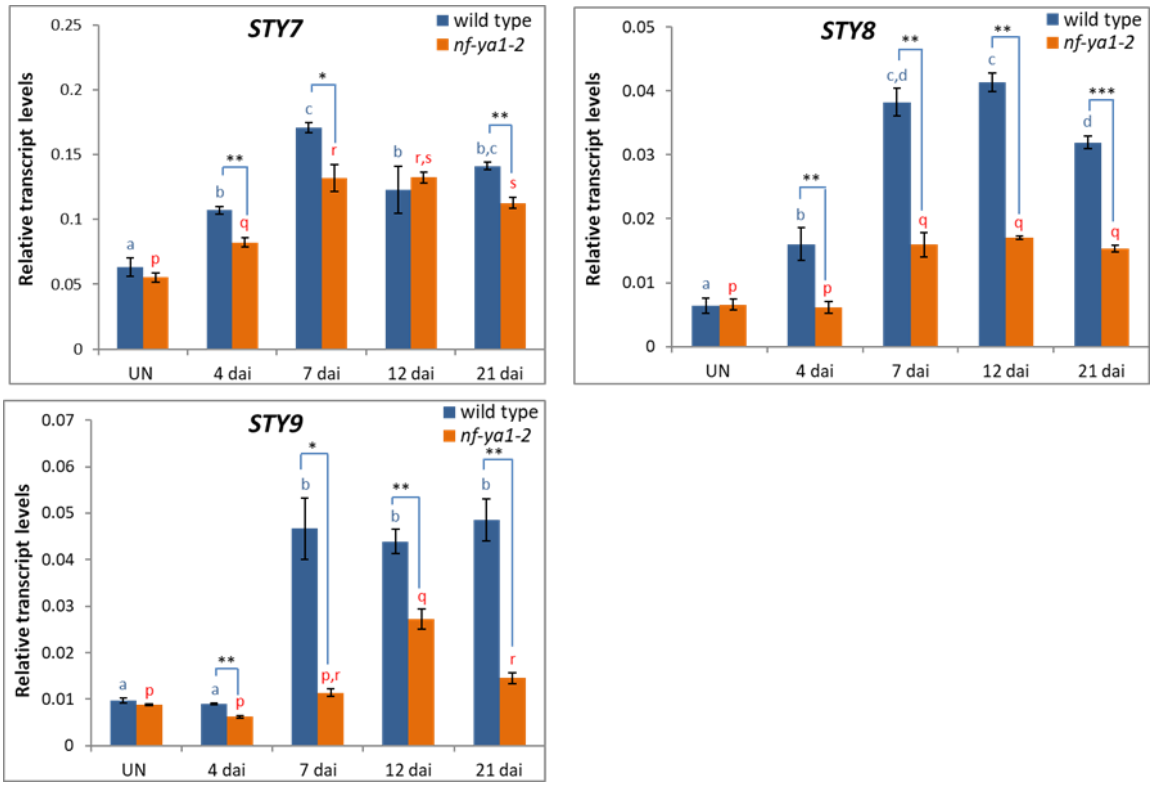

Figure 3.8 Expression of *STY* genes is regulated upon *M. loti* infection. Quantitative RT-PCR data showing steady-state levels of *STY* mRNAs in un-inoculated (UN) control roots of *L. japonicus* wild type (blue) and the *nf-ya1-2* mutant (orange) and in samples collected at various time-points (days) after inoculation (dai) with *M. loti*. The mean ± SE are given for three biological replicates. Statistical groupings across different time-points, reflected by the same letters, have been determined separately for each genotype using one-way ANOVA with the Tukey HSD post hoc test ($P<0.05$). The Student's t-test was used to carry out pair-wise comparisons between wild-type and *nf-ya1-2* at each time-point (*$P<0.05$; **$P<0.01$; *** $P < 0.001$).

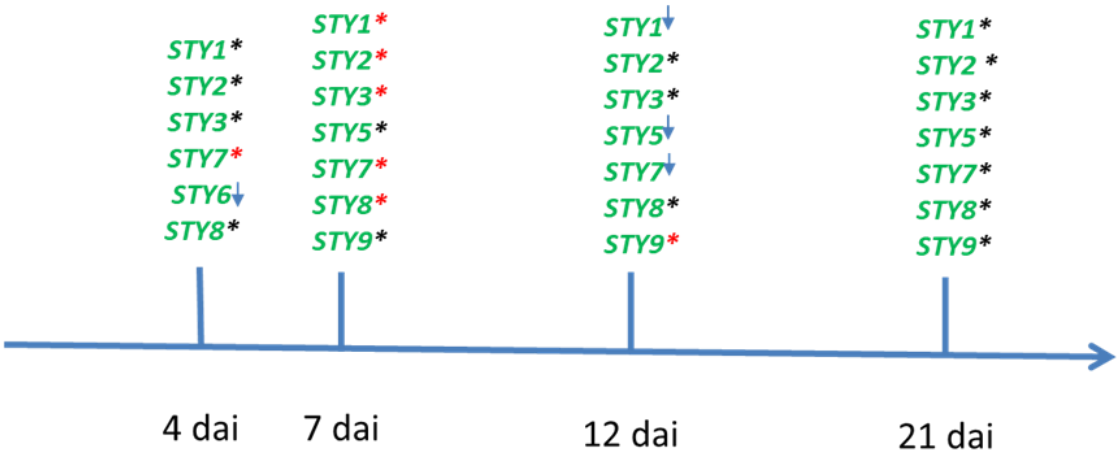

Figure 3.9 Summary of *STY* genes that responded to *M. loti* infection and the relative dependency of expression changes on presence of functional *NF-YA1*. dai: days after inoculation with *M. loti*. Black asterisks reflect complete dependency of regulation on presence of functional *NF-YA1*, while red asterisks indicate both *NF-YA1*-dependent and independent control of expression. Arrows indicate downregulated levels of a given mRNA.

upregulated levels of their mRNAs in *nf-ya1-2* also, although these were not as high as in wild-type roots (Figure 3.8). These observations suggested that in addition to *NF-YA1*, other regulators are likely to partake in mediating *STY* gene expression and this may be dependent on a particular developmental stage.

In comparison to un-inoculated roots, levels of all seven *STY* mRNAs described above were also significantly upregulated at subsequent 12 and 21 dai time-points (Figures 3.8 and 3.9). However, the corresponding expression patterns varied between different *STY*s and were loosely put into two categories. The first group included *STY3*, *STY7*, *STY8* and *STY9*, for which levels of mRNAs while significantly upregulated from the control roots remained more or less constant from 7 to 21 dai with *M. loti*. In contrast, *STY1*, *STY2* and *STY5* showed more dynamic, time point-dependent expression patterns, with either lowered mRNA levels at both (*STY1*) or only one of the 12 and 21 dai time-points (*STY2* and *STY5*) (Figure 3.8).

Notably, in *nf-ya1-2*, no further significant increase, beyond the 7 dai level, was observed for any of the seven *STY*s, except for *STY9* for which mRNA levels were elevated between 7 and 12 dai time-points, perhaps reflecting a partial redundancy of the *NF-YA1* function. Finally, *STY4* did not respond significantly and *STY6* mRNA showed decreased levels upon *M. loti* infection (Figure 3.8).

Using steady-state mRNA levels as sole indicators, Figure 3.9 summarises the expression patterns of *L. japonicus STY*s. Together with histochemical data (see above), these results indicated a strong likelihood for *STY*s acting in a highly redundant manner during *L. japonicus* root nodule development.

3.5 *L. japonicus sty* mutants

To begin addressing the functional relevance of *STY* genes during root nodule development, a reverse genetic resource of *L. japonicus* LORE1 retrotransposon insertion lines (https://lotus.au.dk/; (Malolepszy et al., 2016; Mun et al., 2016) was surveyed in order to identify mutant *sty* alleles.

LORE1 is a long terminal repeat retrotransposon that propagates in the *L. japonicus* genome by a copy-and-paste mechanism (Malolepszy et al., 2016). Insertions of the 5.041 kb long LORE1 sequence in coding (exonic) regions of a gene introduce multiple premature, translational stop codons (Fukai et al., 2012; Urbanski et al., 2012), which in many cases generates strong, null alleles (Madsen et al., 2005; Hossain et al., 2016).

Insertions of LORE1 in exonic regions were identified for all but the *STY3* gene (Figure 3.10). One of the *L. japonicus* lines (*sty3-10*; Plant ID 30010699; https://lotus.au.dk/) was characterized as containing an intronic LORE1 insertion at the *STY3* locus. However, this insertion was considered unlikely to be deleterious to the gene function based on previous observations and data showing an unimpeded splicing of LORE1 containing introns (K. Szczyglowski, unpublished data). Therefore, a Targeted Induced Localised Lesions IN Genomes (TILLING) approach was used as an alternative to identify deleterious mutations at the *STY3* locus. This was successful in selecting two alleles, called *sty3-1* and *sty3-9*, that carried independent single nucleotide substitutions (C_{187} to T and C_{493} to T, respectively) which were predicted to result in premature translation termination (STOP) codons (Figure 3. 10). Unfortunately, the *L. japonicus* line carrying the *sty3-1* allele showed significantly stunted growth with altered leaf morphology and was infertile (data

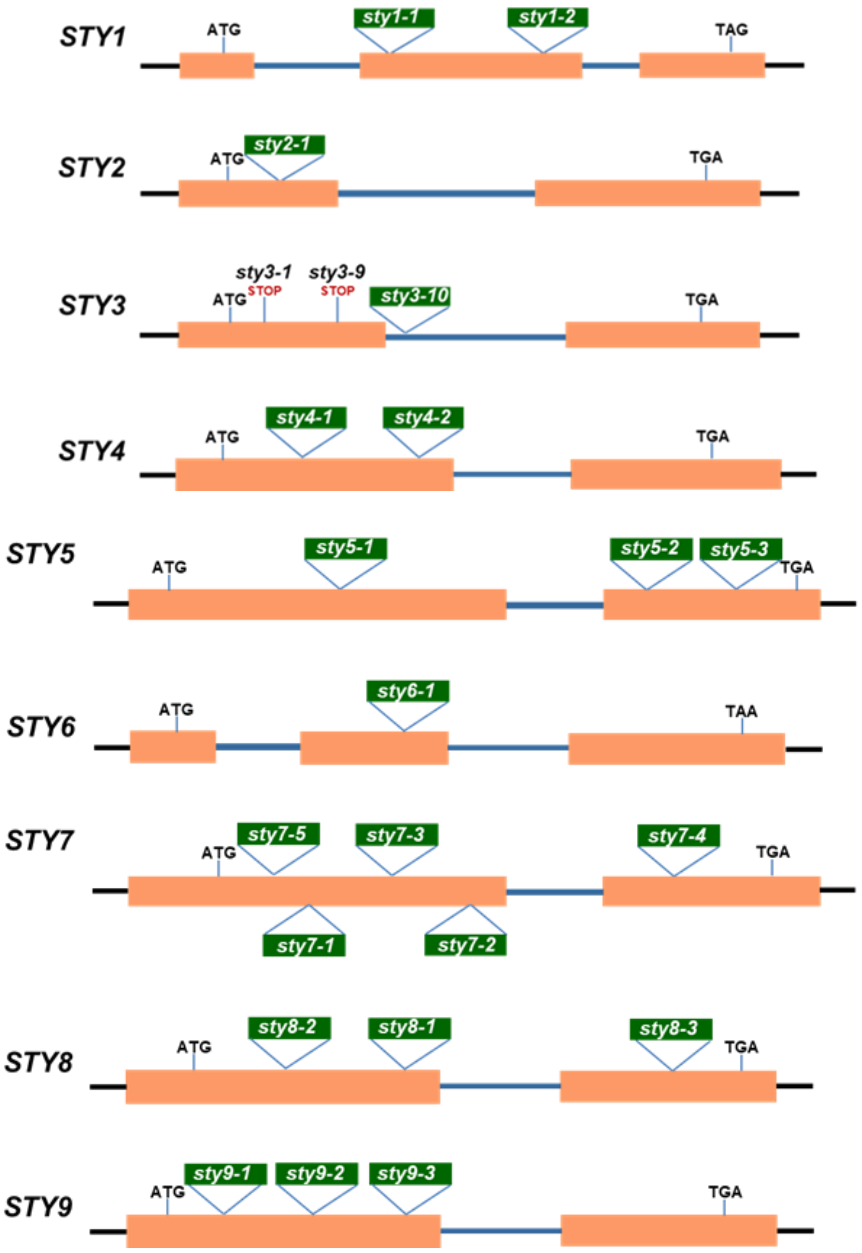

Figure 3.10 *Lotus japonicus* mutant *sty* alleles. Schematic structures of the nine *L. japonicus STY* genes are shown with the approximate positions of LORE1 retrotransposon insertions (green boxes) indicated. Names in the green boxes denote corresponding mutant alleles. Note that, for example, *sty4-1* and *sty4-2* represent two mutant *sty4* alleles, each present in independent *L. japonicus* mutant lines. The same concept applies to all other *STY* loci. For *STY3*, two point mutations, *sty3-1* and *sty3-9*, which are predicted to generate premature stop codons (STOP), were also identified using a TILLING approach.

not shown). By contrast, the line containing the *sty3-9* allele appeared healthy and was therefore used in subsequent analyses. The stunted growth of *sty3-1* was unlikely to be the result of a LORE1 insertion at the *STY3* locus. If this was the case, a similar growth phenotype would be expected for *sty3-9*, which like *sty3-1* carried a premature stop codon in the first exon.

In terms of characterizing individual *sty* mutants, the effort was purposefully focused on a group of the five *STY* genes (i.e. *STY1*, *STY2*, *STY3*, *STY7* and *STY8*) that were first to respond to *M. loti* infection by upregulating their expression at the 4 dai time-point (Figures 3.8 and 3.9). As further described below, a dominant negative approach to simultaneously affect the functioning of all relevant *STY*s was also undertaken, in order to account for the high likelihood of their redundant function during symbiosis.

3.6 *sty* mutants show weak symbiotic phenotypes

Where available, two independent LORE1 insertion lines for a given *STY* locus (e.g. *sty1-1* and *sty1-2*) were used to evaluate both symbiotic and non-symbiotic plant growth. For the symbiotic phenotype, number of epidermal infection threads (eITs), nodule primordia and mature nodules were scored. At 7 dai, no significant differences between wild type and the *sty* mutant lines could be found with regard to eIT formation (Figure 3.11), indicating no major role for any of the five *STY* genes in this process. Surprisingly, however, while forming the wild-type or close to wild-type number of nodules, *sty1*, *sty2*, *sty7* and *sty8* developed a significantly lower number of nodule primordia. By contrast, *sty3-9* was wild type in this respect (Figure 3.12A). These somewhat attenuated nodulation phenotypes persisted at the 21 dai time-point and were also consistent between different

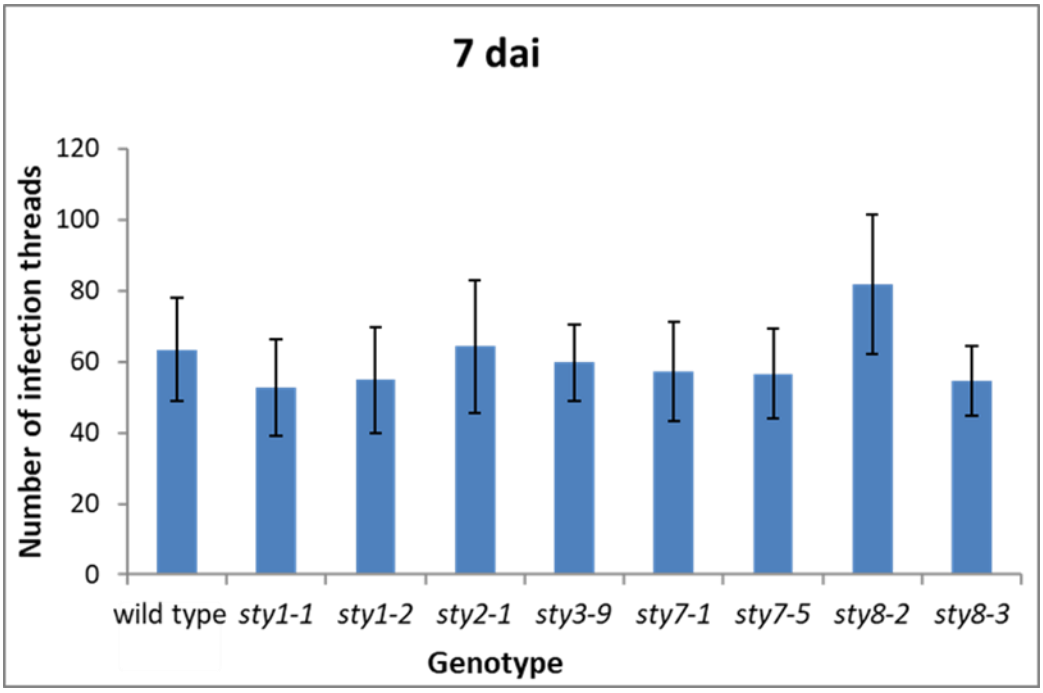

Figure 3.11 *sty* mutants form epidermal infection threads. The epidermal infection threads were scored in *L. japonicus* wild type and the selected *sty* mutant lines at 7 dai with an *M. loti* strain NZP2235 tagged with the *hemA::LacZ* reporter. Note that where available, two independent mutant lines carrying different *sty* alleles (e.g. *sty1-1* and *sty1-2*) at the same locus were used. In all cases, values reported are the mean ± 95% confidence intervals (n = 10). Statistical differences between wild type and the individual mutant lines were evaluated using Dunnett's test but none were found.

allelic lines used, suggesting that they are likely reflective of a given *STY* gene function (Figure 3.12A).

Follow-up experiments were performed to determine whether the observed decreased nodule primordia phenotypes could be correlated with defects in overall plant growth. Development of shoots and roots in wild type and the *sty* mutants were comparatively evaluated at 14 and 28 days after sowing (das) under non-symbiotic conditions, in sterile soil supplemented with the B&D nutrient solution containing 1mM KNO_3.

In comparison to wild-type, the shoot mass, used as one of the measures of plant performance, was significantly diminished in all but the sty3-9 and *sty8-2* mutants (Figure 3.13A and B). This was especially evident for the 21 dai time-point (Figure 3. 13B). Similarly, the root growth was negatively impacted by the *sty* mutations, affecting in most cases root weight (Figures 3.14). However, a simple correlation between the degree of plant growth retardation under non-symbiotic conditions and the number of nodule primordia could not be fully supported. For example, in spite of having the most retarded growth, *sty8-3* did not have the most extreme mutant nodulation phenotype. Also, at 21 dai, *sty3-9* had wild-type nodulation despite showing some diminished shoot and root growth under non-symbiotic conditions (Figures 3.12, 3.13 and 3.14). These data did not entirely rule out the possibility that the diminished growth of at least some of the *sty* mutants had a negative impact on the number of nodule primordia. Nonetheless, they showed that other, as yet uncharacterized factors were likely to be pertinent, which was not entirely surprising considering that each of the *sty* lines carried additional LORE1 insertions that could have impacted the phenotypic outcome. These data also indicated that developing and interpreting phenotypes of higher order (i.e. double, triple, etc.) *sty* mutants could be

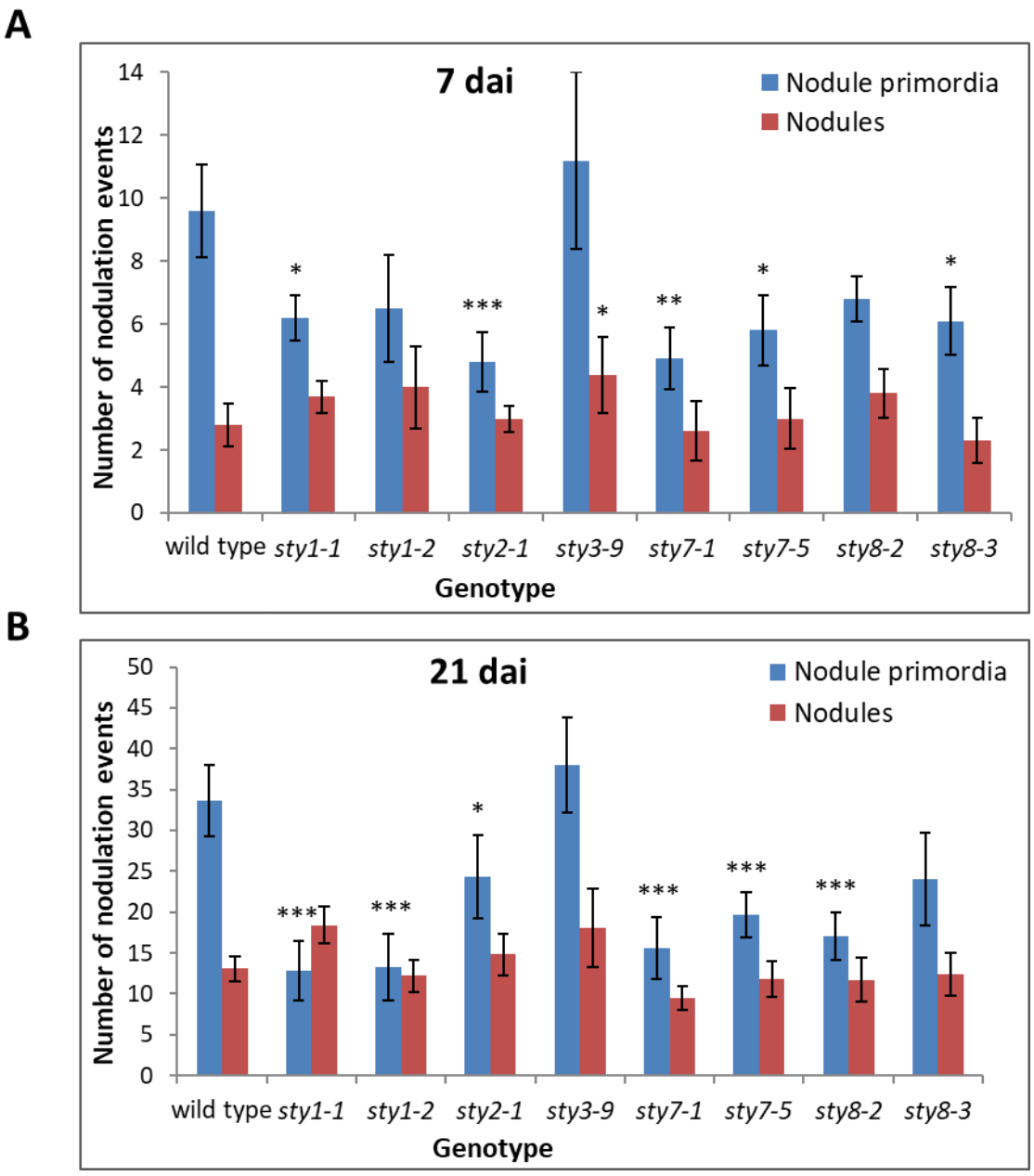

Figure 3.12 *sty* mutants form fewer nodule primordia. The number of nodule primordia and nodules were scored 7 (A) and 21 dai (B) with *M. loti* strain NZP2235 tagged with the *hemA::LacZ* reporter. Ten individuals were scored for each genotype and average ± 95% confidence intervals are given. Asterisk denotes a significant difference from the wild-type control (Dunnett's test, *P <0.05; **P <0.01; *** P < 0.01).

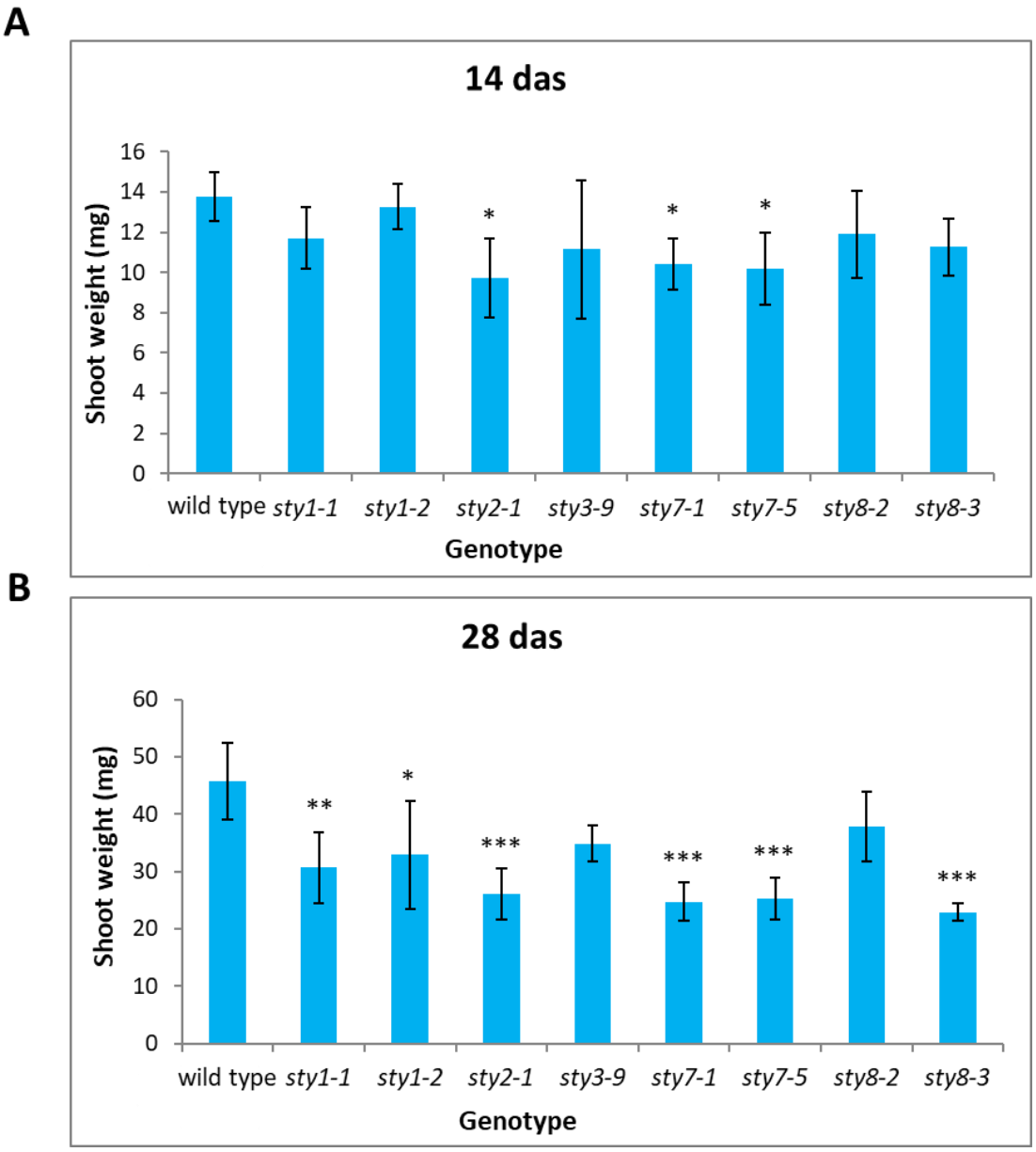

Figure 3.13 Mutations at most *STY* loci affect shoot growth. Plants were grown under sterile conditions, in the absence of *M. loti*, and the fresh shoot weight was evaluated 14 (A) and 28 (B) days after sowing (das). Ten plants were scored for each genotype. Averages ± 95% confidence intervals are given. Asterisk denotes a significant difference from the wild-type control (Dunnett's test, *P <0.05; **P <0.01; *** P < 0.01).

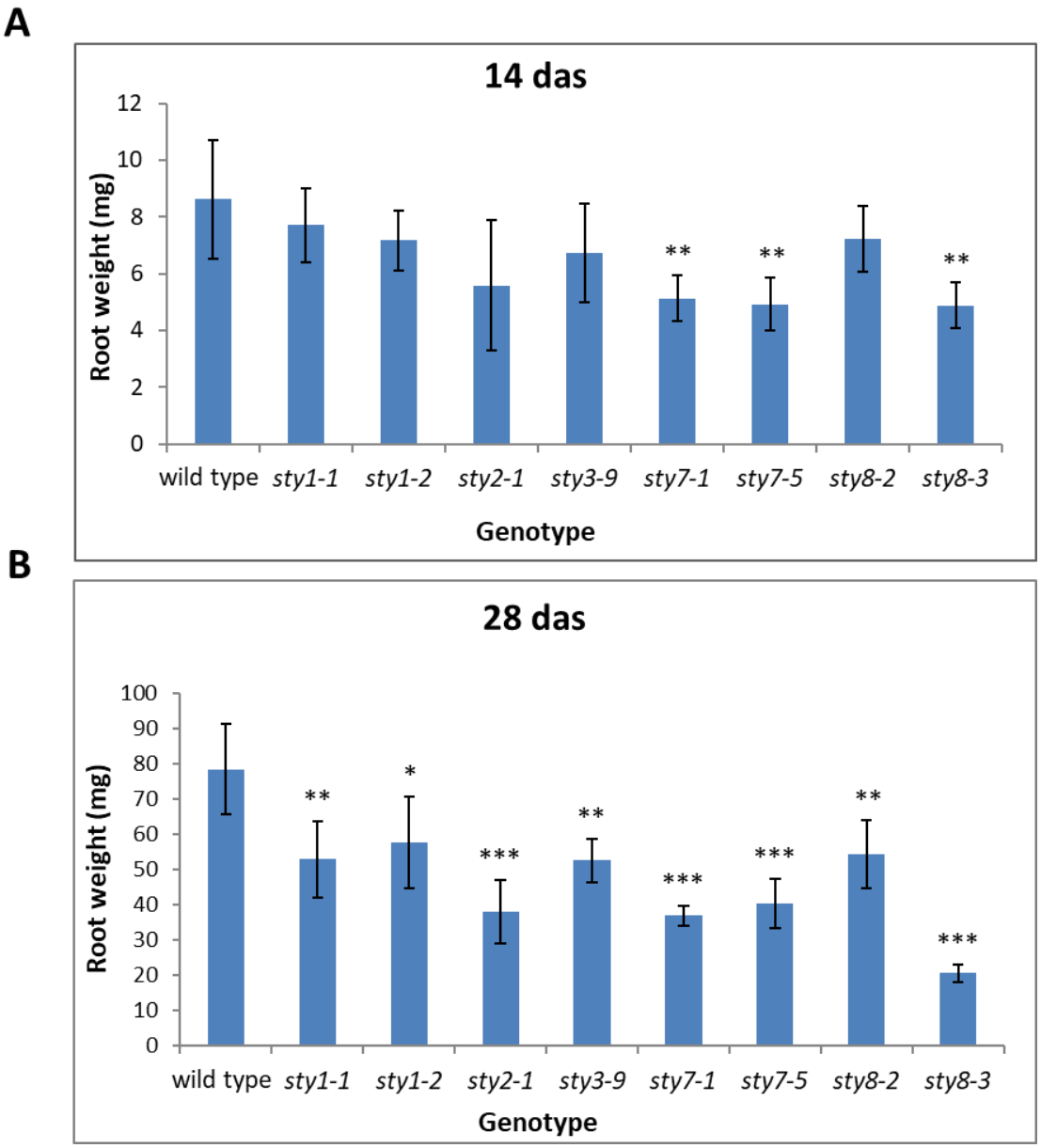

Figure 3.14 (see next page for the figure legend)

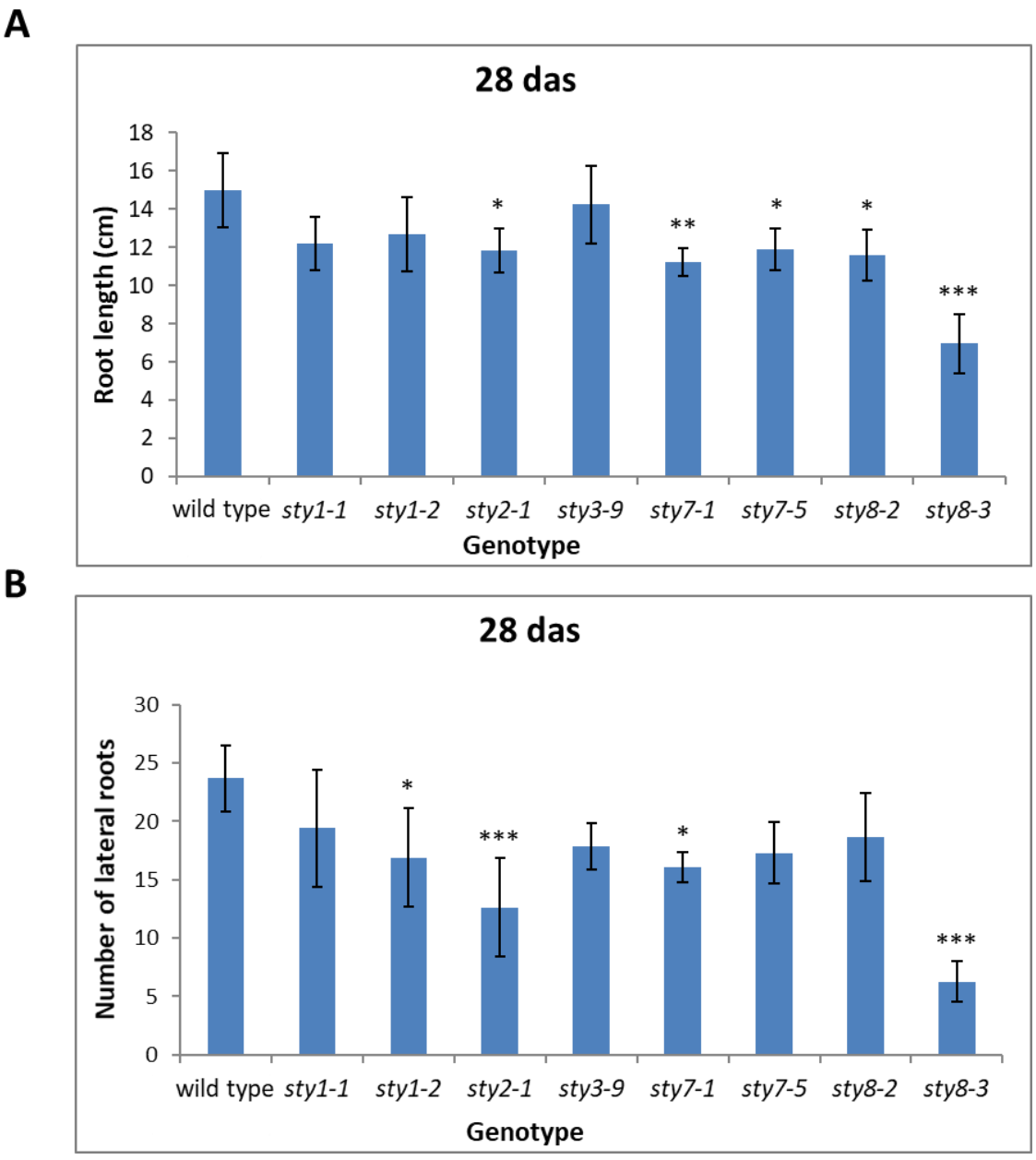

Figure 3.14 Root growth is affected in *sty* mutants. Plants were grown under sterile conditions, in the absence of *M. loti* and root weight was measured 14 (A) and 28 (B) days after sowing (das). In addition, the root length (C) and the number of lateral roots (D) were evaluated 28 das. Ten plants were scored for each genotype. Averages ±95% confidence intervals are given. Asterisk denotes a significant difference from the wild-type control (Dunnett's test, *P <0.05; **P <0.01; *** P < 0.01).

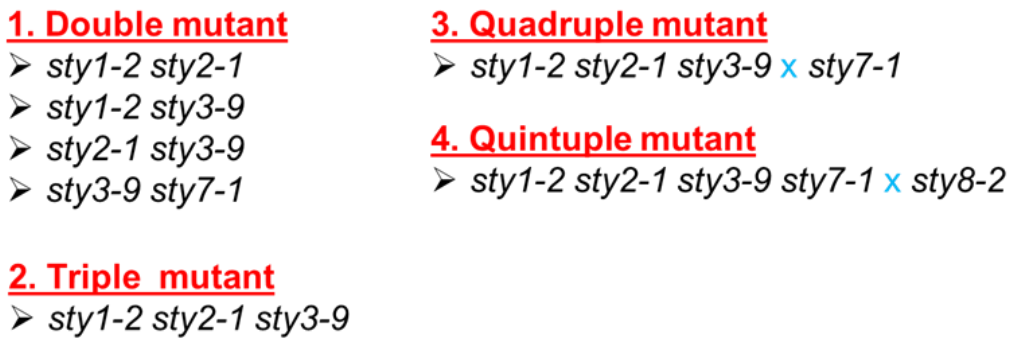

Figure 3.15 A list of double and higher order *sty* mutants.

challenging due to an increased accumulation of LORE1 insertions. Nonetheless building such mutant lines was undertaken and four double mutants and the *sty1-2 sty2-1sty3-9* triple mutant were obtained, while construction of the relevant quadruple and quintuple mutant lines is currently under way (Figure 3.15).

Symbiotic phenotypes of three of the four double *sty* mutants were evaluated by scoring visible nodules only. At 21 dai no significant differences from the wild-type control were detected (data not shown). The triple mutant showed a weak mutant symbiotic phenotype. When evaluated at 21 dai, it formed the same number of nodule primordia as wild type but had a significantly diminished, circa 30%, nodule number (Figure 3.16A). Under non symbiotic conditions, at 28 das, the triple mutant had diminished shoot and root growth (Figures 3.16B, 3.16C and 3.16D). Whether adding *sty7-1* and/or *sty8-2* alleles into the triple mutant background will result in a more severe nodulation phenotype remains to be determined.

3.7 STY3::SRDX blocks infection thread and nodule formation

In order to gain a swifter insight into the significance of *STY*s during symbiosis, a dominant negative approach was implemented. If successful, this was also expected to help determine whether continuing with the construction of higher order *sty* mutants is indeed warranted. To this end, a chimeric construct composed of the entire *L. japonicus STY3* coding (i.e. CDS) region translationally fused with a DNA fragment encoding the 12-amino acid-long Ethylene-Responsive Element Binding Factor (ERF)-associated amphiphilic repression domain, called SRDX (for SUPERMAN REPRESSOR DOMAIN X) was developed (Figure 3.17). The presence of the SRDX domain was expected to convert the

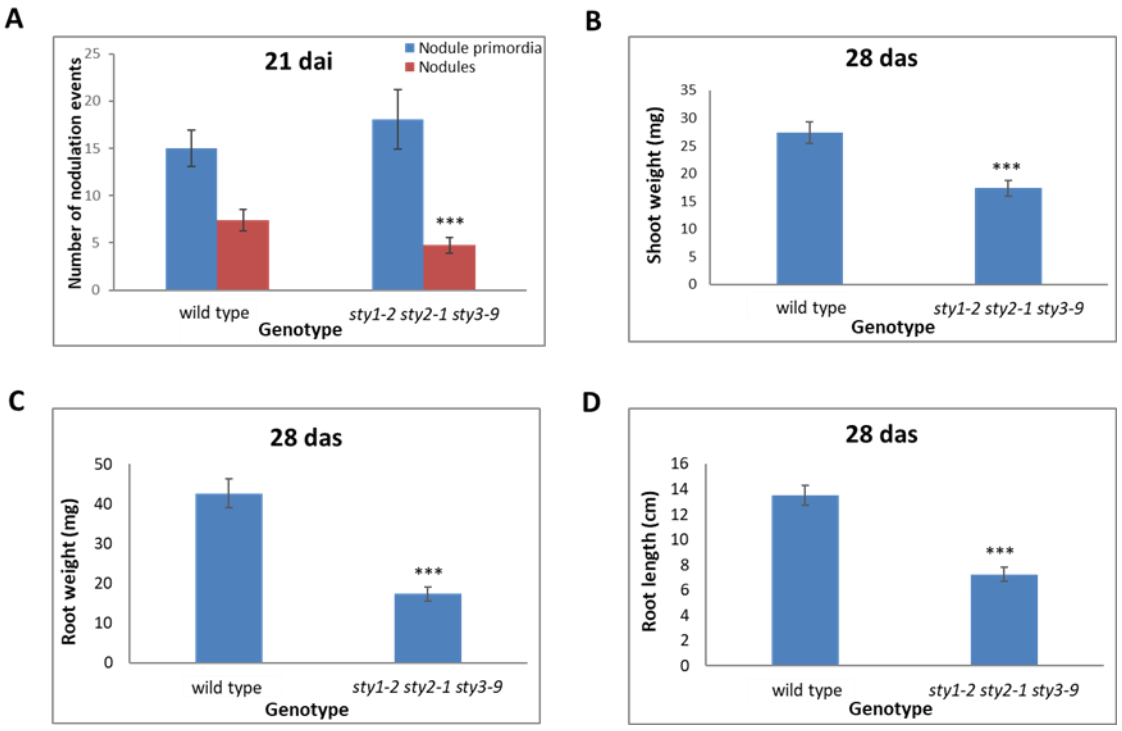

Figure 3.16 Plant development is affected in *sty1-2 sty2-1 sty3-9* triple mutant. (A) Nodulation events (nodule primordia and nodules) were scored in wild type and the triple mutant 21 days after inoculation (dai) with *M. loti*. Non-symbiotic phenotypes, including shoot weight (B), root weight (C) and root length (D) of plants grown under sterile conditions, in absence of *M. loti*, were evaluated at 28 days after sowing (das). 15 and 30 individuals per genotype were analyzed for symbiotic and non-symbiotic phenotypes, respectively. Averages ±95% confidence intervals are given. Asterisks(*** P<0.001) represent a significant difference from wild type (Student's t-test).

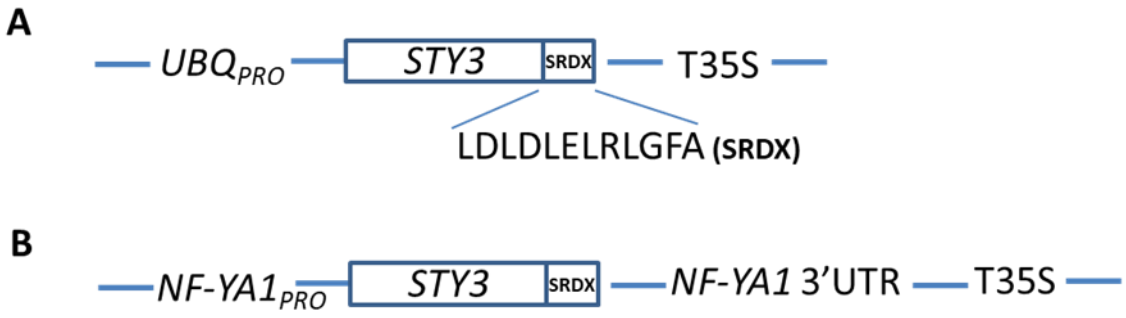

Figure 3.17 Outlines of constructs used for expression of a presumed STY3 dominant repressor. Two different promoters (PRO), *Ubiquitin* (A), and *NF-YA1* (B) were used to drive expression of a chimeric protein, as encoded by a cDNA sequence composed of the entire coding region of the *STY3* gene translationally fused with the 36 nucleotide sequence for the 12 amino acid ERF-associated amphiphilic repression domain, known as the Superman Repressor Domain X (SRDX). T35S, the CAMV 35s terminator sequence; *NF-YA1 3'* UTR, 3' untranslated region of the *NF-YA1* mRNA.

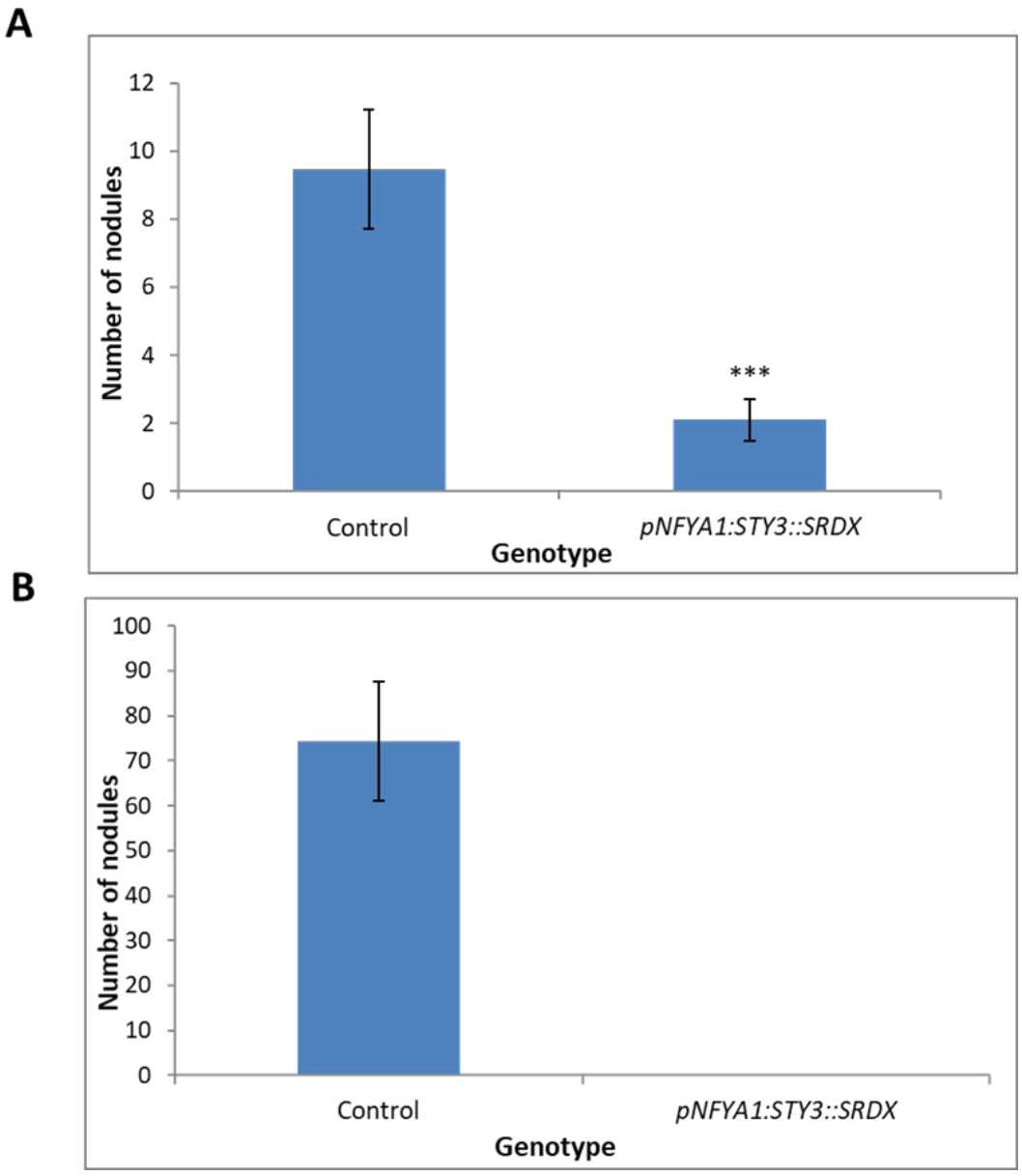

Figure 3.18 *pNF-YA1:STY3::SRDX* inhibits nodule formation. (A) Scores of nodules on transgenic hairy roots in the absence (control) or presence of *pNF-YA1*:*STY3::SRDX* transgene. For Control and *pNF-YA1*:*STY3-SRDX*, 45 and 43 independent hairy root systems were evaluated, respectively. (B) Scores of nodules developed on fully transgenic (T0) *L. japonicus* control and *pNF-YA1*:*STY3-SRDX* containing plants (n=10 for each category). Control: plants transformed with the empty pKGWD,0 vector. The scores in A and B represent means +/- 95% confidence intervals and were taken 21 days and 6 weeks after *M. loti* inoculation, respectively.

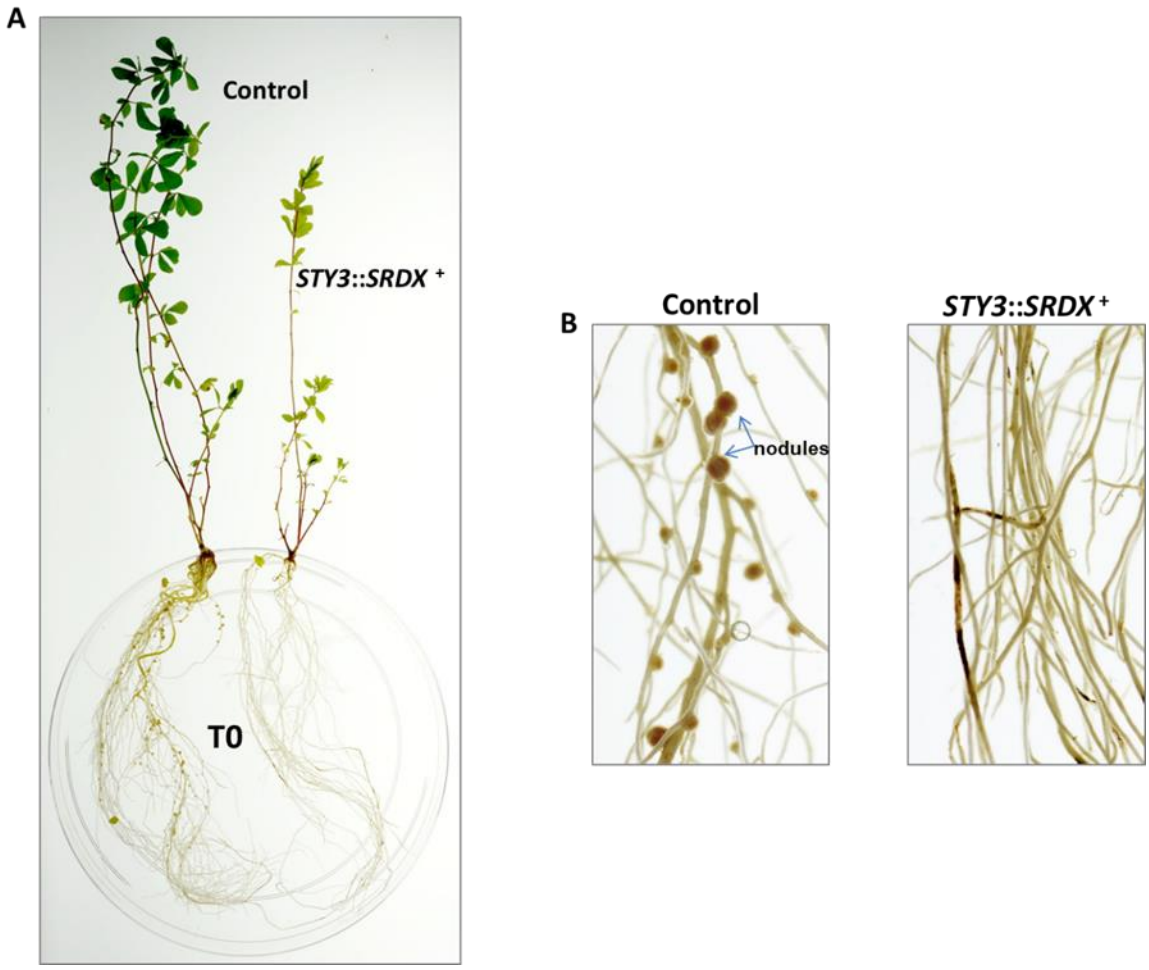

Figure 3.19 Transgenic plants carrying *pNF-YA1:STY3::SRDX* do not form nodules. (A) Images of representative fully transgenic *L. japonicus* control and the *pNF-YA1:STY3::*SRDX transgene-containing plants. The images were taken 28 days after inoculation with *M. loti*. (B) Close-up images depicting segements of roots shown in (A). Control: Plant transformed with the empty pKGWD,0 vector.

presumed STY3 transcriptional activator into a transcriptional repressor, as previously demonstrated for several independent transcriptional activators (Hiratsu et al., 2003), including *Arabidopsis* STY1 (Eklund et al., 2010a). *STY3* was chosen for this approach because among the *L. japonicus STY*s it was expressed at a relatively high level and at 4 dai with *M. loti* this was entirely dependent on *NF-YA1* (Figures 3.8 and 3.9).

The activation of any downstream targets of STY3 was expected to be attenuated in tissues expressing *STY3::SRDX*, possibly also overcoming the presumed functional redundancy. To account for the latter, the chimeric *STY3::SRDX* mRNA was expressed in transgenic hairy roots formed on wild-type *L. japonicus* shoots under the control of a strong, constitutive *L. japonicus UBIQUITIN* (UBI_{Pro}) promoter. In addition, the nodule-specific *LjNF-YA1* promoter was used, which provided an alternative that was meant to minimize any pleiotropic effects as possibly associated with the ubiquitous expression of *STY3::SRDX* in roots (Figure 3.17). Furthermore, the $LjNF\text{-}YA1_{Pro}$*:STY3::SRDX* construct was presumed to allow silencing of only a subset of genes that operate downstream of *NF-YA1* and are targeted by STYs within the same cellular domain.

Activity of the green fluorescent protein (GFP) marker present in the T-DNA region of the binary vector was used to select for the relevant, co-transformed transgenic hairy roots (see Materials and Methods). GFP-positive hairy roots were induced by *A. rhizogenes* carrying either control, empty binary vector or the same vector containing $LjNF\text{-}YA1_{Pro}$*:STY3::SRDX*. By contrast, only non-fluorescing (i.e. GFP minus) hairy roots were formed when *A. rhizogenes* carrying the UBI_{Pro}*:STY3::SRDX* containing binary vector was used for transformation. This result indicated that ubiquitous expression of *STY3::SRDX* is detrimental to hairy root development. Consequently, subsequent experiments involved

A

Transgenic T0 Plants	Total T1 plants	*pNF-YA1:STY3::SRDX* -		*pNF-YA1:STY3::SRDX* +	
		Nod +	Nod -	Nod +	Nod -
STY3::SRDX5	85	23	0	0	62
STY3::SRDX6	72	21	0	0	51

B

STY::SRDX5	*pNF-YA1:STY3::SRDX* -	*pNF-YA1:STY3::SRDX* +
Observed no. (O)	23	62
Expected no. (E)	21.25	63.75
$\chi 2$ calculated	0.192156863	
$\chi 2$ critical (P = 0.05)	3.841	

STY3::SRDX6	*pNF-YA1:STY3::SRDX* -	*pNF-YA1:STY3::SRDX* +
Observed no. (O)	21	51
Expected no. E	18	54
$\chi 2$ calculated	0.666666667	
$\chi 2$ critical (P = 0.05)	3.841	

Table 3.2 Segregation of the *pNF-YA1:STY3::SRDX* transgene in two T1 populations, derived from *STY3::SRDX5* and *STY3::SRDX6* independent T0 transgenic plants.

(A) Number of plants segregating the *pNF-YA1:STY3::SRDX* transgene and the corresponding nodulation phenotypes. (-/+) symbols denote presence and absence of the transgene and nodules (Nod), respectively. (B) The corresponding Chi-square ($\chi 2$) test results for segregation of the transgene in T1 population derived from the indicated T0 plant (P = 0.05).

evaluation of nodulation phenotypes as associated with either control or *LjNF-YA1$_{Pro}$:STY3::SRDX* containing hairy roots. When examined 21 dai with *M. loti*, the former developed on average 9.5 ± 1.7 nodules (n = 54), while the latter showed a low nodulation phenotype ($\bar{x}$ = 2.1 ± 0.6; n = 43) (Figure 3.18A). In fact, of the 43 independent hairy root systems transformed with *LjNFYA1$_{Pro}$:STY3::SRDX*, 15 did not form nodules at all, while the remaining 28 had a low-nodulation phenotype that included a mixture of primarily small but also some regular-size nodules.

In order to characterize the impact of the transgene on nodule formation in more detail, fully trangenic *L. japonicus* plants were developed. Ten independent T0 plants carrying *LjNF-YA1$_{Pro}$:STY3::SRDX* were characterized and compared with the equivalent, control T0 plants that lacked the construct. When examined 6 weeks after inoculation with *M. loti*, none of the *LjNF-YA1$_{Pro}$:STY3::SRDX* containing plants formed any visible nodules. In contrast, control transgenic T0 plants were profusely nodulated (Figures 3.18B and 3.19).

The T0 plants were allowed to self and produced segregating T1 populations. Two T1 populations, derived from *STY3::SRDX*-5 and *STY3::SRDX*-6 independent T0 transgenic plants, were characterized by genotyping for the presence of the *LjNF-YA1$_{Pro}$:STY3::SRDX* transgene and evaluating the associated symbiotic phenotypes. Out of 85 and 72 T1 segregants genotyped for each of the two populations, 62 and 51 individuals were *STY::SRDX* positive (*STY::SRDX* $^{+}$), respectively and showed non-nodulating phenotypes.

The remaining 23 and 21 *STY::SRDX* lacking (*STY::SRDX* $^{-}$) plants, respectively, formed wild-type looking nodules (Table 3.2 and Figure 3.20). These segregation values were consistent with a 3:1 ratio (P = 0.05), showing that the corresponding T0 plants

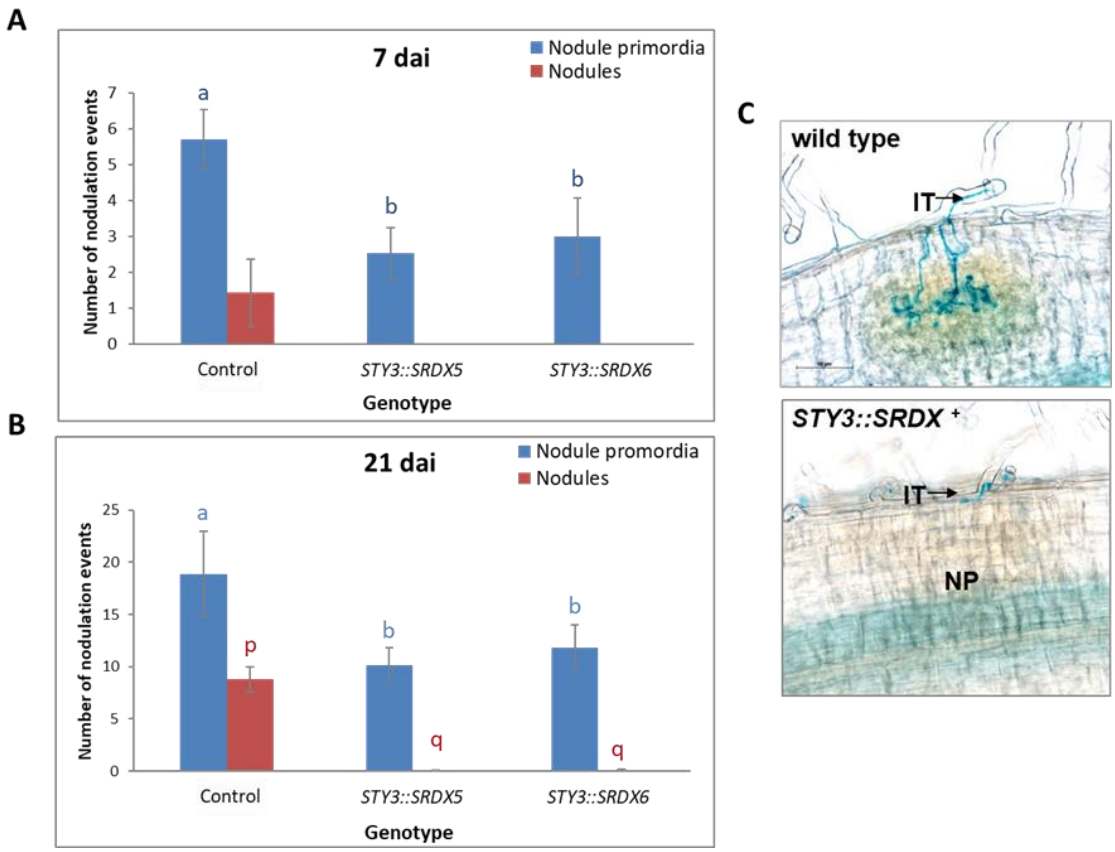

Figure 3.20 *STY*s are required for nodule formation. (A and B) Average scores of nodulation events (i.e. nodule primordia and nodules) in *L. japonicus* T1 plants segregating for presence/absence of the *pNF-YA1*:*STY3*::*SRDX* transgene. Control: T1 plants lacking the transgene; *STY3::SRDX5* and *STY3::SRDX6:* T1 plants carrying the transgene and derived from two independent, 5 and 6, T0 plants, respectively. The nodulation phenotypes were evaluated at (A) 7 days after inoculation (dai) (control, n=7; *STY3::SRDX5*, n=19; *STY3::SRDX6*, n=16 and (B) 21 dai with *M. loti* (control, n=25 *STY3::SRDX5*; n=30 and *STY3::SRDX6*, n=30). The scores in A and B represent means +/- 95% confidence intervals (C) Representative images of wild-type nodule primordia and a nodule primordia formed in transgenic plants carrying the *pNF-YA1*:*STY3*::*SRDX (STY3::SRDX*$^{+}$*)*transgene. Statistical groupings, reflected by the same letters, have been determined separately for nodule and nodule primordia using one-way ANOVA with the Tukey HSD post hoc test.

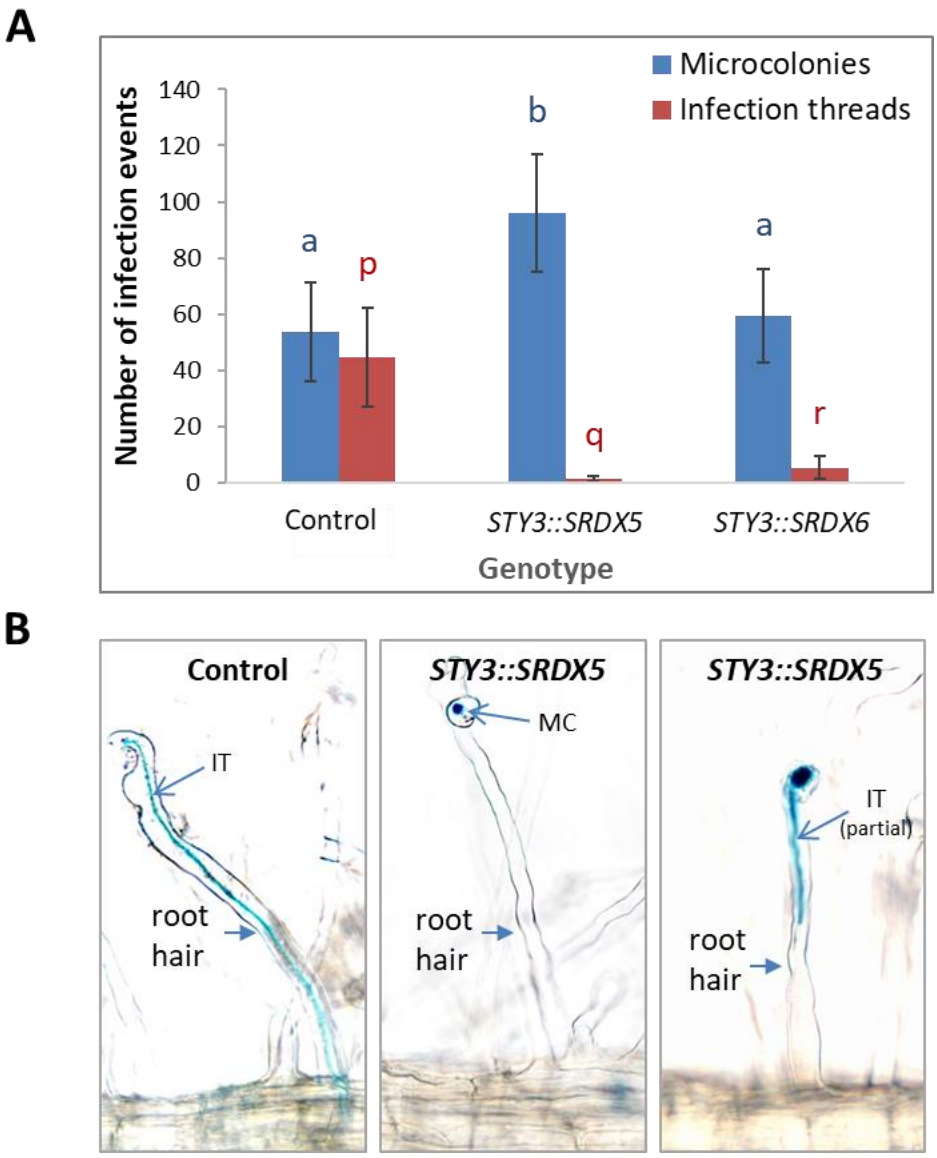

Figure 3.21 *STY*s are required for infection thread formation. (A) Scores of infection events (i.e microcolonies and epidermal infection threads) in *L. japonicus* T1 plants that either lack (control n =7) or carry (*STY3::SRDX5*, n=19, and *STY3::SRDX6*, n=16) the *pNF-YA1*:*STY3*::*SRDX* transgene. The scores represent means +/- 95% confidence intervals. Statistical groupings, reflected by the same letters, have been determined separately for MC and IT using one-way ANOVA with the Tukey HSD post hoc test. (B) Representative images of epidermal infection events in control or the transgene-containing (*STY3::SRDX5*) T1 plants. IT: Infection thread; MC: micro-colony; IT (partial): IT that is not fully elongated. Control: Plants without *STY3::SRDX* transgene.

contained a single locus transgene insertions, which segregated with the non-nodulating phenotype (Table 3.2 and Figure 3.20).

Closer inspection of the *STY::SRDX* $^{+}$ plants performed at 7 and 21 dai showed that although unable to develop mature nodules, they were capable of initiating the organogenesis, such that small nodule primordia were formed (Figure 3.20A and 3.20B). These were represented by foci of limited cortical cell divisions (Figure 3.20C) that were less frequent in comparison to control, *STY::SRDX*$^{-}$ roots (Figure 3.20A and 3.20B). The *STY3::SRDX*$^{+}$ T1 plants also formed very few eIT (Figure 3.21A) and those that managed to initiate appeared to terminate prematurely within root hairs (Figure 3.21B). Noteworthy, *STY3::SRDX*$^{+}$ T1 plants had many microcolonies, even more than wild type in the case of *STY3::SRDX5*$^{+}$plants. Together, these data indicated an essential role for *STY*s during eIT formation and nodule organogenesis.

3.8 STYs are required to regulate *YUCCA1* and *YUCCA11* expression during symbiosis

In order to begin identifying downstream targets of *L. japonicus STY*-dependent regulation in the context of symbiosis, two approaches were considered (Figure 3.22). An untargeted approach, such as RNAseq, CHIP-seq, and other genomic techniques would require an appropriate mutant *sty* background, with a clearly defined symbiotic phenotype, to be available. Work continues toward developing such a background either by pyramiding more *sty* mutations (i.e. generating quadruple and quintuple) into a single plant or by developing a stable, homozygous *L. japonicus* line expressing the STY3::SRDX chimeric protein under the control of the *NF-YA1* promoter (see above). In the meantime,

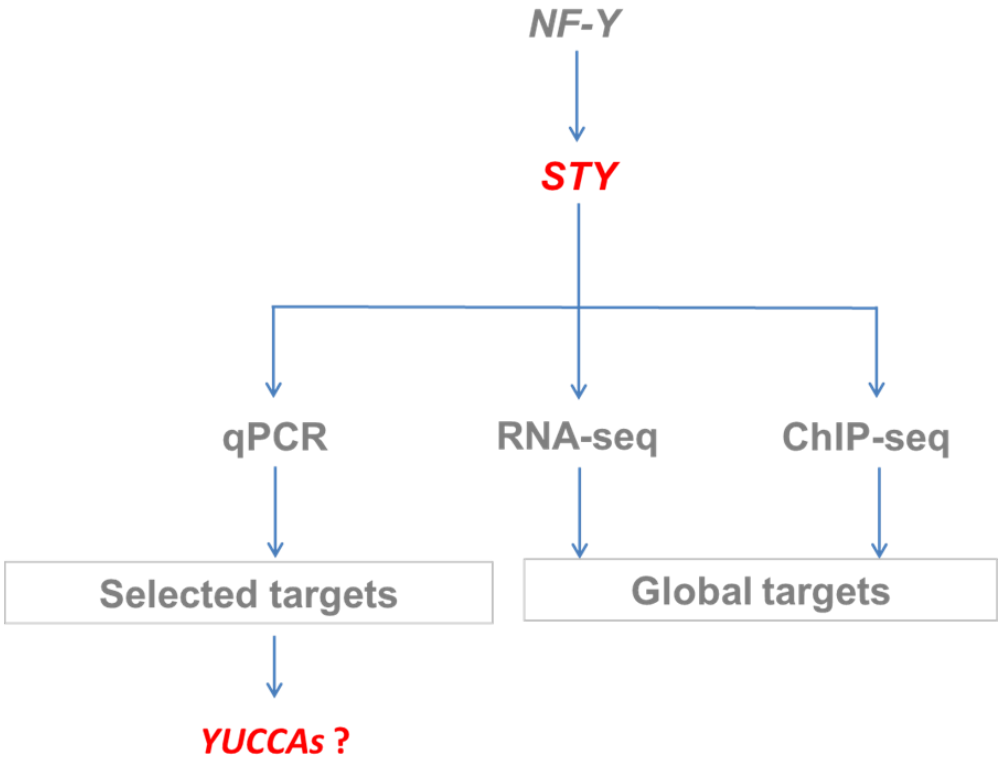

Figure 3.22 A conceptual outline for identification of downstream STY targets.

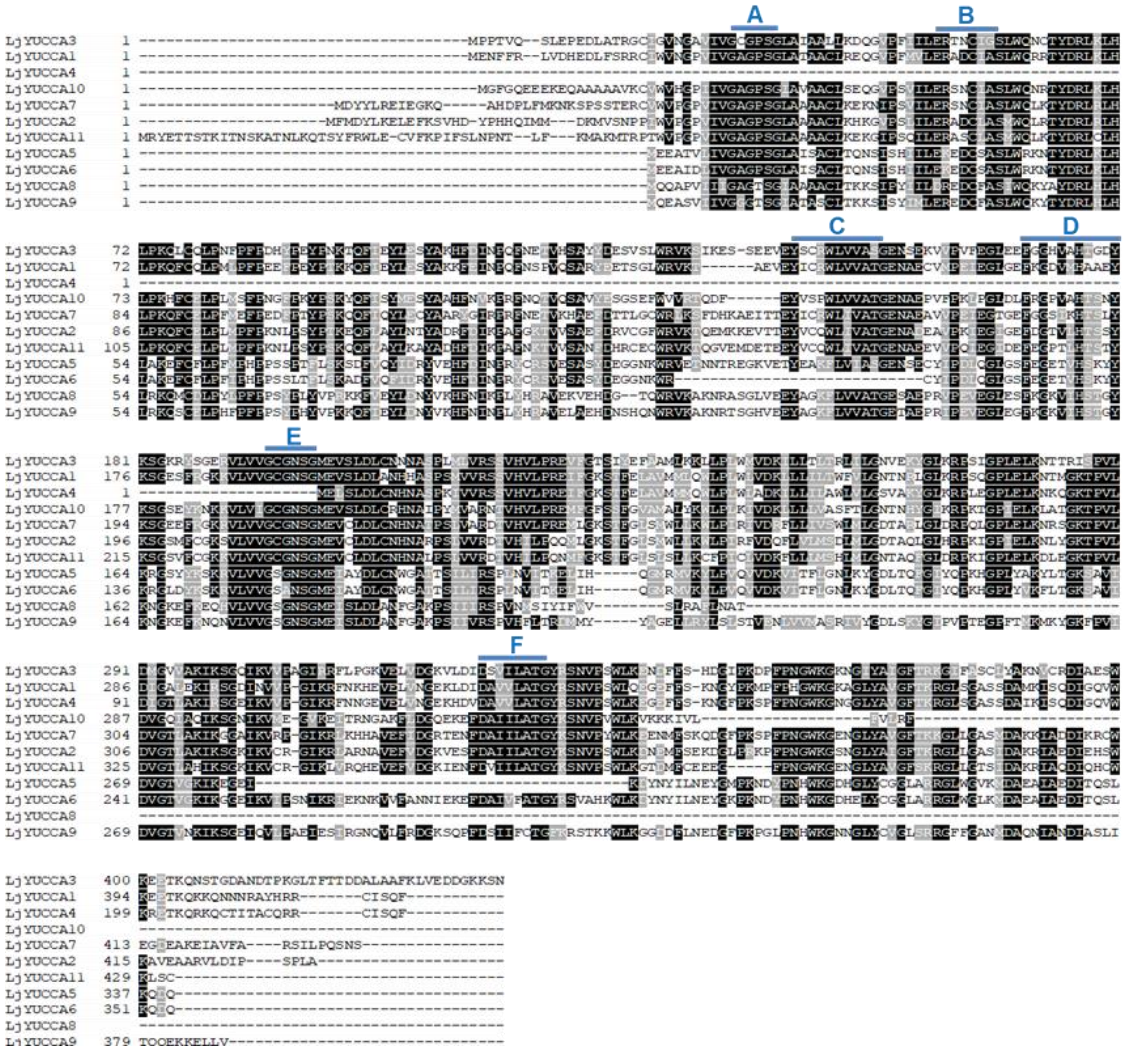

Figure 3.23 *L. japonicus* YUCCA proteins have six conserved domains characteristic of flavin monooxygenases. (A) FAD-binding domain, (B) GC-motif, (C) ATG-Containing motif 1, (D) FMO-identifying sequence, (E) NADPH domain, (F) ATG-Containing motif 2. The alignment was created with Clustal Omega using default settings and analyzed by the BoxShade software version 3.21. A threshold of ≥ 60% conservation was used. Black shading indicates identical residues, whereas gray indicates presence of conservative substitutions. The corresponding domains of known *Arabidopsis* thaliana STY/SHI protein were used for comparison. For accession numbers see Figure 3.24.

a targeted approach was commenced to determine whether any of the *L. japonicus YUCCA* genes are subjected to *STY*-dependent regulation and if this is relevant to symbiosis (Figure 3.22).

YUCCA genes encode flavin monooxygenase (FMO)-like enzymes that catalyze the rate-limiting step in tryptophan-dependent auxin biosynthesis and *Arabidopsis YUCCA4* and *YUCCA8* were shown to be regulated by STY1 (Eklund et al., 2010a). As auxin signaling was shown to be important for both the symbiotic infection and nodule formation (Suzaki et al., 2012; Suzaki et al., 2013; Breakspear et al., 2014) and it has been suggested that NF-YA1 may regulate the relevant auxin maxima during symbiosis by orchestrating the *STY* gene expression (Hossain et al., 2016), focusing on *YUCCA* genes as potential downstream targets of NF-YA1/STY-dependent regulation was deemed relevant.

Using *Arabidopsis* YUCCA protein sequences as Blast queries (Cheng et al., 2006; Zhao, 2018), 11 YUCCA-like proteins were predicted to be encoded by the *L. japonicus* genome (http://www.kazusa.or.jp/lotus/index.html; https://lotus.au.dk/) (Figure 3.23). Six of these proteins, namely YUCCA1-3, YUCCA7, YUCCA9 and YUCCA11 were found to contain all of the relatively conserved domains characteristic of FMOs (Yan et al., 2016). These included FAD-binding, GC, FMO-identifying, ATG-containing 1, NADP-biding and ATG-containing 2 motifs (Figure 3.23). YUCCA5, YUCCA6 and YUCCA8, were each missing one of the domains and YUCCA8 was also lacking the C-terminal region, as present in all other *L. japonicus* YUCCA proteins. Finally, YUCCA4 had a much shorter N-terminus, missing the first five FMO motifs (Figure 3.23).

An *in-silico* analysis of the RNAseq data showed that at 4 dai with *M. loti* the steady-state level of only *YUCCA11* mRNA was significantly (FDR<0.05) upregulated in *L.*

Gene ID	Gene name	log2FC	Fold change	P-value	FDR-value
Lj1g3v4528740	*YUCCA1*	0.67	1.59	0.00359	0.1555
Lj0g3v0049349	*YUCCA2*	0.26	1.20	0.4650	0.9999
Lj0g3v0085899	*YUCCA3*	-0.44	-1.35	0.0294	0.6376
Lj0g3v0308259	*YUCCA4*	0.07	1.05	0.8035	0.9999
Lj3g3v3189630	*YUCCA5*				
Lj3g3v3189640	*YUCCA6*				
Lj1g3v2036560	*YUCCA7*	-0.76	-1.70	0.0069	0.2488
Lj1g3v4764550	*YUCCA8*	-0.09	-1.07	0.7477	0.9999
Lj1g3v4764680	*YUCCA9*	0.01	1.01	0.9678	0.9999
Lj0g3v0101099	*YUCCA10*	3.18	9.06	0.0945	0.9999
Lj4g3v3081700	*YUCCA11*	8.31	317.23	0.0006	0.0404

Table 3.3 *YUCCA11* is expressed upon *M. loti* inoculation. The wild-type, un-inoculated roots and the roots of the same age collected 4 days after inoculation with *M. loti* were analyzed using next-generation RNA sequencing. Of the 11 *YUCCA* genes, only *YUCCA11* was found to be significantly (FDR<0.05) regulated by *M. loti* inoculation (highlighted in yellow) Log2FC: log2 fold change; Fold change: absolute fold change value; P-value: uncorrected P-value; FDR-value: false discover rate (corrected P value).

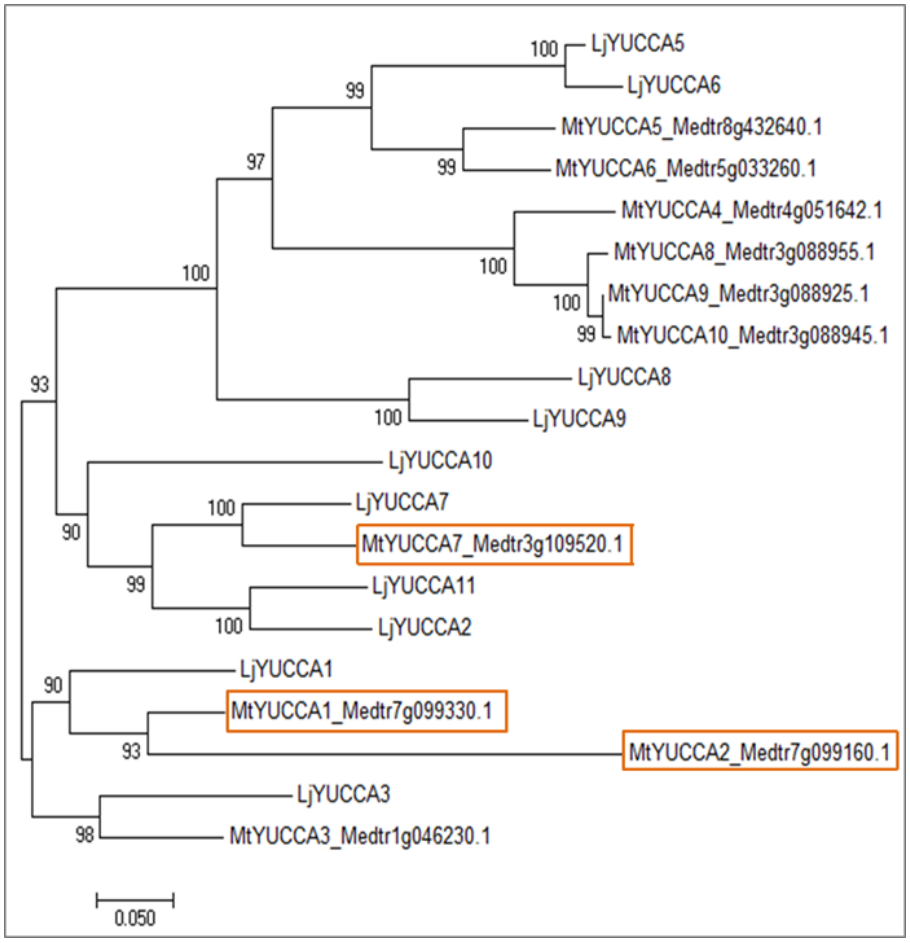

Figure 3.24 Relationship tree of predicted *L. japonicus* and *M. truncatula* YUCCA proteins. The protein sequences were aligned with ClustalW and the tree was generated using MEGA 7 (Molecular Evolutionary Genetics Analysis) software and neighbor-joining method with bootstrap replicates of 1000. The corresponding accession numbers are as follows: *L. japonicus* LjYUCCA1 (Lj1g3v4528740.1), LjYUCCA2 (Lj0g3v0049349.1), LjYUCCA3 (Lj0g3v0085899.1), LjYUCCA4 (Lj0g3v0308259.1), LjYUCCA5 (Lj3g3v3189630.1), LjYUCCA6 (Lj3g3v3189640.1), LjYUCCA7 (Lj1g3v2036560.1), LjYUCCA8 (Lj1g3v4764550.1), LjYUCCA9 (Lj1g3v4764680.3), LjYUCCA10 (Lj0g3v0101099.1), LjYUCCA11 (Lj4g3v3081700.1), and *M. truncatula* MtYUCCA1 (Medtr7g099330.1), MtYUCCA2 (Medtr7g099160.1), MtYUCCA3 (Medtr1g046230.1), MtYUCCA4 (Medtr4g051642.1), MtYUCCA5 (Medtr8g432640.1), MtYUCCA6 (Medtr5g033260.1), MtYUCCA7 (Medtr3g109520.1), MtYUCCA8 (Medtr3g088955.1), MtYUCCA9 (Medtr3g088925.1), MtYUCCA10 (Medtr3g088945.1). Three *M. truncatula* YUCCAs in red boxes are known to be regulated in a Nod factor-dependent manner.

japonicus roots (Table 3.3). Subsequently, a phylogenetic tree constructed with the corresponding *L. japonicus* and *M. truncatula* sequences revealed that *L. japonicus* YUCCA11 (LjYUCCA11) showed the highest primary sequence homology with the *M. truncatula* MtYUCCA7 protein (Figure 3.24). Interestingly, this protein is encoded by the *Medtr3g109520.1* gene, the expression of which was reported to be significantly enhanced upon Nod factor application to *M. truncatula* roots (Larrainzar et al., 2015). Two other *Medicago YUCCA* genes, namely *Medtr7g099160.1* and *Medtr7g099330.1.1*, were also shown to positively respond to Nod factor application with upregulated mRNA levels (Larrainzar et al., 2015). Their predicted protein products, MtYUCCA1 and MtYUCCA2, had the highest homology to LjYUCCA1 (Figure 3.24). Thus, based on these observations, both *LjYUCCA1* and *LjYUCCA11* were chosen for subsequent analyses.

qRT-PCR analyses showed that both *L. japonicus YUCCA1* and *YUCCA11* expression was regulated during symbiosis (Figure 3.25). *YUCCA1* mRNA was detectable already in un-inoculated *L. japonicus* roots and its level was significantly increased upon *M. loti* infection (Figure 3.25A). By contrast, *YUCCA11* mRNA could be detected only in *M. loti* inoculated roots (Figure 3.25B). Importantly, the responsiveness of the two genes was entirely lost or significantly attenuated in *STY3::SRDX-5* and *STY3::SRDX-6* roots, indicating that *STY3* and possibly other redundantly acting *STY*s are essential for the regulation of *YUCCA1* and *YUCCA11* gene expression upon *M. loti* infection (Figure 3.25).

The binding site for STYs has been identified as ACTCTAC/A and is present in promoters of at least five *Arabidopsis YUCCA* genes (i.e. *YUCCA1*, *4*, *5*, *8* and *9*) (Eklund et al., 2010a). However, in trans-activation assays with STY1, this recognition site was shown to be essential only for *YUCCA4* and *YUCCA8* expression, suggesting that other

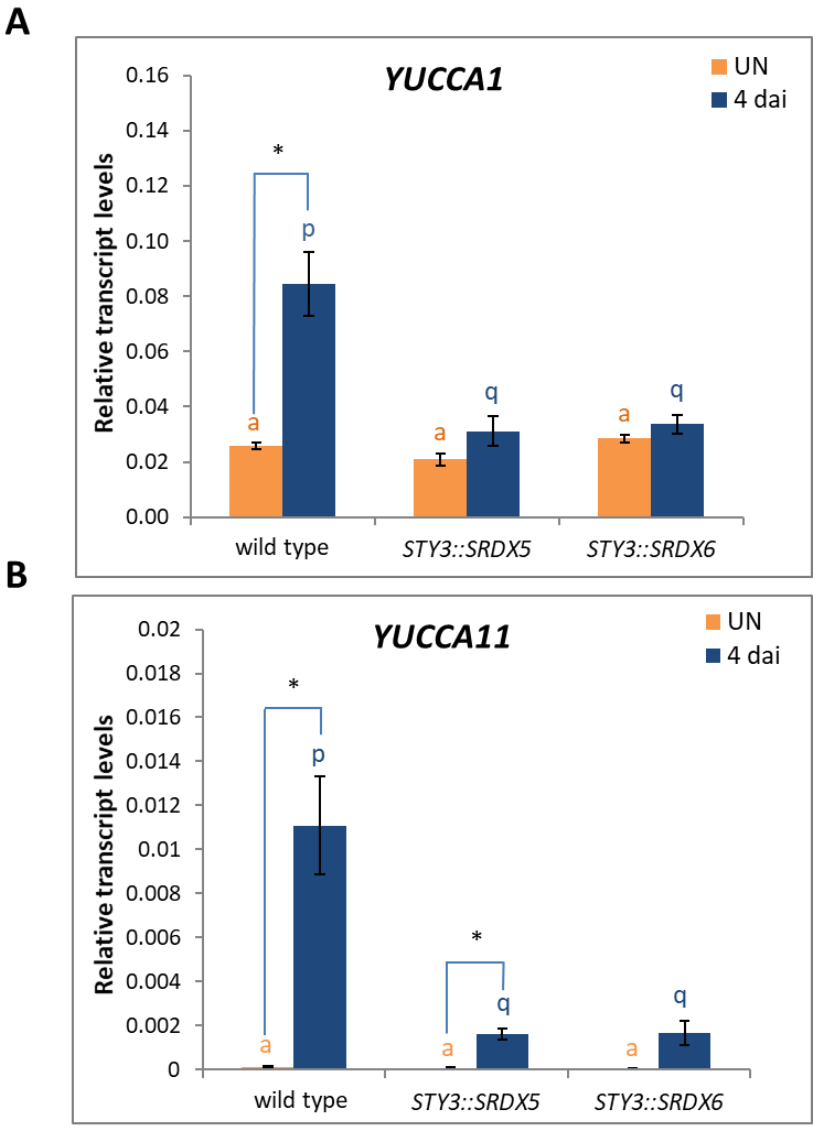

Figure 3.25 *YUCCA1* and *YUCCA11* respond to *M. loti* infection and this is dependent on *STY*s. Using qRT-PCR, the steady-state levels of *YUCCA1* and *YUCCA11* mRNAs were determined in un-inoculated (control) *L. japonicus* roots of the wild-type genotype and the corresponding roots from T1 transgenic plants carrying the *STY3-SRDX* transgene These were compared to equivalent root samples collected 4 days after inoculation (dai) with *M. loti*. The mean ± SE is given for three biological replicates. Statistical groupings across different genotypes, reflected by the same letters, have been determined separately for *M. loti* inoculated and un-inoculated samples using one-way ANOVA with the Tukey HSD post hoc test. Asterisks (*) denote significant differences between un-inoculated and inoculated samples (Student's t-test: [*], $P < 0.05$).

Gene ID	Gene name	Upregulated by infection	STY binding motif	Distance from TSS
Lj1g3v4528740	***YUCCA1***	+	Yes (ACTCTAC)	-663
Lj0g3v0049349	*YUCCA2*	-	Yes (ACTCTAA)	-253
Lj0g3v0085899	*YUCCA3*	-	No	
Lj0g3v0308259	*YUCCA4*	-	No	
Lj3g3v3189630	*YUCCA5*	nd	No	
Lj3g3v3189640	*YUCCA6*	nd	No	
Lj1g3v2036560	*YUCCA7*	-	Yes (ACTCTAC)	-1831
Lj1g3v4764550	*YUCCA8*	-	Yes (ACTCTAA)	-1682
Lj1g3v4764680	*YUCCA9*	-	No	
Lj0g3v0101099	*YUCCA10*	-	Yes (ACTCTAA)	-704
Lj4g3v3081700	***YUCCA11***	+	Yes (ACTCTAA)	-1509

Table 3.4 *In silico* analysis of *YUCCA* gene promoters for the presence of a STY binding (ACTCTAC/A) motif.

regulatory sequences might also be required (Eklund et al., 2010a). Indeed, using a protein binding microarray, a palindromic CTAG sequence was also identified as a potential regulatory element and was shown to be enriched in *Arabidopsis STY1* and *STY2* co-regulated genes (Franco-Zorrilla et al., 2014).

Inspection of the 4.0 kb promoter regions of *L. japonicus YUCCA* genes showed that *YUCCA1* and *YUCCA11* each contain a single copy of the ACTCTAC/A motif at the 663 or 1509 nucleotide position, respectively, upstream from the predicted transcriptional start site (Table 3.4). This motif was also present in promoters of *YUCCA2*, *7*, *8* and *10* (Table 4), while the CTAG palindromic sequences were present in multiple copies in both promoter and coding regions of all *L. japonicus YUCCA* sequences (data not shown).

3.9 *YUCCA1* and *YUCCA11* promoters are active in nodule primordia and nodules

To further explore expression patterns of *YUCCA1* and *YUCCA11* during root nodule symbiosis, the activity of their promoters was monitored in transgenic hairy roots, induced by *A. rhizogenes*-dependent transformation of wild-type *L. japonicus* shoots, using the GUS reporter (Figure 3.26). The *YUCCA1* promoter showed activity along the entire root vasculature and also in dividing cortical cells of nodule primordia (Figure 3.26A). In growing (small) nodules, this activity appeared to be present in all centrally-located cells, only to be confined later to the nodule vasculature in fully developed nodules (Figure 3.26A). The activity of the *YUCCA11* promoter resembled *YUCCA1*, except that it was mostly if not exclusively confined to the root regions that formed nodules. This included

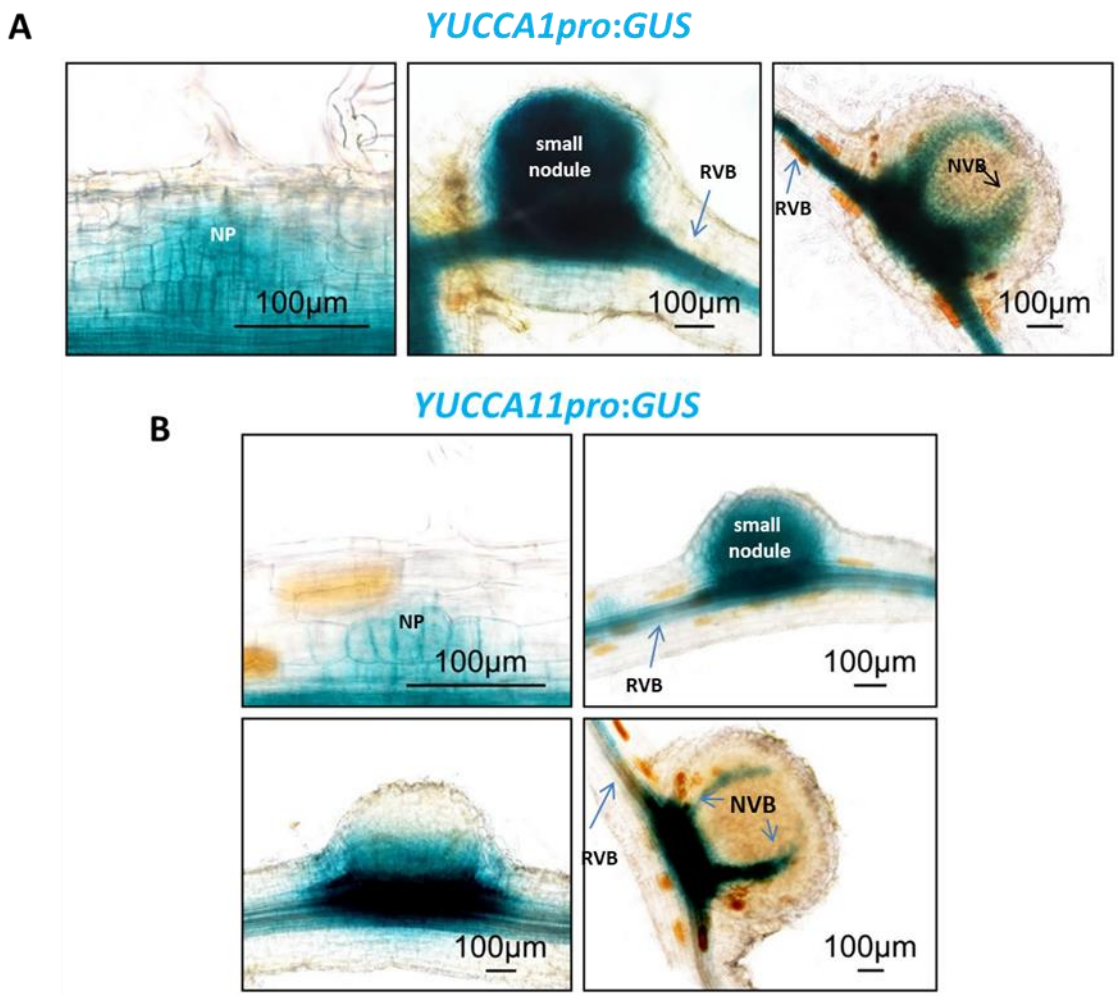

Figure 3.26 The activity of *YUCCA1* and *YUCCA11* promoters associates with nodule development. Representative images of nodules at different stages of development, showing the activity of GUS reporter gene (blue colour), as driven by *YUCCA1* (A) and *YUCCA11* (B) promoters. NP, nodule primordium; NVB, nodule vascular bundle. The images were captured at 10 days after inoculation with *M. loti*.

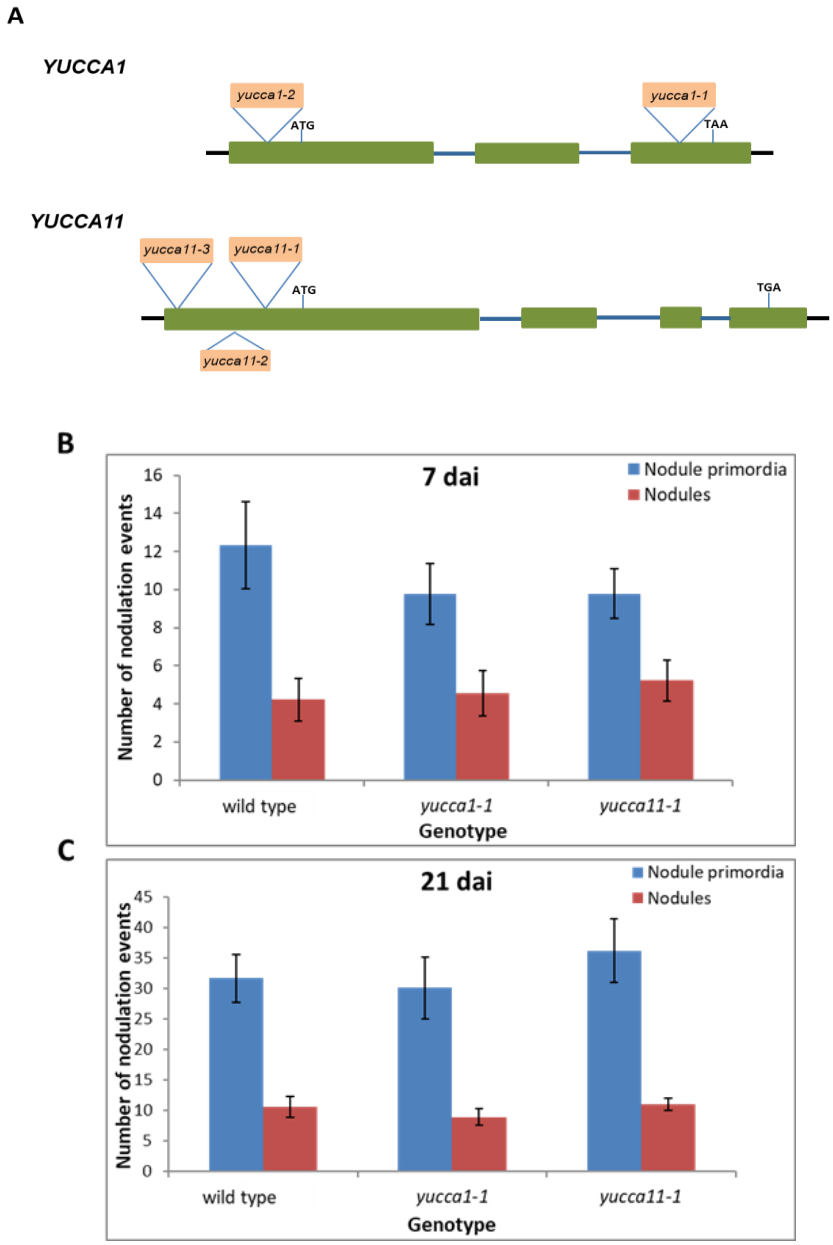

Figure 3.27 *Lotus japonicus* mutant *yucca* alleles. (A) Schematic exon-intron structures of *YUCCA1* and *YUCCA11* genes are shown with the positions of LORE1 insertions (orange boxes) indicated. Names in the orange boxes denote corresponding mutant alleles. The number of nodule primordia and nodules were scored 7 (B) and 21 (C) days after inoculation (dai) with *M. loti* strain NZP2235 tagged with the *hemA*::*LacZ* reporter. Ten individuals were scored for each genotype and average ± 95% confidence intervals are given. Statistical differences between wild type and the individual mutant lines were evaluated using the Student's t-test ($P<0.05$).

the associated root vasculature at the place of nodule emergence, where the GUS activity appeared to be the most intense (Figure 3.26B).

To assess the functional relevance of *YUCCA1* and *YUCCA11* during nodule development, the *L. japonicus* LORE1 insertion line resource (Malolepszy et al., 2016; Mun et al., 2016) was examined to identify the corresponding mutants. For the *YUCCA1* locus two lines, L8288 and 30120352, were identified that carried the LORE1 insertion either 60 bp upstream from the predicted ATG initiation codon or 143 bp upstream from the TAA termination codon, respectively (Figure 3.27A). As seeds were not available for the former, likely due to the plant sterility, only the latter line, called *yucca1-1*, was used. For *YUCCA11*, three lines, named *yucca11-1*, *-2* and *-3* were obtained, each carrying LORE1 within the predicted 5'UTR sequence, at 369, 445 and 597 bp upstream of the ATG initiation codon, respectively (Figure 3.27A), and *yucca11-1* was chosen for downstream analyses.

Both *yucca1-1* and *yucca11-1* were assessed with respect to their capacity for nodule primordia and nodule formation. At 7 and 21 dai with *M. loti*, these mutants showed wild-type symbiotic phenotypes (Figure 3.27B and C).

3.10 Expression of *YUCCA1* and *YUCCA11* is regulated by NF-YA1

As the upregulated levels of *YUCCA1* and *YUCCA11* mRNA upon *M. loti* infection required S*TY*-dependent functions (Figure 3.25) and *STYs* were regulated by *NF-YA1* (see Figure 3.1 and 3.8), this predicted that the two *YUCCA* genes are likely subjected to the

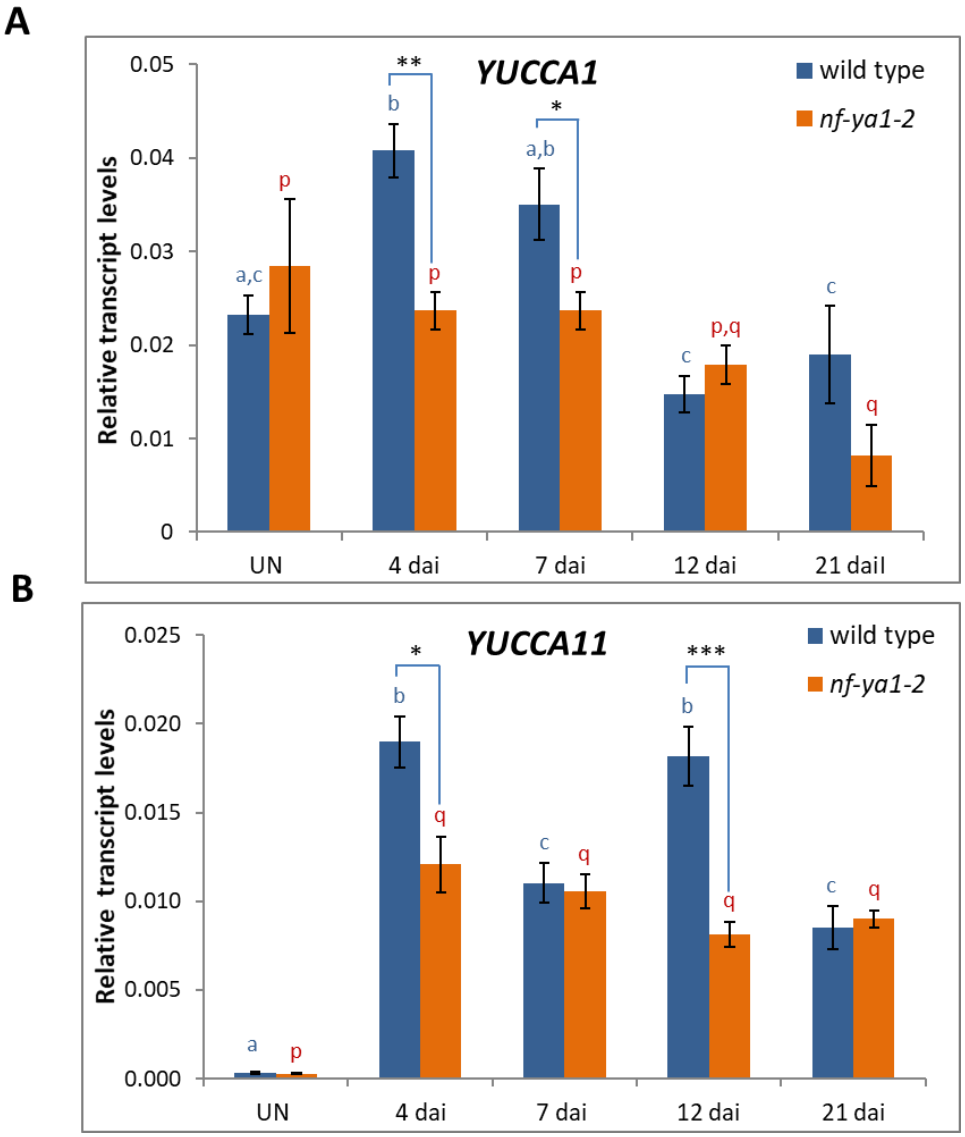

Figure 3.28 *NF-YA1* participates in the regulation of *YUCCA1* and *YUCCA11* expression upon *M. loti* infection. Quantitative RT-PCR data showing steady-state levels of *YUCCA1* (A) and *YUCCA11* (B) mRNAs in roots of *L. japonicus* wild-type (blue) and *nf-ya1-2* mutant (orange). The un-inoculated (UN) control roots and root samples collected at various time-points days after inoculation (dai) with *M. loti* were analyzed. The mean ± SE are given for three biological replicates. Small letters denote significant differences between time-points, as determined separately for each genotype by one-way ANOVA with post-hoc Tukey HSD; Asterisks denote significant differences in pair-wise comparisons between wild-type and *nf-ya1-2* mutant allele (Student's t-test: [*], $P < 0.05$; [**], $P < 0.01$; [***], $P < 0.001$).

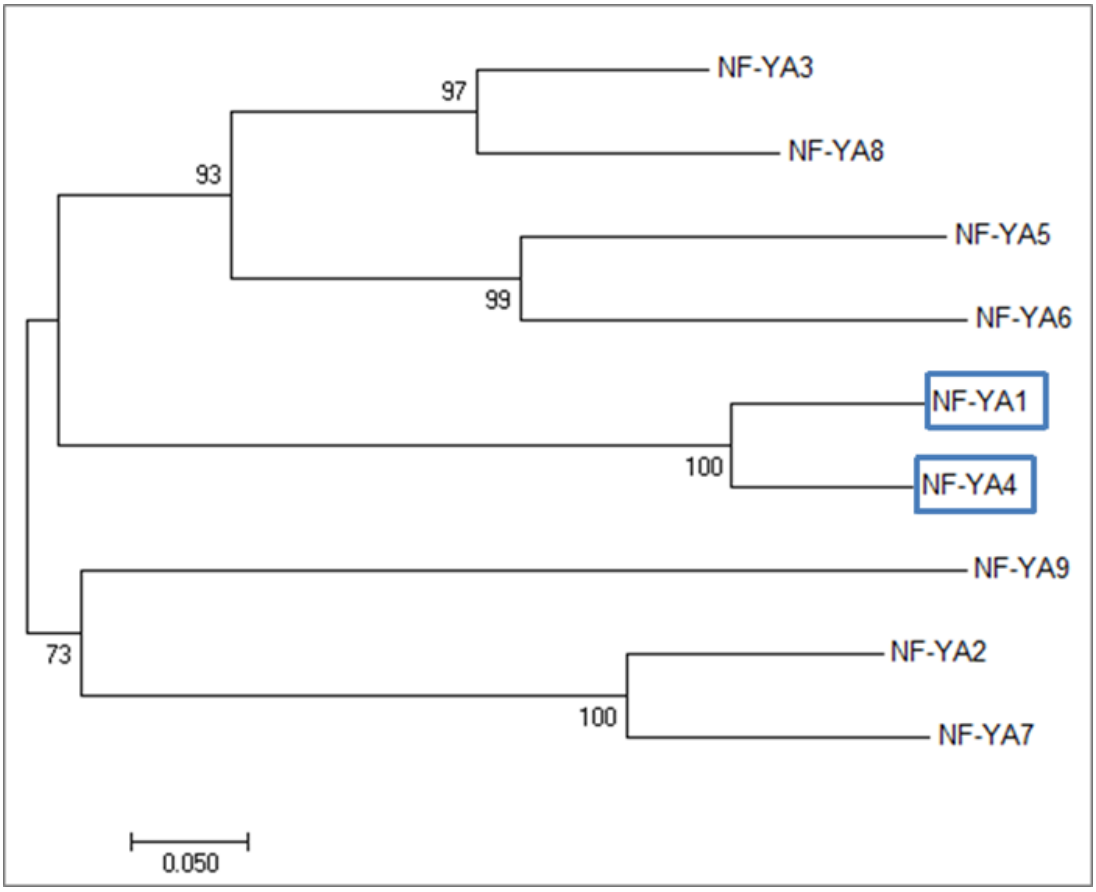

Figure 3.29 *L. japonicus* has nine predicted *NF-YA* genes. The relationship tree based on an amino acid alignment of predicted, full-length *L. japonicus* NF-YA proteins. NF-YA1 and its closest paralog, NF-YA4, are highlighted in blue boxes. The following accession numbers were used: LjNF-YA1 (Lj5g3v0841080.1; same as Genbank BAG50060.1); LjNF-YA2 (Lj6g3v0647470.1); LjNF-YA3 (Lj4g3v2179250.1); LjNF-YA4 (Lj1g3v4752710.1); LjNF-YA5 (Lj3g3v2657800.1); LjNF-YA6 (Lj3g3v0338970.1); LjNF-YA7 (Lj2g3v3336090.1); LjNF-YA8 (Lj0g3v0252369.1); LjNF-YA9 (deduced based on the predicted consensus sequence of three cDNAs with the following GenBank Accession. no: FS318732, FS333631 and FS360245). The protein sequences were aligned using ClustalW and the tree was generated using MEGA 7 (Molecular Evolutionary Genetics Analysis) software and neighbor-joining method with bootstrap replicates of 1000.

NF-YA1-dependent regulation. To test this assumption, qPCR experiments were carried out, comparing steady-state levels of *YUCCA1* and *YUCCA11* mRNA at various stages of nodule development in both wild-type and *nf-ya1-2* mutant roots.

Confirming previous data (see Figure 3.25), levels of *YUCCA1* and *YUCCA11* mRNAs were regulated upon *M. loti* infection (Figure 3.28). For *YUCCA1* this was most apparent at 4 dai, where the mRNA level was significantly upregulated above the control, un-inoculated roots and this was entirely dependent on *NF-YA1*. By contrast, levels of *YUCCA11* mRNA remained high in *M. loti* inoculated roots at all time-points analyzed, although they fluctuated significantly, being at their highest at 4 and 12 dai. Interestingly, reaching these relatively high levels required *NF-YA1*, while maintaining more modest levels at 7 and 21 dai time-points was *NF-YA1*-independent (Figure 3.28).

3.11 NF-YA1 and NF-YA4 regulate the *YUCCA11* gene expression in a partially redundant manner

Given that the *L. japonicus* genome contains ten *NF-YA* genes (Hossain et al., 2016), it was surmised that a partially redundantly operating *NF-YA* could be responsible for the observed incomplete dependency of the *YUCCA11* gene expression on *NF-YA1*. In the *L. japonicus* genome *NF-YA4* is the closest paralog of *NF-YA1* (Figure 3.29). Although dispensable for root nodule formation, the presence of the *nf-ya4-1* mutation potentiates the defective symbiotic phenotype of *nf-ya1-2*, indicating a partially redundant function of the two genes in this process (S. Zhong, L. Ross and K. Szczyglowski, unpublished data). It was, therefore, tested whether this is pertinent to *YUCCA1* and *YUCCA11* expression during symbiosis.

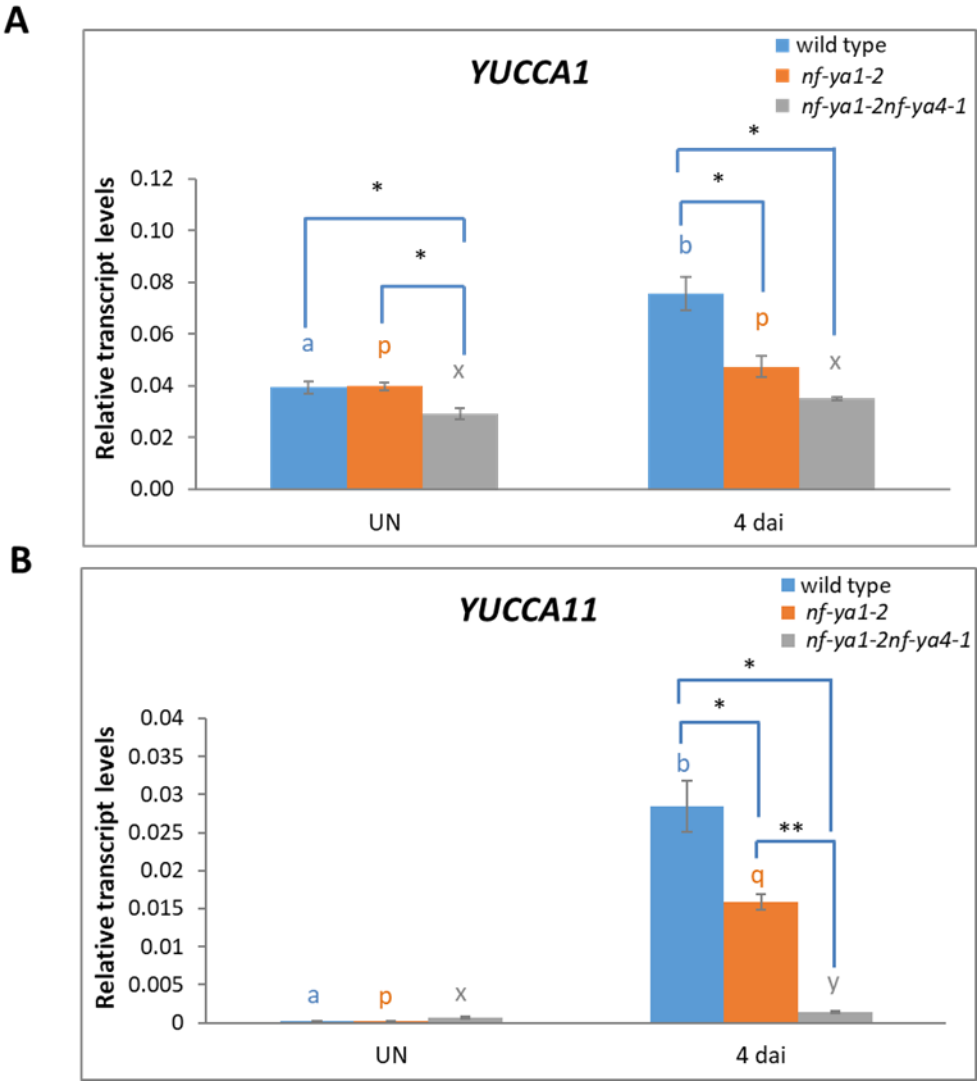

Figure 3.30 *NF-YA1* and *NF-YA4* work partially redundantly to regulate *YUCCA11* gene expression. Quantitative RT-PCR data showing steady-state levels of *YUCCA1* (A) and *YUCCA11* (B) mRNAs in roots of *L. japonicus* wild-type, *nf-ya1-2*, and *nf-ya1-2 nf-ya4-1* mutants. The un-inoculated (UN) control roots and root samples collected at 4 dai with *M. loti* were analyzed. The mean ± SE are given for three biological replicates. Small letters denote significant differences, as determined separately for each genotype by one-way ANOVA with post-hoc Tukey HSD; Asterisks (*) denote significant differences between wild-type and the mutants for the given treatment (Student's t-test: [*], $P < 0.05$; [**], $P < 0.01$.

qRT-PCR experiments were conducted in order to determine levels of the two *YUCCA* mRNAs in the *nf-ya1-2 nf-ya4-1* double mutant and compared them with corresponding mRNA levels in wild type and *nf-ya1-2* (Figure 3.30). At 4 dai with *M. loti*, the steady-state level of *YUCCA1* mRNA was significantly upregulated in wild-type but not in *nf-ya1-2* mutant roots, confirming our previous data (Figure 3.28). Absence of *NF-YA4*, in *nf-ya1-2 nfya4-1,* had no significant impact, such that levels of *YUCCA1* mRNA in the single and double mutants were similar (Figure 3.30). By contrast, the level of *YUCCA11* mRNA was further significantly diminished in *M. loti* inoculated *nf-ya1-2 nf-ya4* roots, well below the corresponding levels in the *nf-ya1-2* single mutant, even though it remained slightly elevated above the level in control, un-inoculated root.

CHAPTER 4

DISCUSSION

4.1 The *L. japonicus SHI/STY* gene family partakes in nodule formation

I show here that the *L. japonicus* genome contains a family of nine *STY/SHI* genes, called *STY1* to *STY9*, which are likely essential for the development of nitrogen-fixing root nodule symbiosis. My observations extend the initial microarray gene expression data (Hossain et al., 2016) by documenting that the activity of all nine *STY* genes is associated with nodule development, with seven of them being regulated by nodule-specific NF-YA1. Combined histochemical localization, RNA sequencing and qRT-PCR gene expression data suggest that the *STY* genes work in a highly redundant manner to regulate symbiosis. Only minor symbiotic defects were detected in single *sty* mutants and the *sty1-2 sty2-1 sty3-9* triple mutant also showed a weak nodulation phenotype. By contrast, expressing a presumed STY3::SRDX dominant negative protein led to a strong impairment in nodule development. By taking a candidate gene approach, I was able to identify two *YUCCA* genes, *YUCCA1* and *YUCCA11*, which are likely involved in auxin biosynthesis, as targets of STY-dependent regulation. Importantly, the same two *YUCCA* genes were found to be regulated by *M. loti* infection and this was dependent on *NF-YA1* and also, in the case of *YUCCA11*, on partially redundantly acting *NF-YA4*. Taken together, my data suggest a cascade of transcriptional reprogramming, wherein the NIN-dependent expression of a heterotrimeric transcription factor containing NF-YA1 activates *STYs*, which in turn regulate expression of the two *YUCCA* genes. I postulate that this leads to the generation of local auxin maxima that drive nodule differentiation, including cell expansion and vascular bundle formation, downstream from the initially formed foci of cortical cell divisions.

4.2 SHI/STY proteins and plant development

In *Arabidopsis*, the *SHI*/*STY* gene family comprises ten members, which includes *LATERAL ROOT PRIMORDIA 1* (*LRP1*), the first characterized member (Smith and Fedoroff, 1995) and *SHORT INTERNODE* (*SHI*), on which the original name of the family was based (Fridborg et al., 1999). The role that the SHI-related proteins, STY1 and STY2, and also several SRS (SHI-related sequences) play in promoting style formation during female reproduction organ development accounts for the second half (i.e. *STYLISH* or *STY*) of the family name (Kuusk et al., 2002; Kuusk et al., 2006).

The SHI/STY proteins are plant-specific transcriptional regulators that span a phylogenetic spectrum from *P. patens*, a moss, to mono- and dicotyledonous species (Fridborg et al., 2001). They were shown to be involved in a variety of processes, such as the development of lateral roots, stems, flowers, leaves, and siliques, primarily at the organ primordia formation stages. This promoted a hypothesis that they may regulate fundamental processes, such as cell proliferation and/or differentiation (Kuusk et al., 2006). Their involvement in modulating responses to gibberellin and/or contributing to auxin signalling has been well documented (Fridborg et al., 1999; Fridborg et al., 2001; Sohlberg et al., 2006; Staldal et al., 2008; Lutken et al., 2010). I show here that in *L. japonicus*, a model legume plant, *STY* genes are required for the differentiation of symbiotic root nodules and that this is mediated, at least in part, by their involvement in regulating *YUCCA1* and *YUCCA11* genes, presumably contributing to auxin biosynthesis.

4.3 *L. japonicus STY*s act in unison to mediate nodule formation

A remarkable feature of *SHI/STY* genes is their functional synergism and redundancy (Kuusk et al., 2006). Different *SHI/STY* paralogues have apparently retained their ancestral function and together with overlapping or partially overlapping expression domains, these characteristics are thought to account for the highly redundant manner with which they mediate various developmental processes (Kuusk et al., 2006). In *Arabidopsis*, at least six *SHI/STY* genes partake in carpel formation while five of the *SHI/STY* family genes, spanning different clades, regulate leaf development (Kuusk et al., 2006). The phenotypic features of single and higher order mutants indicate that members of the *Arabidopsi*s *SHI*/*STY* family act in a dosage-dependent manner and this has been considered as a protective mechanism against effects of dominant negative mutations, a notion for which some experimental support was found (Kuusk et al., 2006).

Here I show that the activity of all nine *L. japonicus STY* genes associates with root and nodule development. Like *Arabidopsis LRP1* (Smith and Fedoroff, 1995), *STY2* (Kuusk et al., 2002), *SRS5* (Kuusk et al., 2006) and *STY1* (Eklund et al., 2011), promoters of the *L. japonicus STY* genes all shared identical or highly overlapping domains of activity, comprising dividing pericyclic cells of young lateral root primordia. Furthermore, most of them remained active later during root development, including at the base of emerging and already emerged lateral roots. They were also operational in lateral root and main root apices, which resembled the expression pattern reported for *Arabidopsis SHI* (Fridborg et al., 2001).

The vastly overlapping if not identical activity domains, encompassing primordia and vasculature, were also apparent for the nine *L. japonicus STY* promoters during nodule

formation. However, unlike roots or carpels, nodules are dispensable plant organs. Thus, finding that all nine *STY* genes were recruited to the symbiotic program, where they appear to operate in a highly redundant manner, was surprising. SHI/STY proteins are known to form homo- and hetero-dimers (Eklund et al., 2010a) and based on the outcome of qRT-PCR experiments, all nine *L. japonicus STY* genes are expressed at a relatively low level. Hence, a dosage-dependency requirement for accurate SHI/STY protein functioning in protein complexes during nodule formation could be a contributing factor. On the other hand, selective constraints for maintaining the participation of such a large number of *SHI/STY* genes in the nodulation program may also be indirect, due to existing functional overlaps with other developmental programs, including lateral root formation.

4.4. *STY* gene expression is regulated by *NF-YA1* dependent and independent mechanisms

For seven of the *L. japonicus STY* genes, the steady-state level of their corresponding mRNAs was significantly upregulated upon *M. loti* infection. *STY1*, *STY2*, *STY3*, *STY7* and *STY8* were upregulated within the first 4 days after inoculation while *STY5* and *STY9* were upregulated during the following three days. The levels of the seven *STY* mRNAs peaked at around the 7 dai time-point, suggesting that a high dose of STY proteins may be needed shortly before or coincident with the onset of N_2-fixation. For at least some of the *STY*s, this relatively high level was maintained at later stages, and was associated with mature nodules and based on the obtained histochemical data, confined to the nodule vascular bundles.

Using an electrophoretic mobility shift assay, it was possible to demonstrate that *NF-YA1* could bind to *STY1*, *STY2* and *STY3* promoters *in vitro*, suggesting that they may be subjected to direct regulation by *NF-YA1*. Interestingly, qRT-PCR experiments, also demonstrated the existence of an *NF-YA1* independent mechanism(s), which positively impacted the steady-state levels of *STY* mRNAs. This was contingent on a particular time-point upon *M. loti* infection. Thus, *STY7* already showed both the *NF-YA1* dependent and independent modes of regulation at 4 dai, while for *STY1*, *STY2*, *STY3*, and *STY8* this became apparent only at 7 dai, and for *STY9* at the 12 dai time-point. The significance of these observations and the underlying mechanism remain unclear. However, some insight was possibly gleaned from *STY7*, for which the steady-state level of mRNA was already relatively high, in un-inoculated *L. japonicus* roots, prior to *M. loti* infection. This predicted the involvement of a non-symbiotic component(s) regulating the *STY7* gene expression. Interestingly in this context, I later found that *NF-YA4*, which is expressed in *L. japonicus* roots but is not regulated by *M. loti* infection (S. Zhong, L. Ross and K. Szczyglowski, unpublished data), acted partially redundantly with the nodule-specific *NF-YA1* to drive *YUCCA11* gene expression. It is conceivable that in addition to *NF-YA1* other *L. japonicus NF-YA* genes, such as *NF-YA4*, also partake in regulating *STY* gene expression, which could explain the observed mixed regulatory mechanism (see Figure 3.8). This assumption is currently being tested using available higher order *nf-ya* mutant lines, including the *nf-ya1-2 nf-ya4* double mutant.

4.5 Deleterious mutations at *STY* loci have only limited impact on symbiosis

Independent *L. japonicus* lines, each carrying a mutant allele at one of the five *STY* loci that showed the earliest responses to *M. loti* infection, were capable of developing wild-type or close to wild-type nodule numbers. However, with the exception of *sty3-9*, all of them showed a reduced number of nodule primordia. This was not well-correlated with the somewhat diminished growth of the mutant lines. Given that *STY1*, *STY7* and *STY8*, two independent LORE1 insertion lines were analyzed, showing a similar impact on nodule primordia formation, I have concluded that this was likely reflective of the role of the *STY* genes during symbiotic development. However, contradicting this notion was the observation that in the *sty1-2 sty2-1 sty3-9* triple mutant the number of nodule primordia was similar to wild-type, even though the nodule number was significantly decreased in the mutant. This apparent conundrum could be due to shortcomings of the triple mutant experiment. Wild-type plants, used as a control in this experiment, grew relatively poorly, underperforming by 30 to 50% the more typically observed *L. japonicus* symbiotic phenotype in terms of both nodule primordia and nodule numbers. Although relevant under any circumstance, repeating the experiment was clearly important but had to be postponed due to scarcity of the triple mutant seeds. Therefore, any further conclusions must await the completion of this part of the research. In the same context, it should be informative to evaluate phenotypes of the relevant quadruple and quintuple *sty* mutants, providing that such mutants will be viable and healthy. This remains of concern because the triple mutant showed significantly diminished root and shoot growth, which already complicates the interpretation of data.

4.6 STY3::SRDX blocks nodule formation

The essential role of *STY*s during *L. japonicus* root development was indirectly suggested by failure to obtain transgenic hairy roots expressing a presumed dominant negative STY3:SRDX chimeric protein under the control of the *UBIQUITIN* promoter. Similarly, a low nodulation phenotype or total lack of nodules in hairy roots and fully transgenic *L. japonicus* plants carrying the *LjNF-YA1*$_{Pro}$*:STY3::SRDX* construct, respectively, were indicative of an important role for these transcriptional regulators during nodule development. This also predicted that *STY3* and likely other redundantly acting *STY* genes must operate in the same cellular domain as NF-YA1, which was consistent with the histochemical data, as obtained for all *STY*s (see above) and also for the *NF-YA1* promoter (Hossain et al., 2016).

At 21 dai, T1 progeny derived from two independent fully transgenic *L. japonicus* plants carrying the *LjNF-YA1*$_{Pro}$*:STY3::SRDX* transgene developed nodule primordia but no nodules. This resembled the prevalent symbiotic phenotype of *nf-ya1* single mutants, where development of the majority of nodules was blocked at the primordium stage (Hossain et al., 2016), and was even more similar with the non-nodulating phenotype of the *nf-ya1-2 nf-ya4* double mutant (S. Zhong and K. Szczyglowski; unpublished data). However, from a purely numerical point of view, the *LjNF-YA1*$_{Pro}$*:STY3::SRDX* transgenic plants formed significantly less, while both *nf-ya1-2* and *nf-ya1-2 nf-ya4* mutants had significantly more nodule primordia than corresponding wild-type plants. This suggested that *STY*s are also likely to be essential early on during nodule primordia formation while *NF-YA1* and *NF-YA4* are not. However, expression of *NF-YA1* is induced within a few hours upon *M. loti* infection, prior to nodule primordium formation (Heckmann et al.,

2011). It is therefore conceivable that the role of *NF-YA1* at earlier stages during symbiosis is masked by redundantly acting paralogues (Hossain et al., 2016), which would have to be beyond the partially redundantly operating *NF-YA4*.

4.7 STY3::SRDX negatively impacts *M. loti* infection

The *LjNF-YA1$_{Pro}$:STY3::SRDX5 and LjNF-YA1$_{Pro}$:STY3::SRDX6* independent transgenic plants also exhibited a significant defect in *M. loti* infection. This was evidenced by strong attenuation of eIT formation. Neither *nf-ya1* (Hossain et al., 2016) nor *nf-ya4* (S. Zhong and K. Szczyglowski; unpublished data) had any detectable impairment in epidermal infections but the *nf-ya1 nf-ya4* double mutant did. It formed slightly but significantly less eITs and more microcolonies in comparison to wild type (S. Zhong and K. Szczyglowski; unpublished data). Thus, both *NF-YA* and *STY* genes could be relevant not only with respect to nodule developement but also for eIT formation. Consistent with this notion, *M. truncatula MtNF-YA1* and *MtNF-YA2*, presumed orthologs of *L. japonicus NF-YA1* and *NF-YA4*, respectively, were shown to be required for symbiotic infection (Laloum et al., 2014; Laporte et al., 2014). Their expression in *S. meliloti* inoculated *M. truncatula* plants was associated, but not causally related, with the activation of auxin and cell-cycle markers within the root epidermis. While the latter accompanied the onset of bacterial infection, the former was shown to be necessary for the initiation of eIT formation (Breakspear et al., 2014; Murray, 2017; Nadzieja et al., 2018). The observation that in *L. japonicus* both *NF-YA1* and *NF-YA4* are required to regulate *YUCCA* gene expression may be important in this context because this could provide for at least one mechanism by which the relevant auxin signalling is generated to support epidermal infections.

4.8 Both *NF-YA* and *STYs* are required for *YUCCA* gene expression

In addition to root epidermis, auxin responses are also known to precede and/or associate with nodule primordium formation (Mathesius et al., 2000b; Mathesius, 2008; Plet et al., 2011; Suzaki et al., 2012; Deinum et al., 2015) and exogenous application of polar auxin transport inhibitors to *M. sativa* (alfalfa) and *M. truncatula* roots was shown to induce nodule-like structures in the absence of rhizobia (Allen et al., 1953; Hirsch et al., 1989; Hirsch and Fang, 1994; Rightmyer and Long, 2011; Suzaki et al., 2013). A model has been proposed in which NF perception and the resulting LHK1-dependent activation of *NIN* expression in the root cortex lead to production of auxin maxima, which mediate nodule organogenesis; however, how NIN contributes to this process remained unresolved (Suzaki et al., 2012).

My work revealed a functional link between the *NIN*-regulated *NF-YA1* and the nodule-associated expression of *SHI/STY* genes. Members of the *Arabidopsis* SHI/STY transcription factor family were shown to regulate the auxin biosynthesis rates by acting as DNA-binding transcriptional activators of *YUCCA4* and *YUCCA8* genes (Kuusk et al., 2002; Kuusk et al., 2006; Sohlberg et al., 2006; Eklund et al., 2010a; Eklund et al., 2010b; Baylis et al., 2013). The identification of the two *L. japonicus* YUCCA genes, *YUCCA1* and *YUCCA11*, as targets of the *NF-YA1/STY* dependent regulation strongly indicates that this signalling pathway may be responsible, at least in part, for auxin production during nodule organogenesis (Figure 4.1).

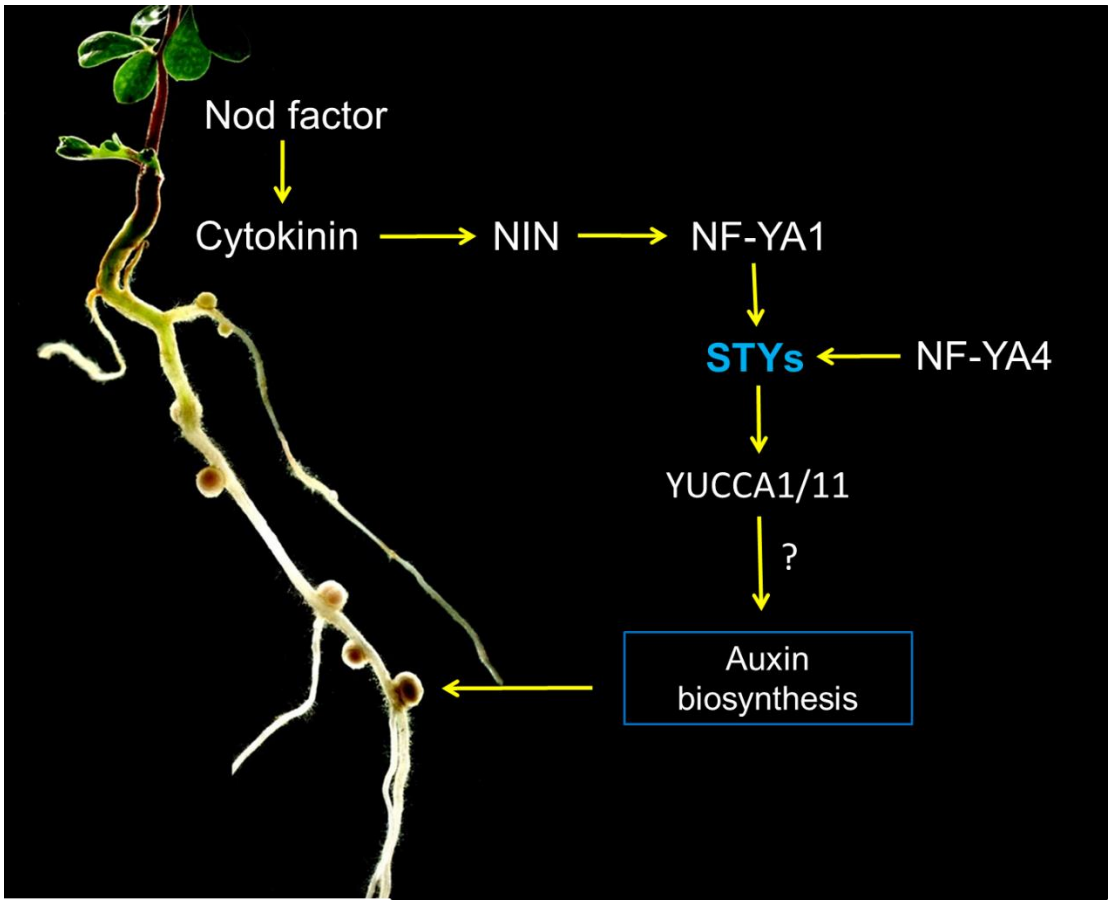

Figure 4.1 A working model for the NF-YA1/STY dependent regulation of nodule organogenesis in a model legume, *L. japonicus*. Perception of *M. loti*-derived nodulation factors by *L. japonicus* roots triggers accumulation of bioactive cytokinins and leads to expression of the NODULE INCEPTION transcriptional regulator NIN. NIN mediates downstream reprogramming, including expression of a nodule-specific *NF-YA1*, which is associated with the initial cell divisions for nodule primordia formation. As a component of a heterotrimeric transcriptional regulator, NF-YA1 regulates expression of *STY* genes, presumably in a partially redundant manner with other NF-YAs, such as NF-YA4. This, in turn, activates *YUCCA* gene expression. YUCCA1 and YUCCA11 are presumed to carry out auxin biosynthesis, which is required for differentiation of fully functional, N_2-fixing nodules.

4.9 Nodule differentiation is mediated by *STY*s

In addition to *YUCCA*s, other targets for the STY1-dependent regulation were characterized in *Arabidopsis*. These included genes involved in cell wall loosening and cell expansion and also genes encoding several different transcription factors, such as those belonging to the APETALA2/Ethylene Responsive Factor (AP2/ERF) protein family (Staldal et al., 2012). In legumes, members of the *AP2*/*ERF* gene family play an important role during both symbiotic infection and nodule formation (Andriankaja et al., 2007; Kawaharada et al., 2017a) and one of the *L. japonicus AP2/ERF* genes was characterized as a target of the *NF-YA1*-dependent regulation (Hossain et al., 2016). Whether this is direct or requires *STY*s as intermediaries remains an interesting question for future investigations.

Determinate nodules formed by *L. japonicus* and also by *Glycine max* (soybean) and *P. vulgaris* (common bean), lack the persistent meristem. After several rounds of cell divisions, which initiate nodule organogenesis, subsequent progress toward a functional N_2-fixing organ is primarily reliant on cellular differentiation (Islas-Flores et al., 2011; Li et al., 2015). This encompasses several interlinked events, such as increase in cell ploidy (endoreduplication) and cell expansion, as well as formation of nodule vascular bundles (Kondorosi and Kondorosi, 2004; González-Sama et al., 2006).

In *Arabidopsis*, *SHI/STY* genes have been implicated as regulators of leaf venation by contributing to local auxin maxima (Baylis et al., 2013). Auxins also have a complex, concentration-dependent role in regulating root cell expansion (Barbez et al., 2017; Majda and Robert, 2018) and together with cytokinins have long been known to be consequential for the early establishment of root vascular tissues (De Rybel et al., 2015). Their role in the development of the *L. japonicus* nodule vasculature and lenticels was also documented

(Takanashi et al., 2011; Suzaki et al., 2012). We previously showed that *NF-YA1* participates in the differentiation of nodule structure, including cell expansion and formation of nodule vascular bundles (Hossain et al., 2016). Presence of cell divisions but lack of any subsequent nodule development in STY3::SRDX expressing transgenic plants support the notion that *STY*s are likely pertinent in the same context as *NF-YA1*. This is further accentuated by the overlapping expression domains, including vascular bundles of mature nodules, for *NF-YA1*, *STY*s, *YUCCA1/11* and also for LHK1 (Held et al., 2014; Hossain et al., 2016). The regulatory relationships uncovered by this work suggest that these genes are likely constituents of the same transduction pathway, which leads to auxin-dependent differentiation of functional nodules (Figure 4.1). However, further research is necessary to more directly demonstrate the involvement of *NF-YA1*, *STYs* and the two *YUCCA* genes in this important signalling circuit.

PERSPECTIVES AND CONCLUSIONS

My thesis work has focused on deciphering the role of the *L. japonicus SHI*/*STY* gene family during symbiotic root nodule development. This was prompted by the initial observation that expression of at least three members of the family is regulated by a nodule specific transcription factor containing NF-YA1 (Hossain et al., 2016). I showed that *SHI/STY* genes are indeed important during root nodule development in *L. japonicus* while also providing the first comprehensive description of *SHI/STY* genes in a legume plant. My results indicate that *SHI*/*STY* participate in lateral root development and also in a mostly legume-specific transcriptional reprograming that begins with the perception of rhizobia-derived NF at the root surface and culminates with the formation of nitrogen-fixing root nodules.

Initially, my aim was to characterize the three *STY* genes, *STY1*, *STY2* and *STY3*, which were defined by previous work in our laboratory as being targeted by NF-YA1. By advancing the research, I ended up characterizing nine *STY* genes, which all apparently participate in nodule formation. This was challenging, especially with regard to functional studies, where achieving absence or significant decline in STY-related functions was difficult due to their apparent redundancy. A dominant negative approach, using SRDX, turned out to be informative. Nonetheless, other experiments are in progress to further solidify current predictions. In addition to building higher order *sty* mutant lines, with possible pitfalls due to anticipated pleiotropic effects, a new chimeric construct expressing a truncated STY3 protein, deprived of the IGGH domain ($STY3^{Truncated}$), under the control of a nodule-specific *NF-YA1* promoter is being prepared and will be used in order to determine whether a dominant negative effect could also be obtained in this way. A similar

approach was successful in *Arabidopsi*s (Kuusk et al., 2006) and, in the context of *L. japonicus*-*M. loti* symbiosis, this could provide important additional support for my conclusions, as made thus far based on the SRDX domain-containing construct. Furthermore, obtaining stable transgenic lines with a nodule-specific decline in STY function(s), either through SRDX or $STY3^{Truncated}$, is important because it will open the possibility of identifying downstream targets of STYs on the genome-wide scale but in a nodule-specific context. When compared to transcriptomic data from *sty* mutant roots, those yet to be identified as carrying a set of *sty* mutations that lead to a significant defect in nodule formation, this could allow for determining whether nodule specific targets other than *YUCCA11* exist and ascertaining the magnitude of the overlap between root (lateral root) and nodule-specific *STY* functions.

The identification of *YUCCA1* and *YUCCA11* as potential downstream targets of *STY*-dependent regulation was exciting because it provided further support for the postulated participation of *NF-YA1* in the generation of auxin maxima downstream from the NF-induced cytokinin signalling (Hossain et al., 2016). However, additional work is needed to directly demonstrate that this relationship indeed exists. Two experiments are currently under way. Firstly, the already available transgenic *L. japonicus* plants carrying the *DR5*:*GUS* auxin reporter (H. Hou, L. Ross and K. Szczyglowski; unpublished data) in the otherwise wild-type and *nf-ya1* mutant backgrounds will be comparatively evaluated using a histochemical approach. This should demonstrate whether significant differences in the activity of the reporter, as associated with either wild-type or the mutant nodule development, are detectable. Secondly, the *YUCCA11* mRNA will be expressed under the control of the *proAtCortex* promoter in the *L. japonicus DR5*:*GUS* reporter line. Derived

from the *Arabidopsis thaliana* aspartyl protease-encoding gene, *proAtCortex* has root cortex-specific activity in *L. japonicus* (Gavrilovic et al., 2016) and was recently used to successfully complement the symbiotic defect of the *lhk1-1* mutation (Miri et al., 2019). If the availability of YUCCA11 limits auxin production in roots, its ectopic production should be reflected in enhanced *DR5*:*GUS* reporter activity. At the same time, within the same experiment, it will be possible to determine whether the ectopic expression of *YUCCA11* in the root cortex will induce cell divisions. As *proAtCortex* is constitutively expressed in the root cortex, an inducible variant is also being prepared (Siligato et al., 2016) to limit global effects and to see whether a spatiotemporal regulation of *YUCCA11* expression would lead to nodule primordia formation.

Like *STYs*, *YUCCA* genes are known to work in a redundant manner (Cheng et al., 2006); hence building a higher order *L. japonicus yucca* mutant line could be informative. Also, it will be interesting to determine whether *L. japonicus sty* and/or *yucca* mutants suffer from defective AM symbiosis. Auxin signalling was shown to be essential for arbuscule formation (Etemadi et al., 2014). Therefore, involvement of *STYs* and *YUCCAs* in this more ubiquitous symbiosis is conceivable.

In summary, my research has opened a new line of investigation toward the main goal of understanding the mechanisms that mediate nodule formation in legumes. It is clear that upon activation by NF, an interplay between ubiquitous plant hormones, cytokinin and auxin, mediates nodule formation, with the former serving as the main plant endogenous stimuli that initiates the entire process (Gamas et al., 2017). Further insight will likely define the reason why most non-leguminous plants are unable to carry out nodule organogenesis in response to cytokinin signalling. This should bring the ultimate goal of

engineering functional nitrogen-fixing symbiosis in important non-legume crops closer to reality, thus possibly advancing the next Green Revolution.

BIBLIOGRAPHY

Allen, E.K., Allen, O.N., and Newman, A.S. (1953). Pseudonodulation of leguminous plants induced by 2-bromo-3,5-dichlorobenzoic acid. Am J Bot **40,** 429-435.

Andriankaja, A., Boisson-Dernier, A., Frances, L., Sauviac, L., Jauneau, A., Barker, D.G., and de Carvalho-Niebel, F. (2007). AP2-ERF transcription factors mediate Nod factor dependent *Mt ENOD11* activation in root hairs via a novel cis-regulatory motif. Plant Cell **19,** 2866-2885.

Ané, J.M., Kiss, G.B., Riely, B.K., Penmetsa, R.V., Oldroyd, G.E.D., Ayax, C., Lévy, J., Debellé, F., Baek, J.M., Kalo, P., Rosenberg, C., Roe, B.A., Long, S.R., Dénarié, J., and Cook, D.R. (2004). *Medicago truncatula* DMI1 required for bacterial and fungal symbioses in legumes. Science **303,** 1364-1367.

Arrighi, J.F., Barre, A., Ben Amor, B., Bersoult, A., Soriano, L.C., Mirabella, R., de Carvalho-Niebel, F., Journet, E.P., Gherardi, M., Huguet, T., Geurts, R., Denarie, J., Rouge, P., and Gough, C. (2006). The *Medicago truncatula* lysin motif-receptor-like kinase gene family includes NFP and new nodule-expressed genes. Plant Physiol **142,** 265-279.

Barbez, E., Dunser, K., Gaidora, A., Lendl, T., and Busch, W. (2017). Auxin steers root cell expansion via apoplastic pH regulation in *Arabidopsis thaliana*. Proc Natl Acad Sci U S A **114,** E4884-e4893.

Battaglia, M., Ripodas, C., Clua, J., Baudin, M., Aguilar, O.M., Niebel, A., Zanetti, M.E., and Blanco, F.A. (2014). A nuclear factor Y interacting protein of the GRAS family is required for nodule organogenesis, infection thread progression, and lateral root growth. Plant Physiol **164,** 1430-1442.

Bauer, P., Ratet, P., Crespi, M.D., Schultze, M., and Kondorosi, A. (1996). Nod factors and cytokinins induce similar cortical cell division, amyloplast deposition and MsEnoD12A expression patterns in alfalfa roots. Plant J **10,** 91-105.

Baylis, T., Cierlik, I., Sundberg, E., and Mattsson, J. (2013). *SHORT INTERNODES*/*STYLISH* genes, regulators of auxin biosynthesis, are involved in leaf vein development in *Arabidopsis thaliana*. New Phytol **197,** 737-750.

Bishopp, A., and Lynch, J.P. (2015). The hidden half of crop yields. Nat Plants **1,** 15117.

Boivin, S., Kazmierczak, T., Brault, M., Wen, J., Gamas, P., Mysore, K.S., and Frugier, F. (2016). Different cytokinin histidine kinase receptors regulate nodule initiation as well as later nodule developmental stages in *Medicago truncatula*. Plant Cell Environ **39,** 2198-2209.

Bonfante, P., and Genre, A. (2010). Mechanisms underlying beneficial plant-fungus interactions in mycorrhizal symbiosis. Nat Commun **1,** 48.

Borden, K.L. (2000). RING domains: master builders of molecular scaffolds? J Mol Biol **295,** 1103-1112.

Borisov, A.Y., Madsen, L.H., Tsyganov, V.E., Umehara, Y., Voroshilova, V.A., Batagov, A.O., Sandal, N., Mortensen, A., Schauser, L., Ellis, N., Tikhonovich, I.A., and Stougaard, J. (2003). The *Sym35* gene required for root nodule development in pea is an ortholog of *Nin* from *Lotus japonicus*. Plant Physiol **131,** 1009-1017.

Breakspear, A., Liu, C., Roy, S., Stacey, N., Rogers, C., Trick, M., Morieri, G., Mysore, K.S., Wen, J., Oldroyd, G.E., Downie, J.A., and Murray, J.D. (2014). The root hair "infectome" of *Medicago truncatula* uncovers changes in cell cycle genes and reveals a requirement for Auxin signaling in rhizobial infection. Plant Cell **26,** 4680-4701.

Broghammer, A., Krusell, L., Blaise, M., Sauer, J., Sullivan, J.T., Maolanon, N., Vinther, M., Lorentzen, A., Madsen, E.B., Jensen, K.J., Roepstorff, P., Thirup, S., Ronson, C.W., Thygesen, M.B., and Stougaard, J. (2012). Legume receptors perceive the rhizobial lipochitin oligosaccharide signal molecules by direct binding. Proc Natl Acad Sci U S A **109,** 13859-13864.

Broughton, W.J., and Dilworth, M.J. (1971). Control of leghaemoglobin synthesis in snake beans. Biochem J **125,** 1075-1080.

Cabeza, R., Koester, B., Liese, R., Lingner, A., Baumgarten, V., Dirks, J., Salinas-Riester, G., Pommerenke, C., Dittert, K., and Schulze, J. (2014). An RNA sequencing transcriptome analysis reveals novel insights into molecular aspects of the nitrate impact on the nodule activity of *Medicago truncatula*. Plant Physiol **164,** 400-411.

Carroll, B.J., and Gresshoff, P.M. (1983). Nitrate inhibition of nodulation and Nitrogen fixation in white clover. Zeitschrift für Pflanzenphysiologie **110,** 77-88.

Chabaud, M., Gherbi, H., Pirolles, E., Vaissayre, V., Fournier, J., Moukouanga, D., Franche, C., Bogusz, D., Tisa, L.S., Barker, D.G., and Svistoonoff, S. (2016). Chitinase-resistant hydrophilic symbiotic factors secreted by *Frankia* activate both Ca(2+) spiking and *NIN* gene expression in the actinorhizal plant *Casuarina glauca*. New Phytol **209,** 86-93.

Chardin, C., Girin, T., Roudier, F., Meyer, C., and Krapp, A. (2014). The plant RWP-RK transcription factors: key regulators of nitrogen responses and of gametophyte development. J Exp Bot **65,** 5577-5587.

Charpentier, M., Bredemeier, R., Wanner, G., Takeda, N., Schleiff, E., and Parniske, M. (2008). *Lotus japonicus* CASTOR and POLLUX are ion channels essential for perinuclear calcium spiking in legume root endosymbiosis. Plant Cell **20,** 3467-3479.

Charpentier, M., Sun, J., Vaz Martins, T., Radhakrishnan, G.V., Findlay, K., Soumpourou, E., Thouin, J., Very, A.A., Sanders, D., Morris, R.J., and Oldroyd, G.E. (2016). Nuclear-localized cyclic nucleotide-gated channels mediate symbiotic calcium oscillations. Science **352,** 1102-1105.

Cheng, Y., Dai, X., and Zhao, Y. (2006). Auxin biosynthesis by the YUCCA flavin monooxygenases controls the formation of floral organs and vascular tissues in *Arabidopsis*. Genes Dev **20,** 1790-1799.

Clavijo, F., Diedhiou, I., Vaissayre, V., Brottier, L., Acolatse, J., Moukouanga, D., Crabos, A., Auguy, F., Franche, C., Gherbi, H., Champion, A., Hocher, V., Barker, D., Bogusz, D., Tisa, L.S., and Svistoonoff, S. (2015). The *Casuarina NIN* gene is transcriptionally activated throughout *Frankia* root infection as well as in response to bacterial diffusible signals. New Phytol **208,** 887-903.

Coba de la Pena, T., Fedorova, E., Pueyo, J.J., and Lucas, M.M. (2017). The Symbiosome: Legume and rhizobia co-evolution toward a nitrogen-fixing organelle? Front Plant Sci **8,** 2229.

Combier, J.P., de Billy, F., Gamas, P., Niebel, A., and Rivas, S. (2008). Trans-regulation of the expression of the transcription factor *MtHAP2-1* by a uORF controls root nodule development. Genes Dev **22,** 1549-1559.

Combier, J.P., Frugier, F., de Billy, F., Boualem, A., El-Yahyaoui, F., Moreau, S., Vernie, T., Ott, T., Gamas, P., Crespi, M., and Niebel, A. (2006). MtHAP2-1 is a key transcriptional regulator of symbiotic nodule development regulated by microRNA169 in *Medicago truncatula*. Genes Dev **20,** 3084-3088.

Cooper, J.B., and Long, S.R. (1994). Morphogenetic rescue of *Rhizobium meliloti* nodulation mutants by trans-zeatin secretion. Plant Cell **6,** 215-225.

Corradi, N., and Bonfante, P. (2012). The arbuscular mycorrhizal symbiosis: origin and evolution of a beneficial plant infection. PLoS Pathog **8,** e1002600.

Curatti, L., and Rubio, L.M. (2014). Challenges to develop nitrogen-fixing cereals by direct *nif*-gene transfer. Plant Sci **225,** 130-137.

De Rybel, B., Mähönen, A.P., Helariutta, Y., and Weijers, D. (2015). Plant vascular development: from early specification to differentiation. Nature Reviews Molecular Cell Biology **17,** 30.

Deinum, E.E., Geurts, R., Hartog, M., Bisseling, T., and Mulder, B.M. (2015). Computational and experimental evidence that auxin accumulation in nodule and lateral root primordia occurs by different mechanisms. Biological Nitrogen Fixation**,** 659-668.

Delves, A.C., Mathews, A., Day, D.A., Carter, A.S., Carroll, B.J., and Gresshoff, P.M. (1986). Regulation of the soybean-*Rhizobium* nodule symbiosis by shoot and root factors. Plant Physiol **82,** 588-590.

Dolfini, D., Gatta, R., and Mantovani, R. (2012). NF-Y and the transcriptional activation of CCAAT promoters. Crit Rev Biochem Mol Biol **47,** 29-49.

Doyle, J.J. (2011). Phylogenetic perspectives on the origins of nodulation. Mol. Plant-Microbe Interact **24,** 1289-1295.

Duc, G., Trouvelot, A., Gianinazzi-Pearson, V., and Gianinazzi, S. (1989). First report of non-mycorrhizal plant mutants (Myc-) obtained in pea (*Pisum sativum* L.) and fababean (*Vicia faba* L.). Plant Sci **60,** 215-222.

Ehrhardt, D.W., Wais, R., and Long, S.R. (1996). Calcium spiking in plant root hairs responding to *Rhizobium* nodulation signals. Cell **85,** 673-681.

Eklund, D.M., Cierlik, I., Ståldal, V., Claes, A.R., Vestman, D., Chandler, J., and Sundberg, E. (2011). Expression of *Arabidopsis SHORT INTERNODES/STYLISH* family genes in auxin biosynthesis zones of aerial organs is dependent on a GCC box-like regulatory element. Plant Physiol **157,** 2069-2080.

Eklund, D.M., Staldal, V., Valsecchi, I., Cierlik, I., Eriksson, C., Hiratsu, K., Ohme-Takagi, M., Sundstrom, J.F., Thelander, M., Ezcurra, I., and Sundberg, E. (2010a). The *Arabidopsis thaliana* STYLISH1 protein acts as a transcriptional activator regulating auxin biosynthesis. Plant Cell **22,** 349-363.

Eklund, D.M., Thelander, M., Landberg, K., Staldal, V., Nilsson, A., Johansson, M., Valsecchi, I., Pederson, E.R., Kowalczyk, M., Ljung, K., Ronne, H., and Sundberg, E. (2010b). Homologues of the *Arabidopsis thaliana SHI/STY/LRP1* genes control auxin biosynthesis and affect growth and development in the moss *Physcomitrella patens*. Development **137,** 1275-1284.

Endre, G., Kereszt, A., Kevei, Z., Mihacea, S., Kalo, P., and Kiss, G.B. (2002). A receptor kinase gene regulating symbiotic nodule development. Nature **417,** 962-966.

Erisman, J.W., Sutton, M.A., Galloway, J., Klimont, Z., and Winiwarter, W. (2008). How a century of ammonia synthesis changed the world. Nature Geoscience **1,** 636.

Etemadi, M., Gutjahr, C., Couzigou, J.M., Zouine, M., Lauressergues, D., Timmers, A., Audran, C., Bouzayen, M., Becard, G., and Combier, J.P. (2014). Auxin perception is required for arbuscule development in arbuscular mycorrhizal symbiosis. Plant Physiol **166,** 281-292.

Falkowski, P.G. (1997). Evolution of the nitrogen cycle and its influence on the biological sequestration of CO2 in the ocean. Nature **387,** 272-275.

Fang, Y., and Hirsch, A.M. (1998). Studying early nodulin gene *ENOD40* expression and induction by nodulation factor and cytokinin in transgenic alfalfa. Plant Physiol **116,** 53-68.

Foley, J.A., Ramankutty, N., Brauman, K.A., Cassidy, E.S., Gerber, J.S., Johnston, M., Mueller, N.D., O'Connell, C., Ray, D.K., West, P.C., Balzer, C., Bennett, E.M., Carpenter, S.R., Hill, J., Monfreda, C., Polasky, S., Rockstrom, J., Sheehan, J., Siebert, S., Tilman, D., and Zaks, D.P. (2011). Solutions for a cultivated planet. Nature **478,** 337-342.

Forde, B.G. (2009). Is it good noise? The role of developmental instability in the shaping of a root system. J Exp Bot **60,** 3989-4002.

Forde, B.G., and Clarkson, D.T. (1999). Nitrate and ammonium nutrition of plants: Physiological and molecular perspectives. Adv. Bot. Res. **30,** 1-90.

Fournier, J., Teillet, A., Chabaud, M., Ivanov, S., Genre, A., Limpens, E., de Carvalho-Niebel, F., and Barker, D.G. (2015). Remodeling of the infection chamber before infection thread formation reveals a two-step mechanism for rhizobial entry into the host legume root hair. Plant Physiol **167,** 1233-1242.

Franco-Zorrilla, J.M., Lopez-Vidriero, I., Carrasco, J.L., Godoy, M., Vera, P., and Solano, R. (2014). DNA-binding specificities of plant transcription factors and their potential to define target genes. Proc Natl Acad Sci U S A **111,** 2367-2372.

Fred, E.B., and Graul, E.J. (1916). The effect of soluble nitrogenous salts on nodule formation. Journal of the American Society of Agronomy**,** 316-328.

Freemont, P.S. (1993). The RING finger. A novel protein sequence motif related to the zinc finger. Ann N Y Acad Sci **684,** 174-192.

Fridborg, A., Kuusk, S., Moritz, T., and Sundberg, E. (1999). The *Arabidopsis* dwarf mutant *shi* exhibits reduced gibberellin responses conferred by overexpression of a new putative zinc finger protein. Plant Cell **11,** 1019-1031.

Fridborg, I., Kuusk, S., Robertson, M., and Sundberg, E. (2001). The *Arabidopsis* protein SHI represses gibberellin responses in *Arabidopsis* and barley. Plant Physiol **127,** 937-948.

Fried, M.G. (1989). Measurement of protein-DNA interaction parameters by electrophoresis mobility shift assay. Electrophoresis **10,** 366-376.

Frugier, F., Kosuta, S., Murray, J.D., Crespi, M., and Szczyglowski, K. (2008). Cytokinin: secret agent of symbiosis. Trends Plant Sci **13,** 115-120.

Fukai, E., Soyano, T., Umehara, Y., Nakayama, S., Hirakawa, H., Tabata, S., Sato, S., and Hayashi, M. (2012). Establishment of a *Lotus japonicus* gene tagging

population using the exon-targeting endogenous retrotransposon *LORE1*. Plant J **69,** 720-730.

Gamas, P., Brault, M., Jardinaud, M.F., and Frugier, F. (2017). Cytokinins in symbiotic nodulation: when, where, what for? Trends Plant Sci **22,** 792-802.

Gavrilovic, S., Yan, Z., Jurkiewicz, A.M., Stougaard, J., and Markmann, K. (2016). Inoculation insensitive promoters for cell type enriched gene expression in legume roots and nodules. Plant Methods **12**.

Genre, A., Chabaud, M., Balzergue, C., Puech-Pages, V., Novero, M., Rey, T., Fournier, J., Rochange, S., Becard, G., Bonfante, P., and Barker, D.G. (2013). Short-chain chitin oligomers from arbuscular mycorrhizal fungi trigger nuclear Ca2+ spiking in *Medicago truncatula* roots and their production is enhanced by strigolactone. New Phytol **198,** 190-202.

Gent, L., and Forde, B.G. (2017). How do plants sense their nitrogen status? J Exp Bot **68,** 2531-2539.

Gewin, V. (2010). Food: An underground revolution. Nature **466,** 552-553.

Giehl, R.F., Gruber, B.D., and von Wiren, N. (2014). It's time to make changes: modulation of root system architecture by nutrient signals. J Exp Bot **65,** 769-778.

Gobbato, E., Marsh, J.F., Vernie, T., Wang, E., Maillet, F., Kim, J., Miller, J.B., Sun, J., Bano, S.A., Ratet, P., Mysore, K.S., Denarie, J., Schultze, M., and Oldroyd, G.E. (2012). A GRAS-type transcription factor with a specific function in mycorrhizal signaling. Curr Biol **22,** 2236-2241.

Gomariz-Fernandez, A., Sanchez-Gerschon, V., Fourquin, C., and Ferrandiz, C. (2017). The role of *SHI/STY/SRS* genes in organ growth and carpel development is conserved in the distant eudicot species *Arabidopsis thaliana* and *Nicotiana benthamiana*. Front Plant Sci **8,** 814.

Gonzalez-Rizzo, S., Crespi, M., and Frugier, F. (2006). The *Medicago truncatula* CRE1 cytokinin receptor regulates lateral root development and early symbiotic interaction with *Sinorhizobium meliloti*. Plant Cell **18,** 2680-2693.

González-Sama, A., De La Peña, T.C., Kevei, Z., Mergaert, P., Lucas, M.M., De Felipe, M.R., Kondorosi, E., and Pueyo, J.J. (2006). Nuclear DNA endoreduplication and expression of the mitotic inhibitor Ccs52 associated to determinate and lupinoid nodule organogenesis. Mol. Plant-Microbe Interact **19,** 173-180.

Good, A.G., and Beatty, P.H. (2011). Fertilizing nature: a tragedy of excess in the commons. PLoS Biol **9,** e1001124.

Govindarajulu, M., Pfeffer, P.E., Jin, H., Abubaker, J., Douds, D.D., Allen, J.W., Bucking, H., Lammers, P.J., and Shachar-Hill, Y. (2005). Nitrogen transfer in the arbuscular mycorrhizal symbiosis. Nature **435,** 819-823.

Griesmann, M., Chang, Y., Liu, X., Song, Y., Haberer, G., Crook, M.B., Billault-Penneteau, B., Lauressergues, D., Keller, J., Imanishi, L., Roswanjaya, Y.P., Kohlen, W., Pujic, P., Battenberg, K., Alloisio, N., Liang, Y., Hilhorst, H., Salgado, M.G., Hocher, V., Gherbi, H., Svistoonoff, S., Doyle, J.J., He, S., Xu, Y., Xu, S., Qu, J., Gao, Q., Fang, X., Fu, Y., Normand, P., Berry, A.M., Wall, L.G., Ane, J.M., Pawlowski, K., Xu, X., Yang, H., Spannagl, M., Mayer, K.F.X., Wong, G.K., Parniske, M., Delaux, P.M., and Cheng, S. (2018). Phylogenomics reveals multiple losses of nitrogen-fixing root nodule symbiosis. Science **361**.

Groth, M., Takeda, N., Perry, J., Uchida, H., Draxl, S., Brachmann, A., Sato, S., Tabata, S., Kawaguchi, M., Wang, T.L., and Parniske, M. (2010). *NENA*, a *Lotus japonicus* homolog of *Sec13*, is required for rhizodermal infection by arbuscular mycorrhiza fungi and rhizobia but dispensable for cortical endosymbiotic development. Plant Cell **22,** 2509-2526.

Guillotin, B., Couzigou, J.M., and Combier, J.P. (2016). NIN is involved in the regulation of arbuscular mycorrhizal symbiosis. Front Plant Sci **7,** 1704.

Handberg, K., and Stougaard, J. (1992). *Lotus japonicus*, an autogamous, diploid legume species for classical and molecular genetics. Plant J **2,** 487-496.

Hayashi, T., Banba, M., Shimoda, Y., Kouchi, H., Hayashi, M., and Imaizumi-Anraku, H. (2010). A dominant function of CCaMK in intracellular accommodation of bacterial and fungal endosymbionts. Plant J **63,** 141-154.

Heckmann, A.B., Sandal, N., Bek, A.S., Madsen, L.H., Jurkiewicz, A., Nielsen, M.W., Tirichine, L., and Stougaard, J. (2011). Cytokinin induction of root nodule primordia in *Lotus japonicus* is regulated by a mechanism operating in the root cortex. Mol. Plant-Microbe Interact **24,** 1385-1395.

Held, M., Hossain, M.S., Yokota, K., Bonfante, P., Stougaard, J., and Szczyglowski, K. (2010). Common and not so common symbiotic entry. Trends Plant Sci **15,** 540-545.

Held, M., Hou, H., Miri, M., Huynh, C., Ross, L., Hossain, M.S., Sato, S., Tabata, S., Perry, J., Wang, T.L., and Szczyglowski, K. (2014). *Lotus japonicus* cytokinin receptors work partially redundantly to mediate nodule formation. Plant Cell **26,** 678-694.

Hiratsu, K., Matsui, K., Koyama, T., and Ohme-Takagi, M. (2003). Dominant repression of target genes by chimeric repressors that include the EAR motif, a repression domain, in *Arabidopsis*. Plant J **34,** 733-739.

Hirsch, A.M., and Fang, Y. (1994). Plant hormones and nodulation: what's the connection? Plant Mol Biol **26,** 5-9.

Hirsch, A.M., Bhuvaneswari, T.V., Torrey, J.G., and Bisseling, T. (1989). Early nodulin genes are induced in alfalfa root outgrowths elicited by auxin transport inhibitors. Proc. Natl. Acad. Sci. USA **86,** 1244-1248.

Hossain, M.S., Shrestha, A., Zhong, S., Miri, M., Austin, R.S., Sato, S., Ross, L., Huebert, T., Tromas, A., Torres-Jerez, I., Tang, Y., Udvardi, M., Murray, J.D., and Szczyglowski, K. (2016). *Lotus japonicus* NF-YA1 plays an essential role during nodule differentiation and targets members of the *SHI/STY* gene family. Mol. Plant-Microbe Interact **29,** 950-964.

Hunter, M.C., Smith, R.G., Schipanski, M.E., Atwood, L.W., and Mortensen, D.A. (2017). Agriculture in 2050: recalibrating targets for sustainable intensification. BioScience **67,** 386-391.

Ikeda, S., Sasaki, K., Okubo, T., Yamashita, A., Terasawa, K., Bao, Z., Liu, D., Watanabe, T., Murase, J., Asakawa, S., Eda, S., Mitsui, H., Sato, T., and Minamisawa, K. (2014). Low nitrogen fertilization adapts rice root microbiome to low nutrient environment by changing biogeochemical functions. Microbes Environ **29,** 50-59.

Islas-Flores, T., Guillen, G., Alvarado-Affantranger, X., Lara-Flores, M., Sanchez, F., and Villanueva, M.A. (2011). PvRACK1 loss-of-function impairs cell expansion and morphogenesis in *Phaseolus vulgaris* L. root nodules. Mol. Plant-Microbe Interact **24,** 819-826.

Jin, Y., Liu, H., Luo, D., Yu, N., Dong, W., Wang, C., Zhang, X., Dai, H., Yang, J., and Wang, E. (2016). DELLA proteins are common components of symbiotic rhizobial and mycorrhizal signalling pathways. Nat Commun **7,** 12433.

Johnson, N.C. (1993). Can fertilization of soil select less mutualistic mycorrhizae? Ecological Applications **3,** 749-757.

Jones, J.D., and Dangl, J.L. (2006). The plant immune system. Nature **444,** 323-329.

Kalo, P., Gleason, C., Edwards, A., Marsh, J., Mitra, R.M., Hirsch, S., Jakab, J., Sims, S., Long, S.R., Rogers, J., Kiss, G.B., Downie, J.A., and Oldroyd, G.E. (2005). Nodulation signaling in legumes requires NSP2, a member of the GRAS family of transcriptional regulators. Science **308,** 1786-1789.

Kanamori, N., Madsen, L.H., Radutoiu, S., Frantescu, M., Quistgaard, E.M., Miwa, H., Downie, J.A., James, E.K., Felle, H.H., Haaning, L.L., Jensen, T.H., Sato, S., Nakamura, Y., Tabata, S., Sandal, N., and Stougaard, J. (2006). A nucleoporin is required for induction of Ca2+ spiking in legume nodule development and essential for rhizobial and fungal symbiosis. Proc Natl Acad Sci U S A **103,** 359-364.

Karimi, M., Inze, D., and Depicker, A. (2002). GATEWAY vectors for *Agrobacterium*-mediated plant transformation. Trends Plant Sci **7,** 193-195.

Kawaharada, Y., James, E.K., Kelly, S., Sandal, N., and Stougaard, J. (2017a). The Ethylene Responsive Factor required for Nodulation 1 (ERN1) transcription factor is required for infection-thread formation in *Lotus japonicus*. Mol. Plant-Microbe Interact **30,** 194-204.

Kawaharada, Y., Nielsen, M.W., Kelly, S., James, E.K., Andersen, K.R., Rasmussen, S.R., Fuchtbauer, W., Madsen, L.H., Heckmann, A.B., Radutoiu, S., and Stougaard, J. (2017b). Differential regulation of the *Epr3* receptor coordinates membrane-restricted rhizobial colonization of root nodule primordia. Nat Commun **8,** 14534.

Kawaharada, Y., Kelly, S., Nielsen, M.W., Hjuler, C.T., Gysel, K., Muszynski, A., Carlson, R.W., Thygesen, M.B., Sandal, N., Asmussen, M.H., Vinther, M., Andersen, S.U., Krusell, L., Thirup, S., Jensen, K.J., Ronson, C.W., Blaise, M., Radutoiu, S., and Stougaard, J. (2015). Receptor-mediated exopolysaccharide perception controls bacterial infection. Nature **523,** 308-312.

Kereszt, A., Mergaert, P., and Kondorosi, E. (2011). Bacteroid development in legume nodules: evolution of mutual benefit or of sacrificial victims? Mol. Plant-Microbe Interact **24,** 1300-1309.

Kiba, T., Kudo, T., Kojima, M., and Sakakibara, H. (2011). Hormonal control of nitrogen acquisition: roles of auxin, abscisic acid, and cytokinin. J Exp Bot **62,** 1399-1409.

Kiers, E.T., Hutton, M.G., and Denison, R.F. (2007). Human selection and the relaxation of legume defences against ineffective rhizobia. Proc Biol Sci **274,** 3119-3126.

Kistner, C., Winzer, T., Pitzschke, A., Mulder, L., Sato, S., Kaneko, T., Tabata, S., Sandal, N., Stougaard, J., Webb, K.J., Szczyglowski, K., and Parniske, M. (2005). Seven *Lotus japonicus* genes required for transcriptional reprogramming of the root during fungal and bacterial symbiosis. Plant Cell **17,** 2217-2229.

Kneip, C., Lockhart, P., Voss, C., and Maier, U.G. (2007). Nitrogen fixation in eukaryotes-new models for symbiosis. BMC Evol Biol **7,** 55.

Kondorosi, E., and Kondorosi, A. (2004). Endoreduplication and activation of the anaphase-promoting complex during symbiotic cell development. FEBS Lett **567,** 152-157.

Konvalinková, T., Püschel, D., Řezáčová, V., Gryndlerová, H., and Jansa, J. (2017). Carbon flow from plant to arbuscular mycorrhizal fungi is reduced under phosphorus fertilization. Plant and Soil **419,** 319–333.

Krouk, G., Ruffel, S., Gutierrez, R.A., Gojon, A., Crawford, N.M., Coruzzi, G.M., and Lacombe, B. (2011). A framework integrating plant growth with hormones and nutrients. Trends Plant Sci **16,** 178-182.

Kurakawa, T., Ueda, N., Maekawa, M., Kobayashi, K., Kojima, M., Nagato, Y., Sakakibara, H., and Kyozuka, J. (2007). Direct control of shoot meristem activity by a cytokinin-activating enzyme. Nature **445,** 652-655.

Kuusk, S., Sohlberg, J.J., Magnus Eklund, D., and Sundberg, E. (2006). Functionally redundant *SHI* family genes regulate *Arabidopsis* gynoecium development in a dose-dependent manner. Plant J **47,** 99-111.

Kuusk, S., Sohlberg, J.J., Long, J.A., Fridborg, I., and Sundberg, E. (2002). *STY1* and *STY2* promote the formation of apical tissues during *Arabidopsis* gynoecium development. Development **129,** 4707-4717.

Laloum, T., De Mita, S., Gamas, P., Baudin, M., and Niebel, A. (2013). CCAAT-box binding transcription factors in plants: Y so many? Trends Plant Sci **18,** 157-166.

Laloum, T., Baudin, M., Frances, L., Lepage, A., Billault-Penneteau, B., Cerri, M.R., Ariel, F., Jardinaud, M.F., Gamas, P., de Carvalho-Niebel, F., and Niebel, A. (2014). Two CCAAT-box-binding transcription factors redundantly regulate early steps of the legume-rhizobia endosymbiosis. Plant J **79,** 757-768.

Laporte, P., Lepage, A., Fournier, J., Catrice, O., Moreau, S., Jardinaud, M.F., Mun, J.H., Larrainzar, E., Cook, D.R., Gamas, P., and Niebel, A. (2014). The CCAAT box-binding transcription factor NF-YA1 controls rhizobial infection. J Exp Bot **65,** 481-494.

Larrainzar, E., Riely, B.K., Kim, S.C., Carrasquilla-Garcia, N., Yu, H.J., Hwang, H.J., Oh, M., Kim, G.B., Surendrarao, A.K., Chasman, D., Siahpirani, A.F., Penmetsa, R.V., Lee, G.S., Kim, N., Roy, S., Mun, J.H., and Cook, D.R. (2015). Deep sequencing of the *Medicago truncatula* root transcriptome reveals a massive and early interaction between nodulation factor and ethylene signals. Plant Physiol **169,** 233-265.

Leff, J.W., Jones, S.E., Prober, S.M., Barberan, A., Borer, E.T., Firn, J.L., Harpole, W.S., Hobbie, S.E., Hofmockel, K.S., Knops, J.M., McCulley, R.L., La Pierre, K., Risch, A.C., Seabloom, E.W., Schutz, M., Steenbock, C., Stevens, C.J., and Fierer, N. (2015). Consistent responses of soil microbial communities to elevated nutrient inputs in grasslands across the globe. Proc Natl Acad Sci U S A **112,** 10967-10972.

Levy, J., Bres, C., Geurts, R., Chalhoub, B., Kulikova, O., Duc, G., Journet, E.P., Ane, J.M., Lauber, E., Bisseling, T., Denarie, J., Rosenberg, C., and Debelle, F. (2004). A putative Ca2+ and calmodulin-dependent protein kinase required for bacterial and fungal symbioses. Science **303,** 1361-1364.

Li, X., Zhao, J., Tan, Z., Zeng, R., and Liao, H. (2015). *GmEXPB2*, a cell wall β-expansin, affects soybean nodulation through modifying root architecture and promoting nodule formation and development. Plant Physiol **169,** 2640-2653.

Liang, Y., Toth, K., Cao, Y., Tanaka, K., Espinoza, C., and Stacey, G. (2014). Lipochitooligosaccharide recognition: an ancient story. New Phytol **204,** 289-296.

Liang, Y., Cao, Y., Tanaka, K., Thibivilliers, S., Wan, J., Choi, J., Kang, C., Qiu, J., and Stacey, G. (2013). Nonlegumes respond to rhizobial Nod factors by suppressing the innate immune response. Science **341,** 1384-1387.

Liese, R., Schulze, J., and Cabeza, R.A. (2017). Nitrate application or P deficiency induce a decline in *Medicago truncatula* N_2-fixation by similar changes in the nodule transcriptome. Sci Rep **7,** 46264.

Limpens, E., and Bisseling, T. (2014). CYCLOPS: a new vision on rhizobium-induced nodule organogenesis. Cell Host Microbe **15,** 127-129.

Limpens, E., Franken, C., Smit, P., Willemse, J., Bisseling, T., and Geurts, R. (2003). LysM domain receptor kinases regulating rhizobial Nod factor-induced infection. Science **302,** 630-633.

Liu, D., Liberton, M., Yu, J., Pakrasi, H.B., and Bhattacharyya-Pakrasi, M. (2018). Engineering nitrogen fixation activity in an oxygenic phototroph. mBio **9**.

Lombari, P., Ercolano, E., El Alaouri, E., and Chiurazzi, M. (2005). *Agrobacterium*-mediated in vitro transformation. Lotus japonicus Handbook**,** 87-95.

Lovering, R., Hanson, I.M., Borden, K.L., Martin, S., O'Reilly, N.J., Evan, G.I., Rahman, D., Pappin, D.J., Trowsdale, J., and Freemont, P.S. (1993). Identification and preliminary characterization of a protein motif related to the zinc finger. Proc Natl Acad Sci U S A **90,** 2112-2116.

Luginbuehl, L.H., Menard, G.N., Kurup, S., Van Erp, H., Radhakrishnan, G.V., Breakspear, A., Oldroyd, G.E.D., and Eastmond, P.J. (2017). Fatty acids in arbuscular mycorrhizal fungi are synthesized by the host plant. Science **356,** 1175-1178.

Lutken, H., Jensen, L.S., Topp, S.H., Mibus, H., Muller, R., and Rasmussen, S.K. (2010). Production of compact plants by overexpression of *AtSHI* in the ornamental *Kalanchoe*. Plant Biotechnol J **8,** 211-222.

Lynch, J. (1995). Root architecture and plant productivity. Plant Physiol **109,** 7-13.

MacLean, A.M., Bravo, A., and Harrison, M.J. (2017). Plant signaling and metabolic pathways enabling arbuscular mycorrhizal symbiosis. Plant Cell **29,** 2319-2335.

Madsen, E.B., Madsen, L.H., Radutoiu, S., Olbryt, M., Rakwalska, M., Szczyglowski, K., Sato, S., Kaneko, T., Tabata, S., Sandal, N., and Stougaard, J. (2003). A receptor kinase gene of the LysM type is involved in legume perception of rhizobial signals. Nature **425,** 637-640.

Madsen, L.H., Fukai, E., Radutoiu, S., Yost, C.K., Sandal, N., Schauser, L., and Stougaard, J. (2005). LORE1, an active low-copy-number TY3-gypsy retrotransposon family in the model legume *Lotus japonicus*. Plant J **44,** 372-381.

Madsen, L.H., Tirichine, L., Jurkiewicz, A., Sullivan, J.T., Heckmann, A.B., Bek, A.S., Ronson, C.W., James, E.K., and Stougaard, J. (2010). The molecular network governing nodule organogenesis and infection in the model legume *Lotus japonicus*. Nat Commun **1,** 10.

Maekawa, T., Kusakabe, M., Shimoda, Y., Sato, S., Tabata, S., Murooka, Y., and Hayashi, M. (2008). Polyubiquitin promoter-based binary vectors for overexpression and gene silencing in *Lotus japonicus*. Mol. Plant-Microbe Interact **21,** 375-382.

Maillet, F., Poinsot, V., Andre, O., Puech-Pages, V., Haouy, A., Gueunier, M., Cromer, L., Giraudet, D., Formey, D., Niebel, A., Martinez, E.A., Driguez, H., Becard, G., and Denarie, J. (2011). Fungal lipochitooligosaccharide symbiotic signals in arbuscular mycorrhiza. Nature **469,** 58-63.

Majda, M., and Robert, S. (2018). The role of auxin in cell wall expansion. Int J Mol Sci **19**.

Malamy, J.E., and Benfey, P.N. (1997). Organization and cell differentiation in lateral roots of *Arabidopsis thaliana*. Development **124,** 33-44.

Malolepszy, A., Mun, T., Sandal, N., Gupta, V., Dubin, M., Urbanski, D., Shah, N., Bachmann, A., Fukai, E., Hirakawa, H., Tabata, S., Nadzieja, M., Markmann, K., Su, J., Umehara, Y., Soyano, T., Miyahara, A., Sato, S., Hayashi, M., Stougaard, J., and Andersen, S.U. (2016). The LORE1 insertion mutant resource. Plant J **88,** 306-317.

Mantovani, R. (1999). The molecular biology of the CCAAT-binding factor NF-Y. Gene **239,** 15-27.

Markmann, K., and Parniske, M. (2009). Evolution of root endosymbiosis with bacteria: how novel are nodules? Trends Plant Sci **14,** 77-86.

Marsh, J.F., Rakocevic, A., Mitra, R.M., Brocard, L., Sun, J., Eschstruth, A., Long, S.R., Schultze, M., Ratet, P., and Oldroyd, G.E. (2007). *Medicago truncatula NIN* is essential for rhizobial-independent nodule organogenesis induced by autoactive calcium/calmodulin-dependent protein kinase. Plant Physiol **144,** 324-335.

Martínez-Hidalgo, P., and Hirsch, A.M. (2017). The nodule microbiome: N_2-fixing rhizobia do not live alone. Phytobiomes **1,** 70-82.

Masclaux-Daubresse, C., Daniel-Vedele, F., Dechorgnat, J., Chardon, F., Gaufichon, L., and Suzuki, A. (2010). Nitrogen uptake, assimilation and remobilization in plants: challenges for sustainable and productive agriculture. Ann Bot **105,** 1141-1157.

Mathesius, U. (2008). Auxin: at the root of nodule development? Functional Plant Biology **35,** 651-668.

Mathesius, U., Weinman, J.J., Rolfe, B.G., and Djordjevic, M.A. (2000a). Rhizobia can induce nodules in white clover by 'hijacking' mature cortical cells activated during lateral root development. Mol. Plant-Microbe Interact **13,** 170-182.

Mathesius, U., Charon, C., Rolfe, B.G., Kondorosi, A., and Crespi, M. (2000b). Temporal and spatial order of events during the induction of cortical cell divisions in white clover by *Rhizobium leguminosarum* bv. *trifolii* Inoculation or localized cytokinin addition. Mol. Plant-Microbe Interact **13,** 617-628.

Messinese, E., Mun, J.H., Yeun, L.H., Jayaraman, D., Rouge, P., Barre, A., Lougnon, G., Schornack, S., Bono, J.J., Cook, D.R., and Ane, J.M. (2007). A novel nuclear protein interacts with the symbiotic DMI3 calcium- and calmodulin-dependent protein kinase of *Medicago truncatula*. Mol. Plant-Microbe Interact **20,** 912-921.

Middleton, P.H., Jakab, J., Penmetsa, R.V., Starker, C.G., Doll, J., Kaló, P., Prabhu, R., Marsh, J.F., Mitra, R.M., Kereszt, A., Dudas, B., VandenBosch, K., Long, S.R., Cook, D.R., Kiss, G.B., and Oldroyd, G.E.D. (2007). An ERF transcription factor in *Medicago truncatula* that is essential for nod factor signal transduction. Plant Cell **19,** 1221-1234.

Miller, A.J., and Smith, S.J. (1996). Nitrate transport and compartmentation in cereal root cells. J Exp Bot **47,** 843-854.

Miri, M., Janakirama, P., Held, M., Ross, L., and Szczyglowski, K. (2016). Into the root: how cytokinin controls rhizobial infection. Trends Plant Sci **21,** 178-186.

Miri, M., Janakirama, P., Huebert, T., Ross, L., McDowell, T., Orosz, K., Markmann, K., and Szczyglowski, K. (2019). Inside out: root cortex-localized LHK1 cytokinin receptor limits epidermal infection of *Lotus japonicus* roots by *Mesorhizobium loti*. New Phytol **0**.

Mitra, R.M., Gleason, C.A., Edwards, A., Hadfield, J., Downie, J.A., Oldroyd, G.E., and Long, S.R. (2004). A Ca2+/calmodulin-dependent protein kinase required for symbiotic nodule development: gene identification by transcript-based cloning. Proc Natl Acad Sci U S A **101,** 4701-4705.

Morieri, G., Martinez, E.A., Jarynowski, A., Driguez, H., Morris, R., Oldroyd, G.E., and Downie, J.A. (2013). Host-specific Nod-factors associated with *Medicago truncatula* nodule infection differentially induce calcium influx and calcium spiking in root hairs. New Phytol **200,** 656-662.

Mortier, V., Holsters, M., and Goormachtig, S. (2012). Never too many? How legumes control nodule numbers. Plant Cell Environ **35,** 245-258.

Mortier, V., Wasson, A., Jaworek, P., De Keyser, A., Decroos, M., Holsters, M., Tarkowski, P., Mathesius, U., and Goormachtig, S. (2014). Role of *LONELY GUY* genes in indeterminate nodulation on *Medicago truncatula*. New Phytol **202,** 582-593.

Mun, T., Bachmann, A., Gupta, V., Stougaard, J., and Andersen, S.U. (2016). *Lotus* Base: An integrated information portal for the model legume *Lotus japonicus*. Sci Rep **6,** 39447.

Murakami, E., Cheng, J., Gysel, K., Bozsoki, Z., Kawaharada, Y., Hjuler, C.T., Sorensen, K.K., Tao, K., Kelly, S., Venice, F., Genre, A., Thygesen, M.B., Jong, N., Vinther, M., Jensen, D.B., Jensen, K.J., Blaise, M., Madsen, L.H., Andersen, K.R., Stougaard, J., and Radutoiu, S. (2018). Epidermal LysM receptor ensures robust symbiotic signalling in *Lotus japonicus*. eLife **7**.

Murray, J.D. (2017). The cell cycle in nodulation. In Molecular cell biology of the growth and differentiation of plant cells, pp. 220-235.

Murray, J.D., Karas, B.J., Sato, S., Tabata, S., Amyot, L., and Szczyglowski, K. (2007). A cytokinin perception mutant colonized by *Rhizobium* in the absence of nodule organogenesis. Science **315,** 101-104.

Mus, F., Crook, M.B., Garcia, K., Garcia Costas, A., Geddes, B.A., Kouri, E.D., Paramasivan, P., Ryu, M.H., Oldroyd, G.E.D., Poole, P.S., Udvardi, M.K., Voigt, C.A., Ane, J.M., and Peters, J.W. (2016). Symbiotic nitrogen fixation and the challenges to its extension to nonlegumes. Appl Environ Microbiol **82,** 3698-3710.

Nadzieja, M., Kelly, S., Stougaard, J., and Reid, D. (2018). Epidermal auxin biosynthesis facilitates rhizobial infection in *Lotus japonicus*. Plant J **95,** 101-111.

Navarro-Gonzalez, R., McKay, C.P., and Mvondo, D.N. (2001). A possible nitrogen crisis for Archaean life due to reduced nitrogen fixation by lightning. Nature **412,** 61-64.

Niu, Y.F., Chai, R.S., Jin, G.L., Wang, H., Tang, C.X., and Zhang, Y.S. (2013). Responses of root architecture development to low phosphorus availability: a review. Ann Bot **112,** 391-408.

Oldroyd, G.E. (2013). Speak, friend, and enter: signalling systems that promote beneficial symbiotic associations in plants. Nat Rev Microbiol **11,** 252-263.

Op den Camp, R.H., De Mita, S., Lillo, A., Cao, Q., Limpens, E., Bisseling, T., and Geurts, R. (2011). A phylogenetic strategy based on a legume-specific whole genome duplication yields symbiotic cytokinin type-A response regulators. Plant Physiol **157,** 2013-2022.

Pan, Y., Cassman, N., de Hollander, M., Mendes, L.W., Korevaar, H., Geerts, R.H., van Veen, J.A., and Kuramae, E.E. (2014). Impact of long-term N, P, K, and NPK fertilization on the composition and potential functions of the bacterial community in grassland soil. FEMS Microbiol Ecol **90,** 195-205.

Panke-Buisse, K., Poole, A.C., Goodrich, J.K., Ley, R.E., and Kao-Kniffin, J. (2015). Selection on soil microbiomes reveals reproducible impacts on plant function. Isme j **9,** 980-989.

Parniske, M. (2008). Arbuscular mycorrhiza: the mother of plant root endosymbioses. Nat Rev Microbiol **6,** 763-775.

Peret, B., Desnos, T., Jost, R., Kanno, S., Berkowitz, O., and Nussaume, L. (2014). Root architecture responses: in search of phosphate. Plant Physiol **166,** 1713-1723.

Perry, J., Brachmann, A., Welham, T., Binder, A., Charpentier, M., Groth, M., Haage, K., Markmann, K., Wang, T.L., and Parniske, M. (2009). TILLING in *Lotus japonicus* identified large allelic series for symbiosis genes and revealed a bias in functionally defective ethyl methanesulfonate alleles toward glycine replacements. Plant Physiol **151,** 1281-1291.

Pingali, P.L. (2012). Green revolution: impacts, limits, and the path ahead. Proc Natl Acad Sci U S A **109,** 12302-12308.

Pirozynski, K.A., and Malloch, D.W. (1975). The origin of land plants: a matter of mycotrophism. BioSystems **6,** 153-164.

Plet, J., Wasson, A., Ariel, F., Le Signor, C., Baker, D., Mathesius, U., Crespi, M., and Frugier, F. (2011). MtCRE1-dependent cytokinin signaling integrates bacterial and plant cues to coordinate symbiotic nodule organogenesis in *Medicago truncatula*. Plant J **65,** 622-633.

Poitout, A., Crabos, A., Petrik, I., Novak, O., Krouk, G., Lacombe, B., and Ruffel, S. (2018). Responses to systemic nitrogen signaling in *Arabidopsis* roots involve trans-zeatin in shoots. Plant Cell **30,** 1243-1257.

Radutoiu, S., Madsen, L.H., Madsen, E.B., Jurkiewicz, A., Fukai, E., Quistgaard, E.M., Albrektsen, A.S., James, E.K., Thirup, S., and Stougaard, J. (2007). LysM domains mediate lipochitin-oligosaccharide recognition and *Nfr* genes extend the symbiotic host range. EMBO J **26,** 3923-3935.

Radutoiu, S., Madsen, L.H., Madsen, E.B., Felle, H.H., Umehara, Y., Gronlund, M., Sato, S., Nakamura, Y., Tabata, S., Sandal, N., and Stougaard, J. (2003). Plant recognition of symbiotic bacteria requires two LysM receptor-like kinases. Nature **425,** 585-592.

Reid, D., Nadzieja, M., Novak, O., Heckmann, A.B., Sandal, N., and Stougaard, J. (2017). Cytokinin biosynthesis promotes cortical cell responses during nodule development. Plant Physiol **175,** 361-375.

Reid, D.E., Heckmann, A.B., Novak, O., Kelly, S., and Stougaard, J. (2016). CYTOKININ OXIDASE/DEHYDROGENASE3 maintains cytokinin homeostasis during root and nodule development in *Lotus japonicus*. Plant Physiol **170,** 1060-1074.

Remy, W., Taylor, T.N., Hass, H., and Kerp, H. (1994). Four hundred-million-year-old vesicular arbuscular mycorrhizae. Proc Natl Acad Sci U S A **91,** 11841-11843.

Rightmyer, A.P., and Long, S.R. (2011). Pseudonodule formation by wild-type and symbiotic mutant *Medicago truncatula* in response to auxin transport inhibitors. Mol. Plant-Microbe Interact **24,** 1372-1384.

Rockström, J., Steffen, W., Noone, K., Persson, A., Chapin, F.S., 3rd, Lambin, E.F., Lenton, T.M., Scheffer, M., Folke, C., Schellnhuber, H.J., Nykvist, B., de Wit, C.A., Hughes, T., van der Leeuw, S., Rodhe, H., Sorlin, S., Snyder, P.K., Costanza, R., Svedin, U., Falkenmark, M., Karlberg, L., Corell, R.W., Fabry, V.J., Hansen, J., Walker, B., Liverman, D., Richardson, K., Crutzen, P., and Foley, J.A. (2009). A safe operating space for humanity. Nature **461,** 472-475.

Rogers, C., and Oldroyd, G.E. (2014). Synthetic biology approaches to engineering the nitrogen symbiosis in cereals. J Exp Bot **65,** 1939-1946.

Ruffel, S., Poitout, A., Krouk, G., Coruzzi, G.M., and Lacombe, B. (2016). Long-distance nitrate signaling displays cytokinin dependent and independent branches. J Integr Plant Biol **58,** 226-229.

Ruffel, S., Krouk, G., Ristova, D., Shasha, D., Birnbaum, K.D., and Coruzzi, G.M. (2011). Nitrogen economics of root foraging: transitive closure of the nitrate-cytokinin relay and distinct systemic signaling for N supply vs. demand. Proc Natl Acad Sci U S A **108,** 18524-18529.

Russo, G., Carotenuto, G., Fiorilli, V., Volpe, V., Chiapello, M., Van Damme, D., and Genre, A. (2018). Ectopic activation of cortical cell division during the accommodation of arbuscular mycorrhizal fungi. New Phytol.

Saito, A., Tanabata, S., Tanabata, T., Tajima, S., Ueno, M., Ishikawa, S., Ohtake, N., Sueyoshi, K., and Ohyama, T. (2014). Effect of nitrate on nodule and root growth of soybean (*Glycine max* (L.) Merr.). Int J Mol Sci **15,** 4464-4480.

Saito, K., Yoshikawa, M., Yano, K., Miwa, H., Uchida, H., Asamizu, E., Sato, S., Tabata, S., Imaizumi-Anraku, H., Umehara, Y., Kouchi, H., Murooka, Y., Szczyglowski, K., Downie, J.A., Parniske, M., Hayashi, M., and Kawaguchi, M. (2007). NUCLEOPORIN85 is required for calcium spiking, fungal and bacterial symbioses, and seed production in *Lotus japonicus*. Plant Cell **19,** 610-624.

Sasaki, T., Suzaki, T., Soyano, T., Kojima, M., Sakakibara, H., and Kawaguchi, M. (2014). Shoot-derived cytokinins systemically regulate root nodulation. Nat Commun **5,** 4983.

Schauser, L., Roussis, A., Stiller, J., and Stougaard, J. (1999). A plant regulator controlling development of symbiotic root nodules. Nature **402,** 191-195.

Sessitsch, A., and Mitter, B. (2015). 21st century agriculture: integration of plant microbiomes for improved crop production and food security. Microb Biotechnol **8,** 32-33.

Sieberer, B.J., Chabaud, M., Fournier, J., Timmers, A.C., and Barker, D.G. (2012). A switch in Ca2+ spiking signature is concomitant with endosymbiotic microbe entry into cortical root cells of *Medicago truncatula*. Plant J **69,** 822-830.

Siligato, R., Wang, X., Yadav, S.R., Lehesranta, S., Ma, G., Ursache, R., Sevilem, I., Zhang, J., Gorte, M., Prasad, K., Wrzaczek, M., Heidstra, R., Murphy, A., Scheres, B., and Mahonen, A.P. (2016). MultiSite gateway-compatible cell type-specific gene-inducible system for plants. Plant Physiol **170,** 627-641.

Singh, S., Katzer, K., Lambert, J., Cerri, M., and Parniske, M. (2014). CYCLOPS, a DNA-binding transcriptional activator, orchestrates symbiotic root nodule development. Cell Host Microbe **15,** 139-152.

Smit, P., Raedts, J., Portyanko, V., Debelle, F., Gough, C., Bisseling, T., and Geurts, R. (2005). NSP1 of the GRAS protein family is essential for rhizobial Nod factor-induced transcription. Science **308,** 1789-1791.

Smith, D.L., and Fedoroff, N.V. (1995). *LRP1*, a gene expressed in lateral and adventitious root primordia of *Arabidopsis*. Plant Cell **7,** 735-745.

Sohlberg, J.J., Myrenas, M., Kuusk, S., Lagercrantz, U., Kowalczyk, M., Sandberg, G., and Sundberg, E. (2006). STY1 regulates auxin homeostasis and affects apical-basal patterning of the *Arabidopsis* gynoecium. Plant J **47,** 112-123.

Soyano, T., and Hayashi, M. (2014). Transcriptional networks leading to symbiotic nodule organogenesis. Curr Opin Plant Biol **20,** 146-154.

Soyano, T., Kouchi, H., Hirota, A., and Hayashi, M. (2013). Nodule inception directly targets NF-Y subunit genes to regulate essential processes of root nodule development in *Lotus japonicus*. PLoS Genet **9,** e1003352.

Sprent, J.I. (2007). Evolving ideas of legume evolution and diversity: a taxonomic perspective on the occurrence of nodulation. New Phytol **174,** 11-25.

Staldal, V., Sohlberg, J.J., Eklund, D.M., Ljung, K., and Sundberg, E. (2008). Auxin can act independently of CRC, LUG, SEU, SPT and STY1 in style development but not apical-basal patterning of the *Arabidopsis* gynoecium. New Phytol **180,** 798-808.

Staldal, V., Cierlik, I., Chen, S., Landberg, K., Baylis, T., Myrenas, M., Sundstrom, J.F., Eklund, D.M., Ljung, K., and Sundberg, E. (2012). The *Arabidopsis thaliana* transcriptional activator STYLISH1 regulates genes affecting stamen development, cell expansion and timing of flowering. Plant Mol Biol **78,** 545-559.

Steffen, W., Richardson, K., Rockstrom, J., Cornell, S.E., Fetzer, I., Bennett, E.M., Biggs, R., Carpenter, S.R., de Vries, W., de Wit, C.A., Folke, C., Gerten, D., Heinke, J., Mace, G.M., Persson, L.M., Ramanathan, V., Reyers, B., and Sorlin, S. (2015). Sustainability. Planetary boundaries: guiding human development on a changing planet. Science **347,** 1259855.

Stracke, S., Kistner, C., Yoshida, S., Mulder, L., Sato, S., Kaneko, T., Tabata, S., Sandal, N., Stougaard, J., Szczyglowski, K., and Parniske, M. (2002). A plant receptor-like kinase required for both bacterial and fungal symbiosis. Nature **417,** 959-962.

Streeter, J. (1988). Inhibition of legume nodule formation and N_2 fixation by nitrate. Critical Reviews in Plant Sciences **7,** 1-23.

Sun, J., Miller, J.B., Granqvist, E., Wiley-Kalil, A., Gobbato, E., Maillet, F., Cottaz, S., Samain, E., Venkateshwaran, M., Fort, S., Morris, R.J., Ane, J.M., Denarie, J., and Oldroyd, G.E. (2015). Activation of symbiosis signaling by arbuscular mycorrhizal fungi in legumes and rice. Plant Cell **27,** 823-838.

Suzaki, T., Ito, M., and Kawaguchi, M. (2013). Genetic basis of cytokinin and auxin functions during root nodule development. Front Plant Sci **4,** 42.

Suzaki, T., Yano, K., Ito, M., Umehara, Y., Suganuma, N., and Kawaguchi, M. (2012). Positive and negative regulation of cortical cell division during root nodule development in *Lotus japonicus* is accompanied by auxin response. Development **139,** 3997-4006.

Szczyglowski, K., and Amyot, L. (2003). Symbiosis, inventiveness by recruitment? Plant Physiol **131,** 935-940.

Takanashi, K., Sugiyama, A., and Yazaki, K. (2011). Auxin distribution and lenticel formation in determinate nodule of *Lotus japonicus*. Plant Signaling and Behavior **6,** 1405-1407.

Taylor, T.N., Remy, W., Haas, H., and Kerp, H. (1995). Fossil arbuscular mycorrhizae from the early Devonian. Mycologia **87,** 560-573.

Timmers, A.C., Auriac, M.C., and Truchet, G. (1999). Refined analysis of early symbiotic steps of the *Rhizobium-Medicago* interaction in relationship with microtubular cytoskeleton rearrangements. Development **126,** 3617-3628.

Tirichine, L., Sandal, N., Madsen, L.H., Radutoiu, S., Albrektsen, A.S., Sato, S., Asamizu, E., Tabata, S., and Stougaard, J. (2007). A gain-of-function mutation in a cytokinin receptor triggers spontaneous root nodule organogenesis. Science **315,** 104-107.

Toby Kiers, E., Palmer, T.M., Ives, A.R., Bruno, J.F., and Bronstein, J.L. (2010). Mutualisms in a changing world: an evolutionary perspective. Ecol Lett **13,** 1459-1474.

Tokunaga, H., Kojima, M., Kuroha, T., Ishida, T., Sugimoto, K., Kiba, T., and Sakakibara, H. (2012). *Arabidopsis lonely guy* (*LOG*) multiple mutants reveal a central role of the LOG-dependent pathway in cytokinin activation. Plant J **69,** 355-365.

Tsikou, D., Yan, Z., Holt, D.B., Abel, N.B., Reid, D.E., Madsen, L.H., Bhasin, H., Sexauer, M., Stougaard, J., and Markmann, K. (2018). Systemic control of legume susceptibility to rhizobial infection by a mobile microRNA. Science **362,** 233-236.

Udvardi, M., and Poole, P.S. (2013). Transport and metabolism in legume-rhizobia symbioses. In Annual Review of Plant Biology, pp. 781-805.

Urbanski, D.F., Malolepszy, A., Stougaard, J., and Andersen, S.U. (2012). Genome-wide LORE1 retrotransposon mutagenesis and high-throughput insertion detection in *Lotus japonicus*. Plant J **69,** 731-741.

van der Heijden, M.G., de Bruin, S., Luckerhoff, L., van Logtestijn, R.S., and Schlaeppi, K. (2016). A widespread plant-fungal-bacterial symbiosis promotes plant biodiversity, plant nutrition and seedling recruitment. Isme j **10,** 389-399.

Van Grinsven, H.J., Ward, M.H., Benjamin, N., and De Kok, T.M. (2006). Does the evidence about health risks associated with nitrate ingestion warrant an increase of the nitrate standard for drinking water? Environmental Health **5,** 26.

van Velzen, R., Holmer, R., Bu, F., Rutten, L., van Zeijl, A., Liu, W., Santuari, L., Cao, Q., Sharma, T., Shen, D., Roswanjaya, Y., Wardhani, T.A.K., Kalhor, M.S., Jansen, J., van den Hoogen, J., Gungor, B., Hartog, M., Hontelez, J., Verver, J., Yang, W.C., Schijlen, E., Repin, R., Schilthuizen, M., Schranz, M.E., Heidstra, R., Miyata, K., Fedorova, E., Kohlen, W., Bisseling, T., Smit, S., and Geurts, R. (2018). Comparative genomics of the nonlegume *Parasponia*

reveals insights into evolution of nitrogen-fixing *rhizobium* symbioses. Proc Natl Acad Sci U S A **115,** E4700-E4709.

van Zeijl, A., Op den Camp, R.H., Deinum, E.E., Charnikhova, T., Franssen, H., Op den Camp, H.J., Bouwmeester, H., Kohlen, W., Bisseling, T., and Geurts, R. (2015). *Rhizobium* lipo-chitooligosaccharide signaling triggers accumulation of cytokinins in *Medicago truncatula* roots. Mol Plant **8,** 1213-1226.

Vandenkoornhuyse, P., Quaiser, A., Duhamel, M., Le Van, A., and Dufresne, A. (2015). The importance of the microbiome of the plant holobiont. New Phytol **206,** 1196-1206.

Vernie, T., Kim, J., Frances, L., Ding, Y., Sun, J., Guan, D., Niebel, A., Gifford, M.L., de Carvalho-Niebel, F., and Oldroyd, G.E. (2015). The NIN transcription factor coordinates diverse nodulation programs in different tissues of the *Medicago truncatula* root. Plant Cell **27,** 3410-3424.

Vessey, J.K., and Waterer, J. (1992). In search of the mechanism of nitrate inhibition of nitrogenase activity in legume nodules: recent developments. Physiologia Plantarum **84,** 171-176.

Vitousek, P.M., Mooney, H.A., Lubchenco, J., and Melillo, J.M. (1997). Human domination of Earth's ecosystems. Science **277,** 494-499.

Vitousek, P.M., Menge, D.N., Reed, S.C., and Cleveland, C.C. (2013). Biological nitrogen fixation: rates, patterns and ecological controls in terrestrial ecosystems. Philos Trans R Soc Lond B Biol Sci **368,** 20130119.

Weese, D.J., Heath, K.D., Dentinger, B.T., and Lau, J.A. (2015). Long-term nitrogen addition causes the evolution of less-cooperative mutualists. Evolution **69,** 631-642.

Wopereis, J., Pajuelo, E., Dazzo, F.B., Jiang, Q., Gresshoff, P.M., De Bruijn, F.J., Stougaard, J., and Szczyglowski, K. (2000). Short root mutant of *Lotus japonicus* with a dramatically altered symbiotic phenotype. Plant J **23,** 97-114.

Xiao, T.T., Schilderink, S., Moling, S., Deinum, E.E., Kondorosi, E., Franssen, H., Kulikova, O., Niebel, A., and Bisseling, T. (2014). Fate map of *Medicago truncatula* root nodules. Development **141,** 3517-3528.

Xie, F., Murray, J.D., Kim, J., Heckmann, A.B., Edwards, A., Oldroyd, G.E., and Downie, J.A. (2012). Legume pectate lyase required for root infection by rhizobia. Proc Natl Acad Sci U S A **109,** 633-638.

Yang, S.Y., and Paszkowski, U. (2011). Phosphate import at the arbuscule: just a nutrient? Mol. Plant-Microbe Interact **24,** 1296-1299.

Yano, K., Yoshida, S., Muller, J., Singh, S., Banba, M., Vickers, K., Markmann, K., White, C., Schuller, B., Sato, S., Asamizu, E., Tabata, S., Murooka, Y., Perry, J., Wang, T.L., Kawaguchi, M., Imaizumi-Anraku, H., Hayashi, M., and Parniske, M. (2008). CYCLOPS, a mediator of symbiotic intracellular accommodation. Proc Natl Acad Sci U S A **105,** 20540-20545.

Yoro, E., Suzaki, T., Toyokura, K., Miyazawa, H., Fukaki, H., and Kawaguchi, M. (2014). A positive regulator of nodule organogenesis, NODULE INCEPTION, acts as a negative regulator of rhizobial infection in *Lotus japonicus*. Plant Physiol **165,** 747-758.

Zanetti, M.E., Blanco, F.A., Beker, M.P., Battaglia, M., and Aguilar, O.M. (2010). A C subunit of the plant nuclear factor NF-Y required for rhizobial infection and nodule development affects partner selection in the common bean-*Rhizobium etli* symbiosis. Plant Cell **22,** 4142-4157.

Zhang, J., and Zhou, J.M. (2010). Plant immunity triggered by microbial molecular signatures. Mol Plant **3,** 783-793.

Zhao, Y. (2012). Auxin biosynthesis: a simple two-step pathway converts tryptophan to indole-3-acetic acid in plants. Mol Plant **5,** 334-338.

Zhao, Y. (2018). Essential roles of local auxin biosynthesis in plant development and in adaptation to environmental changes. Annu Rev Plant Biol **69,** 417-435.

Zipfel, C., and Oldroyd, G.E. (2017). Plant signalling in symbiosis and immunity. Nature **543,** 328-336.

Zürcher, E., and Muller, B. (2016). Cytokinin synthesis, signaling, and function-advances and new insights. Int Rev Cell Mol Biol **324,** 1-38.

APPENDICES

Appendix A Primers used for *STY* gene study

Name of primer	Primer sequences (5'-3')
Genotyping primers for LORE1 insertion *sty* alleles	
sty1-1- LORE1-F	ATTGCGGACACAGGAGGTGCAGGT
sty1-1- LORE1-R	CACGCACTTGACGAGGCAACGACT
sty1-2- LORE1-F	ACCTGCACCTCCTGTGTCCGCAAT
sty1-2- LORE1-R	TGGTCAGCCACTCCTCCATCCTCC
sty2-1- LORE1-F	TGCTTGTTGTTGCTTGCTTCTTC
sty2-1- LORE1-R	GACGACGCCCTCACAAACC
sty3-10- LORE1-F	CGCAACCGATCTTCCTTTGGAGCA
sty3-10-LORE1-R	CGCAACCGATCTTCCTTTGGAGCA
sty4-1- LORE1-F	GCCACTCCTTGCATGCCACAACAA
sty4-1- LORE1-R	CATCACCACCACCACCCTCAC
sty4-2- LORE1-F	CATGTTGTAAGGGGCGCGGGTATG
sty4-2- LORE1-R	CCTCCAGGACAACCAAATTGCCTTTCA
sty5-1- LORE1-F	CTCTGCAACGCCGCCATGGAAACT
sty5-1- LORE1-R	TGCATGGCTACGTCTCCCTTTTACCA
sty5-2- LORE1-F	TGAGATATGGCCACCGCAGCAGAA
sty5-2- LORE1-R	CACACACCGAAACACCGCCGTAGA
sty5-3- LORE1-F	TGGTTGTGGCCGTGTTAGTGGCAG
sty5-3- LORE1-R	GTTTCCGTGCCAAACGCATGTCAA
sty5-4- LORE1-F	GGAAGCGGGGCAATTCCCTACTGA
sty5-4- LORE1-R	TCACACCGGAAATACACCAGCACCA
sty6-1- LORE1-F	GAAGCTAATGAGCGCGGCTGAGGA
sty6-1- LORE1-R	TCCCTCCCCCAAATGTTACCTAACTCA
sty7-1- LORE1-F	GCATGTTGGTGGTTGCGTTGTCGT
sty7-1- LORE1-R	TGCAGCCTTCAGATTCTGGCGCTT
sty7-2- LORE1-F	ACGACAACGCAACCACCAACATGC
sty7-2- LORE1-R	CCAAAGCCAAAATCATACGGTGGGC
sty7-3- LORE1-F	CCGGCACTTCCAGGTCACCATCTC
sty7-3- LORE1-R	CTTGCAGCAGGGACCCAAGTGCTC
sty7-4- LORE1-F	GATGAGGCCCCATTTCTCCCTCCA
sty7-4- LORE1-R	GCCCACCGTATGATTTTGGCTTTGG
sty7-5- LORE1-F	TGCAGCCTTCAGATTCTGGCGCTT
sty7-5- LORE1-R	CTTGCAGCAGGGACCCAAGTGCTC
sty8-1- LORE1-F	TGAAAAACCATTCGTTACGGCTGAGACC
sty8-1- LORE1-R	CGACGATGTTTCGGTGTCTTTCTCCG

Appendix A continued	
sty8-2- LORE1-F	TTGCTGTCTCTCACGGCGTTTTGC
sty8-2- LORE1-R	TCATCATCACAACAACATGGCTGGG
sty8-3- LORE1-F	GCCAGCCCCCTTTAATTTCGAGCA
sty8-3- LORE1-R	CCTGAGCTTAACTCTCCGGCGGTGT
sty9-1- LORE1-F	CAGACCTTGTTGCTGTTTCCATGAGCA
sty9-1- LORE1-R	GCACCACCACCATCACTGTCACCC
sty9-2- LORE1-F	GCACCACCACCATCACTGTCACCC
sty9-2- LORE1-R	GCCACTCCTTGCATGCCACAACCT
sty9-3- LORE1-F	GATGCAGGACATGTTGCAAGGGGC
sty9-3- LORE1-R	CATGTCCCCCTCCCTTCACCCACT
P2 (LORE1 reverse)	CCATGGCGGTTCCGTGAATCTTAGG
Genotyping primers for *sty3* TILLING alleles	
sty3-1-F	TCTTCTTACAGAGGCTTTGAGATATGGAACCACCGG
sty3-1-R	AGAGTGCAAGCGAGTGATGAA
sty3-9-F	CGCTAGGTGTTGGGCCGTCG
sty3-9-R	ATCTCTCTGCTGCCTTGTAGGAACCAGCT
Sequencing primers for *sty3-1* and *sty3-9*	
sty3-1-seq-F	ATGGCGGGTTTATTCTCACTAG
sty3-1-seq-R	TCCTCCTCCACCTCCACTTC
sty3-1-seq-R1	AGCAAGTTCTGCACCTCACA
sty3-9-seq-F	GAAGTGGAGGTGGAGGAGGA
sty3-9-seq-R	TGCACTCTGCAGGATTCTGTT
sty3-9-seq-F1	TGTGAGGTGCAGAACTTGCT
sty3-9-seq-R1	ACACGCAACCGATCTTCCTT
qRT-PCR Primers for *STYs*	
STY1-qPCR-F	ACGCTCTTGTTGAGCACGAT
STY1-qPCR-R	CTCCTGTGTCCGCAATCCTT
STY2-qPCR-F	GGTACAAACCAAACGACGATG
STY2-qPCR-R	CTTAACCCTGCTCCTCCAACT
STY3-qPCR-F	GGCCAGACGGCAATAGTTACAC
STY3-qPCR-R	GAGCCGGATACAAGGAAGAAGG
STY4-qPCR-F	TGGAACCTCAAAATGTGCCC
STY4-qPCR-R	TCAGGACCGTAAACACCGTT
STY5-qPCR-F	TGATGATGAGTAGGCGTGGTG
STY5-qPCR-R	TGTGGTGGAGGATGGAGGATT
STY6-qPCR-F	ATGGCGGTATTCAGCAGTGTT
STY6-qPCR-R	ATCATGGCTGTGGATTGTGG
STY7-qPCR-F	GAGGATGGGAAGGATGAGTATG

Appendix A continued	
STY7-qPCR-R	CTCCACCACCAACAGTACCAC
STY8-qPCR-F	AGGCCAAGACAATGCTCCTA
STY8-qPCR-R	GCGTACCAGCCATGAAAGCA
STY9-qPCR-F	GTGGCTGATGGTGGTAGTGG
STY9-qPCR-R	TTAGTGGCGGTGGAACTGTG
UBQ-F	ATGTGCATTTTAAGACAGGG
UBQ-R	GAACGTAGAAGATTGCCTGAA
PP2A-F	GTAAATGCGTCTAAAGATAGGGTCC
PP2A-R	ACTAGACTGTAGTGCTTGAGAGGC
ATPs-F	AACACCACTCTCGATCATTTCTCTG
ATPs-R	CAATGTCGCCAAGGCCCATGGTG
Genotyping primers for *STY3::SRDX* transgene	
STY3-SRDX-F	AAGTGAGAGAAGAATGGCGGG
STY3-SRDX-R	GCCAAGGATGGATTTCCTAAGC
qPCR primers for *STY3::SRDX* transgene	
STY3-SRDX-qPCR-F	GGGCCAGACGGCAATAGTTA
STY3-SRDX-qPCR-R	AGCAAATCCAAGTCTAAGCTCAA

Appendix B Primers used for *YUCCA* gene study

Genotyping primers LORE1 insertion *yucca* alleles	
yucca1-1-LORE1-F	TGGGGCTGAAAAGGCCATCACAAG
yucca1-1-LORE1-R	TGGGTCTTCGGAGAGGGCTCTGTTG
yucca11-1-LORE1-F	TCAGGCCCTTGCAAACCACAGTGA
yucca11-1-LORE1-R	CCCGGAACCCATGTAGGCCTTGTC
yucca11-2 LORE1-F	TGACTGTGTGCATCCCCTGAAGCT
yucca11-2 LORE1-R	TCCGCATGCATTAATTGGTGAGTGC
yucca11-3 LORE1-F	GGATGTTCTAGGTTCGAACACGATTGCC
yucca11-3 LORE1-R	TGACTGTGTGCATCCCCTGAAGCT
qRT-PCR Primers for *YUCCAs*	
YUCCA1-qPCR-F	GAGTTGGCGGTTATGATGCTG
YUCCA1-qPCR-R	CAGGGGTTTTTCCCATTGTGTT
YUCCA11-qPCR-F	ACAGCACGAAGTGGAGTTTG
YUCCA11-qPCR-R	AAGCAGGCCACGTTTAGAGA
***YUCCA1* and *YUCCA11* promoter amplification primers**	
pYUCCA1-DT-F	CACCTCATCCACTGTCTGTTAAG
pYUCCA1-DT-R	TTTGAATTTTGTGTGTGTTATG
pYUCCA11-DT-F	CACCAATGCAAGACATTGAC
pYUCCA11-DT-R	ATGAATTGAAAACCAAACATATAC
***YUCCA1* and *YUCCA11* promoter sequencing primers**	
pYUCCA1-F1	ATAACCTCCGATCCACTTC
pYUCCA1-F2	TGGAGTGTTATTCTAACA
pYUCCA1-F3	TACGTGTCAGTATGTCCTGC
pYUCCA1-F4	ATTTCTTCCATACCACTTG
pYUCCA1-F5	TCTCACAGAATATAGTGT
pYUCCA1-F6	TCAATCCAACACTCTCAAC
pYUCCA1-R1	CAACGATGCAGTGGAGCA
pYUCCA1-R2	ACATCACAGTCCTCCTCATTC
pYUCCA1-R3	ATCTATACAGTCTCTCTT
pYUCCA1-R4	GTATATGCATTTTCCATGCAC
pYUCCA1-R5	GACAATCCTTTGGTTATGTATG
pYUCCA11-F1	GTACTAGTGTCGCTACCAGATTG
pYUCCA11-F2	CGTCACATAGTTCTTGTCAGGAG
pYUCCA11-F3	TCAAAGCAAGGAATTTGTGAC
pYUCCA11-F4	CTATGAGTCATTCAAGCAATA
pYUCCA11-F5	CAAGTAGTCAGTTGTAGTGTG
pYUCCA11-F6	CAGTCCTTTCTTGAGGACAGTC
pYUCCA11-R1	GCATTGCTCGTATTAGGAG

Appendix B continued	
pYUCCA11-R2	GTGACAGCCTTATATTTCGTC
pYUCCA11-R3	GTGACAGAATCTTAGAGAG
pYUCCA11-R4	CGAATCATGGATCAGGTACCT
pYUCCA11-R5	CACACAGACATTGGGAGTCAG
pYUCCA11-R6	GAGCACACAGCAGGAAGCAATGT
pYUCCA11-R7	CTCGTCACTCAGTGCATGT

CURRICULUM VITAE

Arina Shrestha

EDUCATION

2013-2018 **PhD Candidate, Cell and Molecular Biology**
Department of Biology, University of Western Ontario
London, Ontario, Canada

2003-2005 **Master of Science, Microbiology**
Department of Microbiology, Tribhuvan University
Kirtipur, Nepal

1999-2002 **Bachelor of Science, Microbiology**
Department of Microbiology, Tri-Chandra Multiple Campus
Kathmandu, Nepal

SCHOLARSHIPS/AWARDS

2013-2018 Western Graduate Research Scholarship
2014 Best Poster Presentation Award, Biological Graduate Research Forum
2014 Best Poster Presentation Award, Canadian Society of Plant Biologists
2016 Graduate Student Travel Award, UWO
2017 Graduate Student Travel Award, UWO
2018 Graduate Student Travel Award, UWO
2018 Early Career Award, Scandinavian Plant Physiology Society, Sweden

WORK EXPERIENCE

2013-2018 **Research Assistant**
Agriculture and Agri-Food Canada, London, Ontario, Canada
2013-2018 **Teaching Assistant**, **Department of Biology**
University of Western Ontario, London, Ontario, Canada
2005-2008 **Research Assistant**
Shi-Gan Health Foundation, Kathmandu, Nepal
2008-2010 **Lecturer, Department of Public Health**
Little Buddha College of Health Sciences, Kathmandu, Nepal
2007-2010 **Lecturer, Department of Microbiology**
Tri-Chandra Multiple Campus, Kathmandu, Nepal

ARTICLES PUBLISHED

Hossain, Md. S*****., **Shrestha, A***., Zhong, S*****., Miri, M., Austin, R., Sato, S., Ross L., Huebert, T., Torres-Jerez, I., Murray, J., Udvardi, M., and Szczyglowski, K. (2016). *Lotus japonicus* NF-YA1 plays an essential role during nodule differentiation and targets members of the *SHI/STY* gene family. MPMI. 29(12):950-64 (PhD work). ***These authors contributed equally to this work.**

Rai, S.K., Gurung, R., Saiju, R., Bajracharya, L., Rai, N., Gurung, K., **Shrestha, A**., Shakya, B., Pant, J., Sharma, P., and Rai, C.K. (2008) Intestinal parasitosis among subjects undergoing cataract surgery at the eye camps in rural hilly areas of Nepal. Nepal Med Coll J. 10(2):100-3 (MSc. work).

Shrestha, **A**., Rai, S.K., Basnyat, S.R.B., and Shakya, B. (2007). Study on soil transmitted helminthiasis in Kathmandu Valley. Nepal Med Coll J. 9:166-9 (MSc. work).

Shakya, B., **Shrestha**, **A**., Rai, S.K., Singh, A., and Rai, C.K. (2007) Analysis of factors associated with intestinal parasitosis among elderly people in Kathmandu Valley. J Med Lab Asso Nepal. 8: 53-6 (MSc. work).

Rai, C.K., **Shrestha**, **A**., Rai, S.K., and Shah, R.D.P. (2007). Study of intestinal parasitosis among health care centre visiting patients in Kathmandu Valley. J Nepal Asso Med Lab Sci. 8:1233-6 (MSc. work).

Shakya, B., Rai, S.K., Singh, A., and **Shrestha**, **A**. (2005). Intestinal parasitosis among the elderly people in Kathmandu Valley. Nepal Med Coll J. 8: 243-7 (MSc. work).

BOOKS PUBLISHED

Shrestha, **A**., and Shrestha, S. (2010). An introduction to public health laboratory science, a textbook for bachelor in public health. Vidhyarthi Publication, ISBN 978-99946-1-400-4.

Shrestha, S., and **Shrestha**, **A**. (2007). A textbook of primary health care and family health. a textbook for health assistant/bachelor in public health. Vidhyarthi Publication, , ISBN 978-99946-065-1.

POSTER PRESENTATIONS

Shrestha, **A**., Janakirama, P., Ross, L., and Szczyglowski, K. (2018). "*Lotus japonicus STYLISH* gene family members act redundantly to mediate *Mesorhizobium loti* and nodule organogenesis," 13th European Nitrogen Fixation Conference, Stockholm, Sweden

(International- PhD work).

Shrestha, **A**., Janakirama, P., Ross L., and Szczyglowski, K. (2018). "*Lotus japonicus STYLISH* gene family members act redundantly to mediate *Mesorhizobium loti* and nodule organogenesis," 24th North American Conference in Symbiotic Nitrogen Fixation, Winnipeg, Canada (International- PhD work).

Shrestha, **A**., Ross, L., and Szczyglowski, K. (2017). "Members of the *Lotus japonicus STY* transcription factor gene family are required for infection thread formation and nodule organogenesis," 20th International Congress on Nitrogen Fixation, Granada Spain (International- PhD work).

Shrestha, **A**., Ross, L., Huebert, T., and Szczyglowski, K. (2016). "*STYLISH* gene family members and their role in symbiotic root nodule development", The joint meeting of Canadian Society of Plant Biologists (CSPB) and the Canadian Association for Plant Biotechnology (CAPB), Queen's University, Kingston, Ontario, Canada (National- PhD work).

Shrestha, **A**., Ross, L., and Szczyglowski, K. (2015). "The *Lotus japonicus STYLISH* gene family and its role during symbiotic root nodule formation," 23rd North American Conference in Symbiotic Nitrogen Fixation, Ixtapa, Mexico (International- PhD work).

Shrestha, **A**., Ross, L., Tromas, A., and Szczyglowski, K. (2014) "*Lotus japonicus STYLISH* gene family and its role during nitrogen fixation symbiosis." Canadian Society of Plant Biologists, East regional meeting, University of Guelph, Ontario, Canada (National- PhD work).

Shrestha, **A**., Ross, L., Tromas, A., and Szczyglowski, K. (2014). "Role of *Lotus japonicus STYLISH/SHORT INTERNODES* gene family member during root nodule development." The 5th Annual Biological Graduate Research Forum (BGRF), University of Western Ontario, Ontario, Canada (Departmental- PhD work).

ORAL PRESENTATIONS

Shrestha, **A**., Rai, SK. (2005). "Study of soil contamination with helminthes parasite eggs and parasitic infection in school children in Kathmandu Valley" Asia Pacific Association of Societies of Pathologists of Nepal, Kathmandu, Nepal (International- MSc. work).

Shrestha, **A**., Rai, CK., and Rai, SK. (2005). "Intestinal Parasitosis among Health Care Center Visiting Patients in Kathmandu Valley." Nepal Association of Medical Laboratory Science, Kathmandu, Nepal (National- MSc. work).